INVESTIGATING PANNEXIN1A MEDIATED MECHANISMS OF PAIN AND NEUROINFLAMMATION USING ZEBRAFISH

Darren Jeyarajah

A THESIS SUBMITTED TO THE FACULTY OF GRADUATE STUDIES IN PARTIAL FULFILLMENT OF THE REQUIREMENTS FOR THE MASTER OF SCIENCE

GRADUATE PROGRAM IN BIOLOGY

YORK UNIVERSITY

TORONTO, ONTARIO

August 2024

Abstract

This thesis explores the role of Panx1a in modulating pain and neuroinflammatory responses in zebrafish (Danio rerio). Nociception was induced using acetic acid (AA) treatments. Behavioral assays conducted on Panx1a knockout (KO) zebrafish larvae demonstrate significant alterations in response to acetic acid (AA)-induced pain. Pharmacological interventions using probenecid, a Panx1 inhibitor, and ibuprofen, a cyclooxygenase (COX) inhibitor, reveal their potential in modulating pain behaviors and rescuing nociceptive deficits. Furthermore, molecular analyses employing quantitative polymerase chain reaction (qPCR) and RNA sequencing (RNA-seq) elucidate the regulatory impact of Panx1a on gene expression related to nociception, neuroinflammation, and synaptic plasticity. In summary, this thesis provides evidence of Panx1a's involvement in pain and neuroinflammation, proposing zebrafish as a viable model for studying nociception.

Acknowledgements

I would like to express my gratitude to my supervisor, Dr. Zoidl, for his exceptional guidance, support, and encouragement throughout my research journey. Thank you for providing me with the opportunity to grow as a scientist.

I am especially grateful to Christiane Zoidl for her support, mentorship, and patience. Thank you for your invaluable assistance in the lab and for always being available to answer my questions and provide guidance.

I would also like to extend my appreciation to all the members of the Zoidl lab. Your camaraderie, collaboration, and support have made my time in the lab both productive and enjoyable. I am thankful for the stimulating discussions, the collaborative efforts, and the friendships that have developed throughout this journey.

A special thanks to the vivarium staff, and the Zoidl lab members at for their work in maintaining the zebrafish and ensuring the smooth conduct of my experiments.

I would like to thank my committee member, Dr. Kwong, for his valuable feedback, guidance, and support. Your constructive criticism and suggestions have contributed to the improvement and completion of this thesis.

Thank you all for making this journey a remarkable and rewarding experience.

Contents

Nomenclature

Humans and non-human primates:

- Full name: Pannexin1
- Gene symbol: *PANX1*
- Protein symbol: PANX1

Mice and rats:

- Full name: Pannexin1
- Gene symbol: *Panx1*
- Protein symbol: PANX1

Zebrafish

- Full name: Pannexin1a
- Gene symbol: *panx1a*
- Protein symbol: Panx1a

List of abbreviations

Panx1 - Pannexin1
KO - Knockout
CFA - Complete Freund's Adjuvant
PAMPs - Pathogen-associated molecular patterns
DAMP - Damage-associated molecular pattern
ATP - Adenosine triphosphate
TRP - Transient receptor potential
NSAID - Nonsteroidal anti-inflammatory drug
COX - Cyclooxygenase
IL-1B - Interleukin-1 beta
IL-6 - Interleukin-6
IL-4 - Interleukin-4
IL-10 - Interleukin-10
CSF-1 - Colony stimulating factor 1
CSF1R - Colony stimulating factor 1 receptor
P2RX4 - P2X purinergic receptor 4
P2RX7 - P2X purinergic receptor 7
P2RY12 – P2Y purinergic receptor 12
PFA - Paraformaldehyde
PBS - Phosphate-buffered saline
BME - Beta-mercaptoethanol
ETBR - Ethidium bromide
DAPI - 4',6-diamidino-2-phenylindole
dpf - Days post-fertilization
ACC - Animal Care Committee
TL - Tupel longfin
RNA - Ribonucleic acid
cDNA - Complementary DNA
qPCR – Quantitative Reverse transcription polymerase chain reaction
OD - Optical density
RT-PCR - Reverse transcription polymerase chain reaction
PGE2 - Prostaglandin E2
PGI2 - Prostaglandin I2
NMDA - N-methyl-D-aspartate
CNS - Central nervous system
NGF - Nerve growth factor
TNF-α - Tumor necrosis factor-alpha

List of Figures

1.0 Introduction

1.1 History of Pannexins

Pannexin channels were first discovered due to their similarities to the invertebrate gap junction proteins, the innexins (Panchin et al., 2000). Pannexins share 25-33% homology in protein structure with innexins. Innexins are gap junction proteins that facilitate communication between adjacent cells. These hemichannels form connecting systems (gap junctions) with the innexins of neighboring cells to promote the diffusion of molecules that aid in intercellular communication. The gap junction proteins in vertebrates are called connexins; these proteins share no sequence homology to pannexins or innexins, despite having a similar function. Another contrasting point about pannexins is that these proteins don't form gap junctions due to extensive glycosylation, preventing the docking of channels in adjacent cells (Figure 1) (Boassa et al., 2007). Instead, pannexins function as integral membrane channels that allow for the passage of ions, ATP, and small metabolites (Scemes et al., 2007, 2009).

There are three isoforms of pannexins named PANX1, PANX2, and PANX3. PANX1 is the most widely expressed of the three. Pannexins, innexins, and connexins share a few similar structural similarities. The proteins all have 4 transmembrane domains, 2 extracellular loops, and intracellular N- and C-terminal domains (Ambrosi et al., 2010).

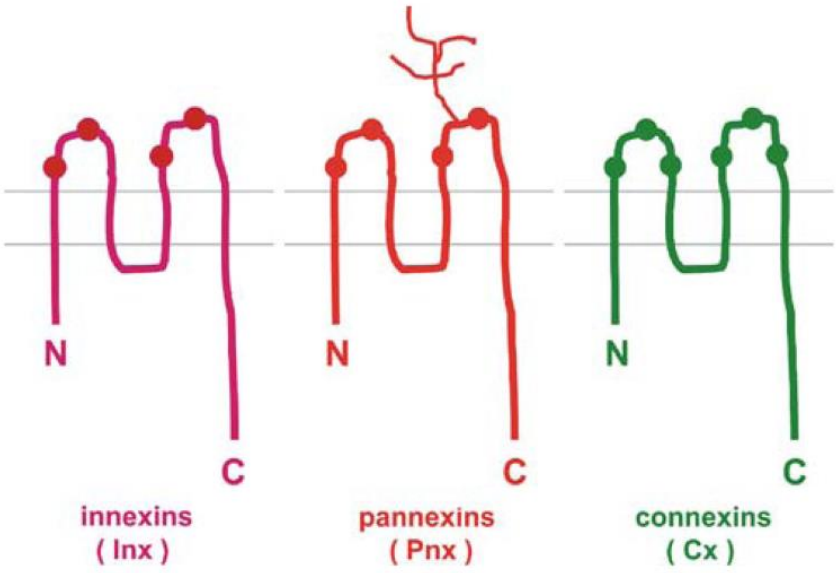

Figure 1: Innexin, pannexin and connexin membrane topography. Pannexin membrane topography is unique as it has a glycosylated protein protruding to the extracellular domain. (Scemes et al., 2009)

1.2 Pannexin1 localization

In the nervous system, immunogold EM methods have revealed pannexin1 (PANX1) to be localized at the post-synapse (Zoidl., 2007). Other studies have shown the presence in neuronal synaptosomes suggesting it has a role in modulating synaptic function. Functional studies in mouse models implicate PANX1 function in regulating NMDAR-dependent plasticity of glutamatergic synapses (Gajardo et al., 2018).

In addition to neuronal expression, PANX1 is expressed in glial cells such as microglia and astrocytes (Burma et al., 2017; Hanstein et al., 2016; Karavis et al., 2023). Microglia play a role in maintaining homeostasis of the Central nervous system (CNS). A topic that is not well understood is what role PANX1 has in the function of microglia. There is evidence that suggests that PANX1-mediated ATP release can modulate the neuroinflammatory function of microglia (Illes et al., 2020; Koizumi et al.,

2013). The mediation of microglial activation via PANX1 is a topic that will be explored in this thesis.

PANX1 function is conserved across species, this allows for the use of animal models to gain valuable insight into the function of PANX1 (Bond et al., 2012a; Penuela et al., 2013). In this project, pannexin channels will be studied in the zebrafish model. In zebrafish, there are two ohnologues of PANX1 named Panx1a and Panx1b, that are primarily expressed in the CNS (Figure 2) (Bond et al., 2012b; Safarian et al., 2020; Whyte-Fagundes et al., 2022). Panx1a and Panx1b expression is ubiquitous and expressed in neurons (Safarian et al., 2021). Past studies have shown evidence of the expression of Panx1a and Panx1b in the retina, KO models have shown a visuomotor deficiency suggesting that it plays a role in the visuomotor response (Safarian et al., 2020, 2021). Panx1a and Panx1b exhibit differences in conductance, opening and activation threshold (Kurtenbach et al., 2013) (Table 1). This project will explore Panx1 and its relation to nociception and neuroinflammation.

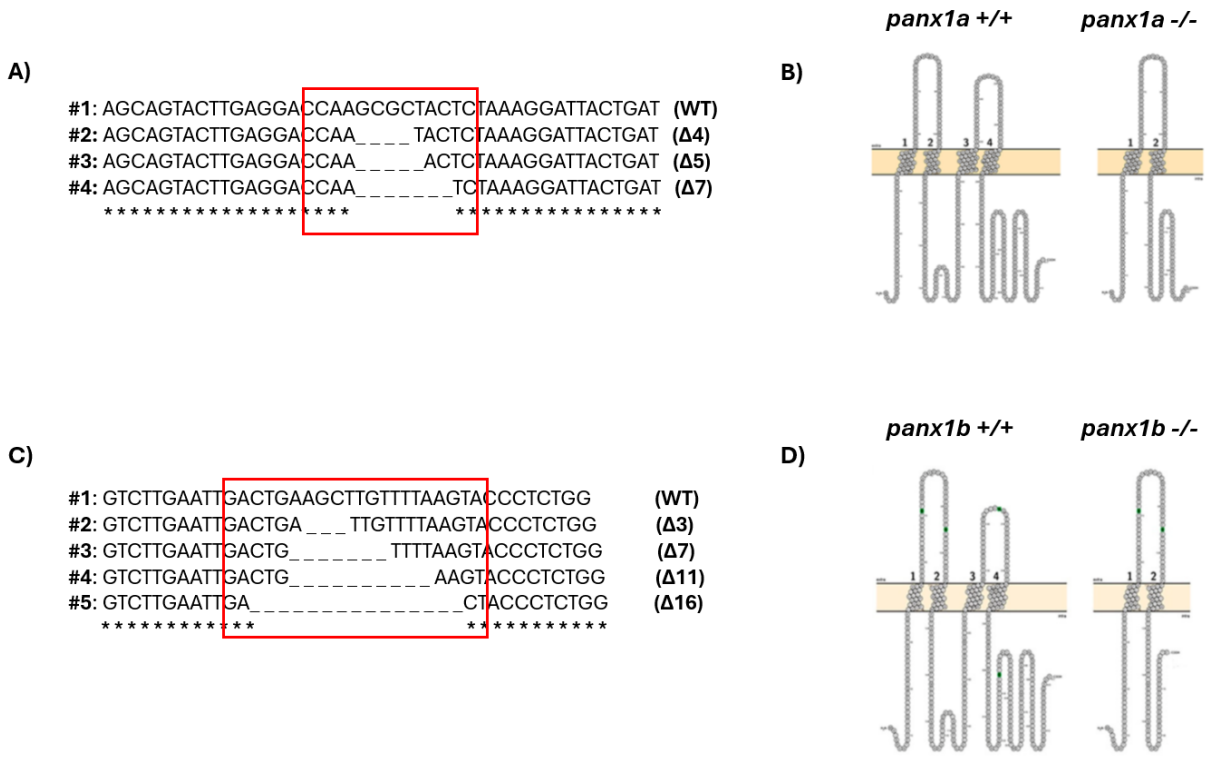

Figure 2: Sequence alignment and predicted topology a) *panx1a* and c) *panx1b* sequence alignment demonstrating small frameshift mutations and predicted topology of mutated b) *panx1a* and d) *panx1b* using potter open-source tool (https://wlab.ethz.ch-/protter). b) A 4 BP deletion to cause a frameshift mutation results in a premature stop codon at amino acid 195. d) A 11 BP deletion to cause a frameshift mutation results in a premature stop codon at amino acid 179 (Safarian et al., 2020, 2021).

Table 1: Shared and distinct properties of Zebrafish *panx1a* and *panx1b*; ohnolouges of mammalian *Panx1* (Kurtenbach et al., 2013; Safarian et al., 2020, 2021; Whyte-Fagundes et al., 2022).

Panx1a	Panx1b
417aa	422aa
ubiquitous	ubiquitous
neurons	neurons/astrocytes
Glycosylated at N246	Glycosylated at N246

Ca2+ and pH - sensitive (half max at pH 6.86)	Ca2+ and pH - sensitive (half max at pH 6.96)
ATP permeable	ATP permeable
Fully open conductance - ≈340 pS	Fully open conductance - ≈500 pS
Open time ≈ 1.4 sec	Open time ≈2.9 sec
Activation threshold ≈ -45 mV	Activation threshold ≈ -60 mV

1.3 Pannexin1 function

PANX1 allows for the passage of molecules smaller than 1000 Da, studies have shown PANX1 mediated diffusion of dyes, Cl^- and ATP (Michalski et al., 2020). PANX1 mediates ATP release in response to pathogens, environmental stressors, and damage (S. Li et al., 2014; Baxter et al., 2014; Muñoz et al., 2021). Neuroinflammatory animal models follow a theme of ATP-mediated signaling, and PANX1 seems to be implicated in the early stages of neuroinflammatory responses (Xing et al., 2024).

PANX1 activation seems to be correlated with increased extracellular ATP levels (Dahl., 2015). In PANX1 KO mice, ATP release was significantly attenuated (Qiu et al., 2011). This study found that ATP release was reduced in PANX1 KO mouse erythrocytes compared to wild-type erythrocytes. Therefore, it seems that PANX1 is functionally capable of mediating the release of ATP.

PANX1 is believed to have a role in nociceptive signaling, in neuropathic mice models, studies have shown that PANX1 KO mice exhibit higher thresholds for pain. Complete Freund Adjuvant (CFA) treatments are injections that elicit an inflammatory response (Hanstein et al., 2016). Researchers showed that following CFA treatments

control mice developed allodynia, which is defined as an increased response to harmless stimuli, suggesting that CFA treatments caused changes to sensory ganglia activity resulting in increased sensitivity. Notably, this effect was ameliorated in PANX1 KO mice. This suggests that PANX1 may be critical in nociceptive signaling.

Recent studies on Japanese flounder (*Paralickthys olivaceus*) provide evidence for the role of PANX1 channels in mediating ATP release during immune responses. In these fish, an immune response was elicited following subjection to pathogen-associated molecular patterns (PAMPs), such as lipopolysaccharide (LPS) and Poly(I) (Li at al., 2014). In this model, the inhibition of PANX1 resulted in reduced ATP release, suggesting the importance of PANX1 in mediating the release of ATP, in response to PAMP treatment. This study reported an upregulation of PANX1 in response to the activation of the immune response. Released ATP acts as a damage-associated molecular pattern (DAMP), which can bind to purinergic receptors and recruit immune cells to the site of damage (Koizumi et al., 2013). These factors are requirements for initiating and regulating inflammation.

Studies provide evidence implicating ATP release via PANX1 channels in various physiological and pathological conditions. This interaction has been studied in the context of the neuroinflammatory/cell death response. Studies have shown PANX1 activation in astrocytes, in response to high extracellular potassium concentrations, leading to cell death. This effect was rescued via pharmacological blockade or genetic KO of PANX1 (W. R. Silverman et al., 2009). This suggests that PANX1 is mediating these neuroinflammatory mechanisms.

Thus, the evidence strongly supports the role of PANX1 in mediating ATP release and contributing to neuroinflammatory signaling, immune response, and nociceptive signaling.

1.4 Nociceptive signaling in mammals

1.4.1 The importance of pain research

Opioids relieve pain by binding to specific opioid receptors (mu, delta, and kappa) in the brain, spinal cord, and peripheral nerves**.** Opioid receptors belong to a family of G-protein-coupled receptors (GPCRs). When a classical opioid agonist binds to its receptor, it results in the inhibition of adenylyl cyclase, which reduces intracellular cAMP levels (Williams., 2010). This leads to increased potassium conductance out of the cell, causing hyperpolarization of the neurons and decreased calcium conductance (Allouche et al., 2014)**.** These events reduce the neuronal firing rate and neurotransmitter release in nociceptive signalling. Opioids and other sedative drugs are problematic because patients who are prescribed these drugs can get addicted to them.

When opioids such as heroin or oxycodone are taken, they attach to mu opioid receptors on brain cells, initiating biochemical processes that result in intense pleasure. This pleasure is mediated by the mesolimbic reward system, where the release of dopamine from the ventral tegmental area (VTA) stimulates the nucleus accumbens (NAc). Over time, repeated use of opioids leads to the development of tolerance, where the brain cells become less responsive to the drugs, requiring higher doses to achieve the same effect. Without the drug, withdrawal symptoms occur, driven by overactive neurons in the locus ceruleus (LC) that produce noradrenaline. Furthermore, opioid

addiction is associated with cognitive deficits, particularly in the prefrontal cortex (PFC), which impair executive function, contributing to compulsive drug use (Kosten & George, 2002).

Opioids create the illusion of euphoria; people often turn to these drugs due to chronic pain issues and can get addicted to them. Individuals abusing opioids use them recreationally, and this can create societal problems if left unchecked (Vadivelu et al., 2018). These issues are directly correlated with the number of opioids being mass-produced today. The development of alternative drug treatments that are less addictive could alleviate the number of people who are being prescribed opioids for pain, in turn minimizing the development of addiction to pain medications. To develop new drugs for pain, it is critical to understand the human nociceptive system and the underlying mechanisms of pain.

1.4.2 How is pain processed?

We classify pain into two categories, acute and chronic. Acute pain is the sharp instant pain that occurs in response to noxious stimuli, it persists as long as the injury exists and goes away with healing. In contrast, chronic pain is gradual and worsens over time due to lifestyle, for example, work-related injuries (Woolf., 2010).

Pain perception begins at the site of trauma, primary afferent nociceptors and the specialized nerve endings will respond to this trauma and generate a neuronal impulse. This signal travels along the axons to the spinal cord. After reaching the spinal cord, the impulses are transmitted to second-order neurons. These neurons relay the pain signal to brain regions: brain stem, thalamus, somatosensory cortex, and limbic system

(Figure 3); these brain structures are implicated in the perception of pain (Bourne et al., 2014).

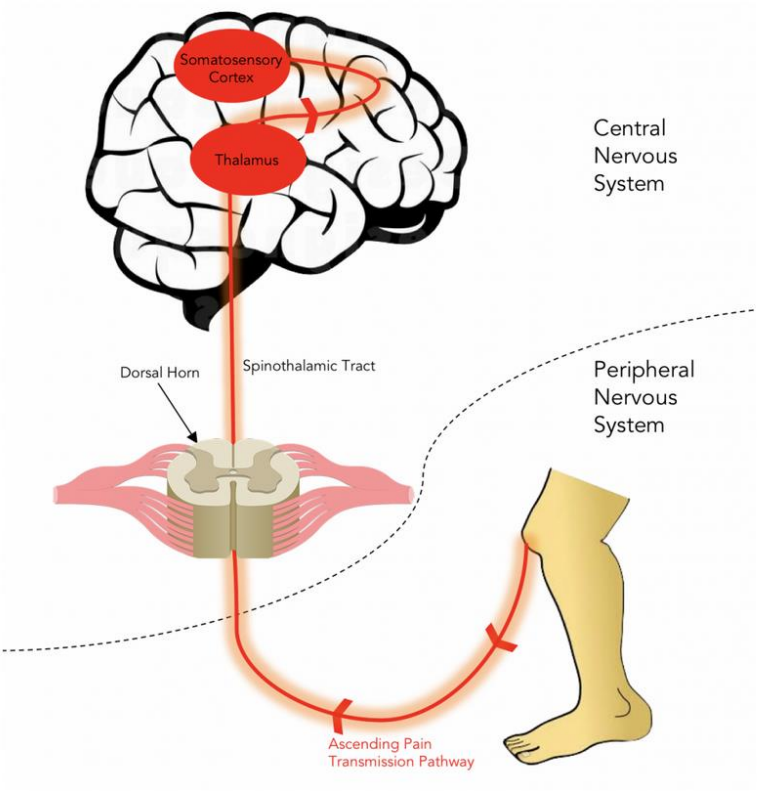

Figure 3: Pathway of nociceptive signaling. This signal travels along the axons to the spinal cord. After reaching the spinal cord, the impulses are transmitted to second-order neurons. These neurons relay the pain signal to brain regions: brain stem, thalamus, somatosensory cortex, and limbic system. (https://sites.tufts.edu/opioidpeptides/-pathways-and-receptors/classical-opioid-signaling/)

The development of chronic pain starts after an insult/injury, leading to the activation of primary sensory neurons. Prolonged activation leads to hyperexcitability of sensory neurons, this phenomenon is referred to as peripheral sensitization (Campbell & Meyer, 2006; Xing et al., 2024). Hyperexcitability of peripheral sensory neurons excites ascending pathways of the spinal cord, resulting in central sensitization. Central

sensitization is a pathological neuroplasticity, that occurs after a lesion to nociceptive neurons; characterized by molecular, cellular, synaptic, and connectivity adaptations of nociceptive neural networks. Consequently, we observe increased spinal neuron signaling in response to stimuli (Bravo et al., 2022).

This increased sensitivity can result in frequent firing of action potentials and increased release of neurotransmitters (glutamate, glycine, GABA) in the dorsal horn of the spinal cord; and are believed to modulate dorsal root ganglion activity (Campbell & Meyer, 2006). Activation of neurons involves the N-methyl-D-aspartate (NMDA) receptors, these receptors bind glutamate, triggering an influx of calcium. This results in the activation of downstream signaling that changes features of the neurons such as plasticity and morphology (Gilron et al., 2015; Weilinger et al., 2016). Changes in plasticity enhance the activation of nociceptive neurons, which is believed to enhance pain perception (Campbell & Meyer, 2006).

Neuropathic mice models attempt to model chronic pain by causing lesions to nerves to elicit changes to peripheral and central nervous systems (Chapman et al., n.d.; Harris, 1998), in this model, we observe behavioral phenomena such as an amplified response to noxious stimuli (hyperalgesia) and/or to normally innocuous stimuli (allodynia) (Hanstein et al., 2016). Neuropathic pain models in mice have provided some insight to the signaling mechanisms associated with nociception (Hanstein et al., 2016; Spray & Hanani, 2019; Xing et al., 2024). Recent studies have been providing evidence of PANX1’s role in nociceptive signaling.

1.5 Pannexin1 and pain

The PANX1 gene is an ATP-release channel that has been implicated in nociceptive signaling (Gusso et al., 2022; Hanstein et al., 2016; Xing et al., 2024). Mouse models of neuropathic pain have explored this topic and evidence supports that upregulation and increased activation of PANX1 contribute to mechanisms of peripheral and central sensitization (Spray & Hanani, 2019). This sensitization is characterized by molecular, cellular, synaptic and connectivity adaptations of nociceptive neural networks. Consequently, we observe increased spinal neuronal signaling in response to stimuli (Bravo et al., 2022).

Due to these changes, we can observe interesting behavioral phenomena that indicate a neuropathic pain response (Bravo et al., 2022). For example, a withdrawal response, evoked by a stimulus that normally does not evoke pain is called allodynia, or an increased response to harmful stimuli is referred to as hyperalgesia

(Costigan et al., 2009). Mouse pain models are treated with a lesion to neurons, resulting in these symptoms of neuropathic pain. Using this model of neuropathic pain, the following studies have given us insight into the function of PANX1 in nociceptive signaling (Spray & Hanani, 2019).

1.5.1 PANX1 mediates activity of sensory ganglia

Research by Zhang et al (2020) showed an upregulation of PANX1 in the dorsal root ganglion (DRG), significantly contributing to the development of neuropathic pain. In this study, neuropathic pain was induced following nerve ligation. Researchers conducted behavioral assays on the mice and defined a withdrawal response to mechanical stimuli as an indication of pain; this behavior suggested that nerve damage

resulted in allodynia and hyperalgesia. They concluded that blockade of PANX1 channels using siRNA and carbenoxolone, significantly rescued the effects of allodynia and hyperalgesia.

Similar findings have been reported in the complete Freund's adjuvant (CFA) orofacial pain model of mice. Following nerve injury, researchers showed an increase in PANX1 in the trigeminal ganglia (Hanstein et al., 2016). Allodynia was characterized following orofacial pain treatment; this effect was ameliorated in the PANX1 KO mice. These studies provide evidence of PANX1's critical role in nociceptive signaling.

1.5.2 PANX1 mediates purinergic signaling

Extracellular ATP has been identified as a nociceptive signal and evidence points to PANX1 as the mediator (Muñoz et al., 2021). The purinergic (P2X/P2Y) receptor family is a class of ATP-gated ion channels, that mediate many developmental processes of neurons (neurogenesis, neuron migration, neuron cell death). It has also been implicated in changes in plasticity and regulating neuroinflammation in response to harmful conditions (Burnstock, 2013). This project will explore purinergic function in nociceptive signaling.

Evidence suggests ATP will bind P2X/P2Y receptors to mediate nociceptive signaling in response to harmful treatments; for example, the P2RX7 channel is implicated in numerous mouse pain models (Adinolfi et al., 2018; Honore et al., 2006; Inoue & Tsuda, 2021; Miteva et al., 2020). The study conducted by Honore et al (2006) looked at pharmacological blockade of P2RX7 in multiple models of pain. One model of

pain-induced allodynia and hyperalgesia following nerve ligation; this effect was ameliorated following pharmacological blockade of P2RX7.

Another study conducted in mice suggested that P2RX7 is critical for nociceptive signaling, and they concluded that blocking PANX1 negatively affected P2RX7-mediated nociceptive signaling. In this study, they tested the effects of P2RX7 agonists on c-reflexive behavior in neuropathic mice. Neuropathic pain was induced via an incision of the sural nerve. The researchers demonstrated that the activation of P2RX7 generated increases in nociceptive behavior that were ameliorated due to the pharmacological blockade of PANX1. Therefore, researchers concluded that P2RX7 requires activation of PANX1 to maintain its pronociceptive signaling in conditions of chronic pain (Bravo et al., 2022). This suggests that P2RX7 is mediating nociceptive signaling and there is evidence that PANX1 activity can modulate P2RX7 function and consequently modulate nociceptive signaling.

In summary, robust evidence supports the involvement of PANX1 channels in pain mechanisms, making them a promising target for novel pain therapies to mitigate pain symptoms.

1.6 Nociceptive signaling in fish

The zebrafish are advantageous to study nociception due to factors such as low maintenance cost, high fecundity, and 70% conservation of proteins and genes with mammals. Pain and nociception are well conserved, as they are critical for an organism's survival. Studying pain in zebrafish offers us new possibilities for drug discovery. This project will attempt to unveil PANX1’s role in nociceptive signaling.

1.6.1 Do fish feel pain?

A topic of contention in the science community is whether fish can feel pain at all. This thesis will argue that fish can feel pain although some topics need to be considered. Firstly, although there are many neuroanatomical similarities between fish and mammals, we have to note, that there are differences. For one, fish lack some neuroanatomical structures found in humans and are implicated in pain perception, such as the neocortex (Rose et al.,2014). To address this, this argument doesn't prove that fish do not experience pain, instead, there could be differences in anatomical structures that may/may not affect nociceptive signaling.

Secondly, researchers have made the argument that behavioral responses observed in fish, when subjected to harmful treatment, could be attributed to an unconscious nociceptive reflex, rather than a conscious pain perception. This argument does not prove that fish don't feel pain. Instead, numerous studies provide evidence that fish may feel pain, and this will be addressed in the following sections.

Fish nociceptors

The physiological evidence that fish can feel pain is based on the presence of nociceptors in the fish (Sneddon, 2002, 2003, 2015) and specialized nerve cells that respond to harmful stimuli. Research by Sneddon has shown that fish possess nociceptors on the head and other regions of their body, that can detect mechanical pressure, extreme temperature, and chemical irritation. Studies have shown the presence of these sensory neurons in the viscera and deeper tissues of fish, indicating a widespread distribution that allows for the detection of harmful stimuli throughout the

body. These nociceptors lay on the nerve endings of nerve fibers: A-delta and C fibers. A-delta fibers are myelinated and transmit sharp and immediate pain sensations. In contrast, C fibers, which are smaller and unmyelinated, are associated with dull, aching pain. In fish, A-fibers make up about 25% of nociceptive fibers, whereas C fibers account for 4%(Sneddon, 2019).

This distribution differs in mammals, where C fibers can constitute up to 50% of all nerve fibers. Despite these differences, the existence of these fibers suggests fish are able to process nociceptive signals. The A-delta and C fibers in fish function much like they do in humans supporting the premise of this project, that fish are capable of experiencing pain and therefore are valuable to the study of pain mechanisms (Sneddon, 2002, 2003, 2015).

Neuroanatomical conservation

In addition to the parallels seen regarding nerve fibers, fish have a conserved neuroanatomical organization that includes sensory ganglia homologous to trigeminal ganglia and dorsal root ganglia found in humans. This organization allows for the transduction and transmission of sensory information from the peripheral nervous system to the central nervous system, suggesting that fish have the hardware to feel and perceive pain (Malafoglia et al., 2013). Painful stimuli (mechanical, physical, or chemical) are captured by nerve endings containing specialized structures to detect and transmit to the spinal cord and then the thalamus. In fish nociceptive processing takes place in the forebrain: epithalamus, thalamus, and hypothalamus (Weber, 2011).

Electrophysiological evidence

The evidence is very limited due to a small number of studies that have used electrophysiology to study pain. It has been shown that the nervous system of fish is capable of processing pain signals through out the CNS. For example, trout have exhibited an electrophysiological response in trigeminal ganglia in response to noxious stimuli (Sneddon et al.,2002). This evidence suggests that the CNS of fish can process harmful stimuli at the level of neuronal networks.

Behavioral evidence

Behavioral studies provide evidence that fish can feel pain. For example, in response to acetic acid injected into the lips of the trout, the fish exhibited changes in feeding behavior. This study showed that this injection resulted in delayed resumption of feeding compared to control groups and they displayed pain-related behaviors, such as rubbing the affected area (Sneddon., 2003). These behaviors were ameliorated when trout were treated with morphine, this suggests that the treatment of analgesics, that inhibit nociceptive signalling, are alleviating symptoms of pain. This study suggests that trout are experiencing discomfort, consequently delaying feeding behavior.

Molecular evidence

At the molecular level, fish have receptors and ion channels similar to those implicated in human pain perception. This includes members of the TRP family and the purinergic receptor family (Babchenko et al., 2022; Bautista et al., 2013; Julius, 2013; Medrano et al., 2017). These channels have been implicated in past pain studies and

neuroinflammation studies in zebrafish. These receptors and channels are critical for the detection and transduction of noxious stimuli. These parallels between mammals and fish suggest that zebrafish have the necessary hardware for pain detection.

In conclusion, based on the evidence supporting that fish have all the necessary hardware for nociception, we can proceed on the premise that fish are processing harmful stimuli. This mechanism of nociception is highly conserved across species and is vital for survival. Therefore, zebrafish are an ideal model for studying nociception.

1.7 The acetic acid pain model in zebrafish

Gusso et al (2020) looked at using acetic acid (AA) to induce a pain response. This model is effective in mimicking nociceptive pain. In zebrafish, AA exposure leads to quantifiable behavioral changes such as decreased locomotion and altered movement patterns. The behavioral parameters that were tested include the distance covered, acceleration, movement duration, and latency to the first entry into the center of a test arena.

In response to acetic acid treatments, we observe changes in zebrafish locomotion. Larvae exhibited a decrease in the distance covered, reduced movement, and altered accelerated patterns. These changes show that the larvae are responding to the harmful treatment, and this suggests that the larvae are experiencing pain. Again, this evidence is not conclusive, the zebrafish larvae may not be experiencing pain. It is well documented that zebrafish will take significant damage to epithelia to acetic acid treatments, and therefore the only thing we can conclude in this model is that zebrafish locomotion is altered in response to harmful treatments (Gusso et al., 2022).

Researchers looked at the pharmacological blockade of pannexin using probenecid in this AA pain model. This drug treatment ameliorated the behavioral changes induced by acetic acid. This suggests that pannexin mediates the behavioral changes caused by acetic acid treatments. This study by Gusso (2020) highlights the potential of blocking pannexin to treat pain and discomfort.

The behavioral assays conducted in this project look at different parameters, which assess the activity of the larvae in response to AA treatments. The specific parameters assess the duration of freeze activity (FDA), which is the fraction of the behavioral assessment time, the larvae exhibited little to no activity. Also, we look at the duration of burst activity (BDA), which is the fraction of the behavioral assessment time, the larvae exhibited a velocity greater than 15mm/s. We aim to build on these results in this AA model by assessing behavior in the PANX1 KO genotype, pharmacological blockade of PANX1, and anti-inflammatory drug treatments. This study aims to unveil mechanisms by which PANX1 is mediating nociceptive signaling.

1.8 Pharmacological block of PANX1 via probenecid

Past studies of PANX1 have looked at the effects of the pharmacological block of this protein. The difference between a pharmacological block vs a genotype KO needs to be stressed. Deficiencies in nociceptive signaling may be attributed to differences in neurodevelopment in the PANX1 KO mice (Hanstein et al., 2016). Therefore, we need to look at the pharmacological blockade of PANX1 to see if we observe the same nociceptive deficiency. This will show that nociceptive deficiencies are a product of PANX1 inhibition rather than developmental differences in the PANX1 KO.

Probenecid is a drug commonly used to treat gout by promoting uric acid secretion (W. Silverman et al., 2008). Although the mechanism of PANX1 inhibition via probenecid is not yet fully understood, it is believed to involve the first extracellular loop (ECL1) of PANX1. This region plays a role in the gating mechanism of PANX1 (Hainz et al., 2016).

Early studies showed probenecid inhibited PANX1 activity in frog oocytes injected with PANX1 mouse RNA (Ransford et al., 2009). In addition to this finding, researchers tested the effects of probenecid in hypotonic stress-induced ATP release assays. Cell cultures subjected to hypotonic stress exhibited increased ATP release, this effect was ameliorated with the blockade of PANX1 using probenecid. This evidence suggests that probenecid is blocking the passage of ATP through PANX1 channels.

The rationale behind using probenecid is its demonstrated ability to inhibit ATP release via PANX1 channels (Fejes-Szabó et al., 2015; Hainz et al., 2016). Functional neuropathic mice models have shown increases in extracellular ATP following nerve damage (Hanstein et al., 2016). We predict that ATP binds to downstream elements modulating the excitation of sensory neurons. By blocking PANX1, we aim to observe how inhibition of PANX1-mediated ATP release modulates behavior. Previous studies have shown that probenecid treatments rescued the behavioral changes to AA treatments (Gusso et al., 2022). Therefore, we hypothesize that the pharmacological blockade of pannexins will modulate the nociceptive response to AA treatments.

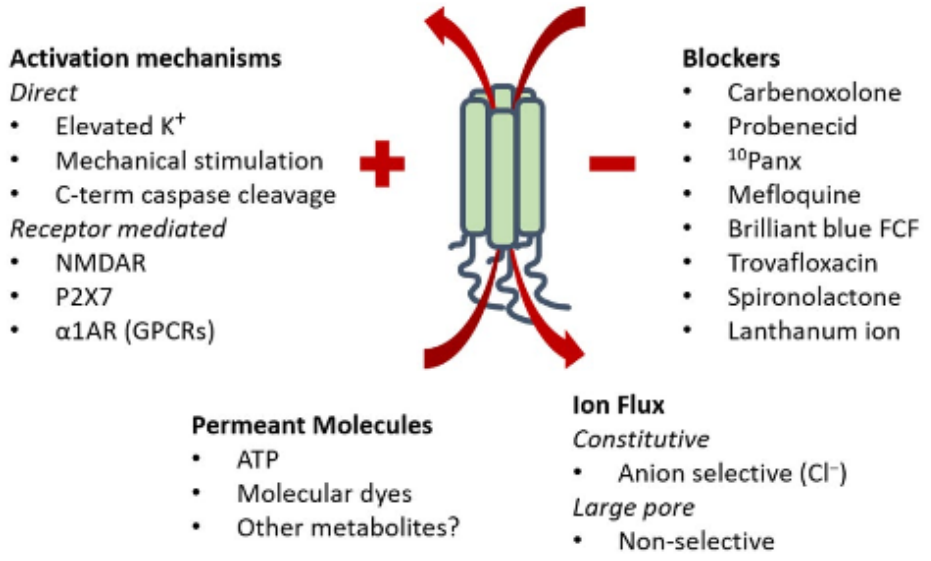

Figure 4. Pannexin1 function and channel properties. PANX1 subunits form a pore in the plasma membrane. Activated PANX1 channels mediate the release of ATP. PANX1 activation is mediated indirectly via NMDA, GPCRs, and P2RX7. Inhibition of PANX1 noted with carbenoxolone, probenecid, 10pans, mefloquine, brilliant blue FCF, trovafloxin, spironolactone and lanthanum ion. (Yeung et al., 2020)

1.9 Ibuprofen and mechanism of action

Ibuprofen is classified as a nonsteroidal anti-inflammatory drug (NSAID) and works by inhibiting cyclooxygenase (COX) enzymes. Ibuprofen specifically inhibits COX-1 and COX2, which are responsible for converting arachidonic acid into prostaglandins (Figure 5). Prostaglandins are mediators of pain, inflammation, and fever. COX-1 typically produces prostaglandins that protect blood vessels and the lining of the digestive tract. In contrast, COX-2 regulates prostaglandin formation that mediates pain, inflammation, and fever (Mazaleuskaya et al., 2015).

The specific prostaglandins mediated by COX-2 include prostaglandin E2 (PGE2) and prostaglandin I2 (PGI2). The reduction of the prostaglandins results in decreased inflammation. These factors enhance vascular permeability allowing for

leukocyte infiltration which leads to inflammation, therefore the reduction of PGE2 and PGI2 levels ameliorates this effect (Mazaleuskaya et al., 2015).

In conclusion, ibuprofen's mechanism of action involves the inhibition of COX enzymes, reduction of prostaglandin synthesis, and modulation of immune cell functions collectively contributing to its anti-inflammatory and analgesic effects. We hypothesize that ibuprofen will modulate nociceptive response to AA treatments.

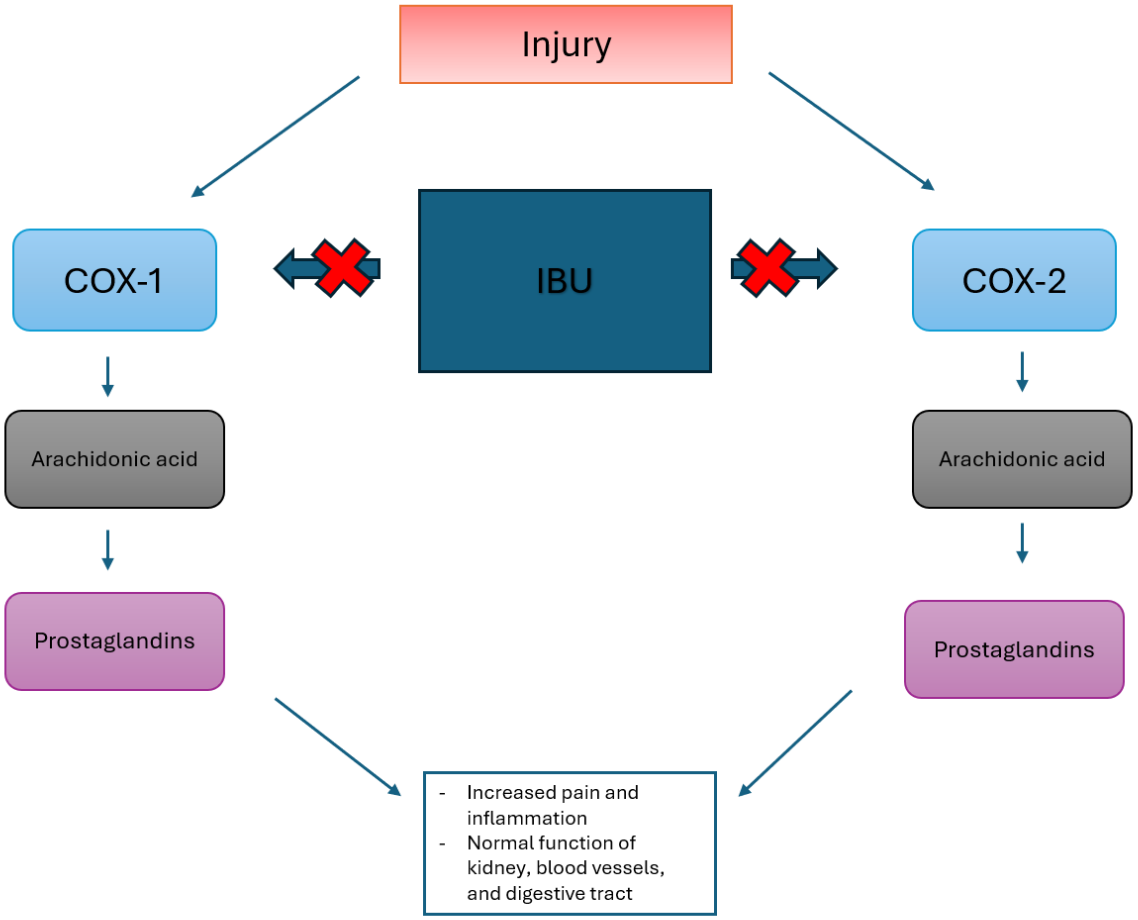

Figure 5: Ibuprofen mechanism of action. Ibuprofen is classified as a nonsteroidal anti-inflammatory drug (NSAID) and works by inhibiting cyclooxygenase (COX) enzymes. Ibuprofen inhibits COX-1 and COX2, which are responsible for converting arachidonic acid into prostaglandins. Prostaglandins are mediators of pain, inflammation

and fever. Therefore, Ibuprofen inhibits inflammatory mechanisms mediated by COX-1 and COX-2. (Health Canada Website)

1.10 The early response gene *c-Fos*

In addition to behavioral assays, this project will attempt to characterize the genes that are implicated in this AA pain model. Using methods such as qPCR and RNA seq we will attempt to identify genes that are regulated in response to AA treatments. Also, we will identify the genes that are regulated by PANX1. This data may reveal molecular mechanisms of nociception and the role of PANX1 in nociceptive signaling. A gene of interest in this study is *c-Fos*, an early response gene that is a biomarker of neuron activity.

1.10.1 Function of c-FOS

C-Fos is an immediate early response gene, playing a critical role in neuron activity and synaptic plasticity (Gallo et al., 2018). The c-FOS protein is induced in response to various stimuli. It is a crucial first step for long-term changes in the brain that underlie learning and memory. It is upregulated in response to environmental stressors in mice models (Harris, 1998). c-FOS upregulation has been identified as a biomarker of neural activity and therefore has been implicated in nociception (Jaworski et al., 2018).

For example, the study by Lin et al (2018) showed that multi-modal stress treatment and electric foot shock treatments resulted in c-FOS activation in the brain. This effect was most prominent at periods from 30-60 mins. This suggests that increased c-FOS expression in neural circuits correlates with stressors in the

environment. This study demonstrates the activation of these pathways during nociceptive events (Lin et al., 2018).

1.10.2 Associative learning and c-FOS

C-FOS has been closely linked to the process of learning and memory. When learning a new task or environment, animals have shown a significant increase in c-FOS expression. c-FOS expression is increased specifically in brain regions associated with memory formation (hippocampus, amygdala). The expression of c-FOS is believed to modulate synaptic changes, which is necessary for encoding and storage of memory (Jaworski et al., 2018).

Studies have also shown that impairing c-FOS activity, can impair learning a fear based memory. In the study by Kwon et al. (2012), researchers investigated the role of c-FOS in fear based memory learning. They found that inhibiting c-FOS expression significantly impaired the mice's ability to learn the association between a tone and a foot shock. In conclusion, c-FOS is a critical gene, in the process of learning fear based memories. Based on this evidence, we suspect that harmful AA treatments can elicit *c-fos* activity.

In the context of this project, c-FOS expression serves as a marker for neuronal activity in response to noxious stimuli (Harris, 1998). In this current study, we will apply methods to study if c-FOS is regulated in response AA treatments. We predict, based on past studies, *c-fos* gene expression will be regulated in response to harmful AA treatments.

1.11 The TRP family of Genes and Pain

The transient receptor potential (TRP) channels are ion channels that have been implicated in the detection of thermal, chemical and mechanical stimuli. They have been identified in zebrafish as chemo-sensitive and acid-sensing ion channels (Prober et al., 2008). In this study researchers showed that frog oocytes expressing TRPA1 showed strong inward currents in response to mustard oil treatments. In addition to mustard oil, this gene has been implicated in the detection of numerous chemical irritants, such as the detection of weak acids and thermal stimuli (Oda et al., 2016; Wang et al., 2011). This channels function could be implicated in our AA model. Therefore, *trpa1a/b* will be further investigated, using qPCR, to uncover underlying mechanisms of pain. We hypothesize that *trpa1a/b* expression is regulated in response to AA treatments.

1.12 Microglia and pain

The microglia are resident macrophages of the CNS, microglia activation has been implicated in response to injury (Tsuda, 2019). Microglia mediate inflammation and maintain homeostasis of the CNS (Karavis et al., 2023). When microglia are in their resting state, they are constantly surveying their environment, assessing the usefulness of neural circuits. Upon activation from stressors in the environment, microglia morphology changes to an ameboid shape (large cell body, short protrusions) which can phagocytose pathogens and release a number of bioactive molecules, such as pro-inflammatory cytokines interleukin-1B (IL-1B) and interleukin-6 (IL-6). This pro-inflammatory state is classified as M1 microglia. In contrast, the alternative M2 microglia

act as anti-inflammatory agents, promoting the release of numerous protective factors (IL-4, IL-13, nerve growth factor (NGF))(Tsuda, 2019).

Functional studies in mice have elucidated the role of microglia in the context of chronic pain. Researchers observed an increase in the number of microglial cells in the spinal cord in response to harmful treatments, a study showed an increase in microglia immunolabeled with Iba1 - a marker for microglia – in the dorsal horn of the spine following peripheral nerve damage (Gilmore, 1970; Tsuda, 2019).

Following nerve ligation colony stimulating factor 1 (CSF-1) is released from the site of nerve damage, the corresponding receptor, CSF1R, is found on the surface of glial cells. This release is believed to act as a chemo attractant for microglia (Karavis et al., 2023). Studies have shown that treatment with an inhibitor of CSF1R (PLX5622), researchers observed significant alleviation of allodynia. Following nerve ligation, neuropathic mice treated with the drug exhibited significant increases in threshold of mechanical stimuli needed to elicit a withdrawal response compared to neuropathic mice. This effect was observed 29 days prior to nerve ligation, suggesting that microglia are mediating central sensitization mechanisms (Lee et al., 2018).

We attempt to elicit microglia activity in zebrafish using AA treatments. Not much is known about microglia activity at early stages of nerve damage, this AA model could possibly give us insight. It is not conclusive whether damage elicited by AA treatments results in nerve damage, though we have documented significant damage to epithelia at higher concentrations. Studying the biomarkers of microglia activity in response to AA treatments may give us insight to the early stages of microglia activation. The following sections go over the gene biomarkers of microglia activity.

1.12.1 Biomarkers of microglia activity

Cytokines

Cytokines are prime biomarkers of pain and inflammation and more specifically microglia activity, as they are regulated in response to harmful treatments. Therefore, we predict these cytokines to be regulated in this AA model.

M1 microglia are associated with pro-inflammatory responses. They secrete a variety of cytokines and chemokines that promote inflammation and are typically involved in the initial response to injury or infection. In this project we study the mRNA levels of pro-inflammatory cytokines: Interleukin-1 beta (IL-1β) and Interleukin-6 (IL-6) (Karavis et al., 2023; Koizumi et al., 2013).

M2 microglia are associated with anti-inflammatory and tissue repair processes. They secrete cytokines and growth factors that promote tissue repair, resolution of inflammation, and restoration of homeostasis. In this project, we study the mRNA levels of anti-inflammatory cytokines: Interleukin-4 (IL-4) and Interleukin-10 (IL-10) (Bottiglione et al., 2020; Karavis et al., 2023).

Previous studies have shown secretion of these cytokines in neuroinflammatory models, more specifically a zebrafish brain lesion model (Gan et al., 2020). The objective was to study whether AA treatments are eliciting an immune response mediated by microglia. We hypothesized that there would be some regulation of pro-inflammatory and anti-inflammatory cytokines in response to AA treatments.

Purinergic receptors

In the CNS, the purinergic receptor system acts as a network for glial and neuron cell communication. Microglia express numerous purinergic receptors that have the potential to be activated by ATP. The literature implicates numerous purinergic receptors in modulating function and morphology of microglia. This following section will cover the function of three main purinergic receptors associated with microglia activity: P2RX7, P2RX4 and P2RY12.

Mice models of neuropathic pain have given us some insight to the role of microglia in nociceptive signalling. The P2RX4 gene has been shown to be upregulated on microglia but not in neurons or astrocytes, following peripheral nerve injury (Tsuda et al., 2003). P2RX4 is a gene that has been associated with neuropathic pain, and studies have shown activation of this receptor was implicated in neuropathic pain symptoms. Studies in mice utilizing the nitroglycerin (NTG) model for chronic migraine, demonstrated increased mechano-sensitivity and upregulation of P2RX4 protein expression. However, treatment with 5-BDBD (P2RX4 antagonist) prevented NTG-induced mechano-sensitivity, indicating a potential therapeutic target (Long et al.,2018). This shows that blocking microglia activity (by targeting inhibition of P2RX4) caused deficiencies in nociceptive signalling.

P2RX7 is another purinergic receptor implicated in the activity of microglia. P2RX7 receptors on microglia have been associated with chronic pain models, and activation of P2RX7 has been shown to drive microglia activation (Bhattacharya & Biber, 2016; Monif et al., 2009; Mousseau et al., 2018). Past studies have shown that P2RX7 activity is critical in nociceptive signalling. The study conducted by Honore et al (2006) looked at pharmacological blockade of P2RX7 in multiple models of pain. One model of

pain induced an increased paw withdrawal response to mechanical stimuli (mechanical allodynia) following nerve ligation; this effect was ameliorated following pharmacological blockade of P2RX7.

Another study showed similar results, after researchers developed a specialized peptide targeting phosphorylation sites of P2RX7 thereby inhibiting activity. Researchers preformed behavioral testing on neuropathic mice and saw recovery of allodynia in response to this peptide treatment, this effect was observed immediately after a 30 min treatment (Dalgarno et al., 2018). This suggests that inhibiting microglia activity (by targeting inhibition of P2RX7) we saw immediate deficits in nociceptive signalling.

P2RY12 activation has shown to change morphology of microglia, to add to this P2RY12 is implicated in the motility function of microglia. In vitro models have shown that P2RY12 KO microglia exhibited amoeboid morphology and deficits in chemotaxis(Haynes et al., 2006). Therefore, it is evident that purinergic signalling can modulate microglia activity. Not a lot is known about microglia activity in nociceptive signalling, the above studies have shown that inhibition of P2X receptors (P2RX4 and P2RX7) found on microglia resulted in deficits in nociceptive signalling, these effects were immediately observed following drug treatments. We hope to elucidate the role of microglia in nociceptive signalling in response to AA treatments.

1.12.2 PANX1 role in modulating microglia function

PANX1 channels are integral membrane proteins that, unlike connexins, do not form gap junctions but function as pores for the passage of ions and small molecules

such as ATP (Michalski et al., 2020). When PANX1 channels are activated, whether it be mechanical stress or environmental stressors, they facilitate the release of ATP into the extracellular space (Baxter et al., 2014; Li et al., 2014). ATP is released at the site of damage and acts as a signaling molecule, it is predicted to bind to the purinergic receptors of the microglia, triggering neuroinflammatory mechanisms (Reoyl Seo et al., 2008; Montilla et al., 2020; Campagno & Mitchell, 2021). This signalling pathway of activation of immune responses by microglia by PANX1 are not well understood in zebrafish. In this current zebrafish acetic acid pain model, PANX1 is predicted to regulate microglia function through ATP release and purinergic signaling (Figure 6).

Purinergic receptors have been associated with a function of microglia. For example, the binding of ATP to P2RX7, on microglia triggers activation, leading to the release of a variety of pro-inflammatory cytokines and chemokines, such as interleukin-1β (IL-1β) and tumor necrosis factor-alpha (TNF-α) (Campagno & Mitchell, 2021). These signaling molecules further propagate the inflammatory response, attracting other immune cells to the site of injury or infection and enhancing the sensitivity of pain pathways. To add to this P2RY12 is a purinergic receptor that plays a role in the motility and migration of microglia (Morillas et al., 2021). Another critical purinergic receptor P2RX4 has been associated with microglia pro-inflammatory function and neuropathic pain (Karavis et al., 2023; Long et al., 2018).

In conclusion, PANX1 is predicted to modulate microglia activity via ATP release and purinergic signaling. By facilitating ATP release in response to various stimuli, PANX1 channels initiate a cascade of events that activate microglia and propagate

inflammatory responses. In this current methodology, we investigate the role of PANX1 in the modulation of microglia activity.

I)

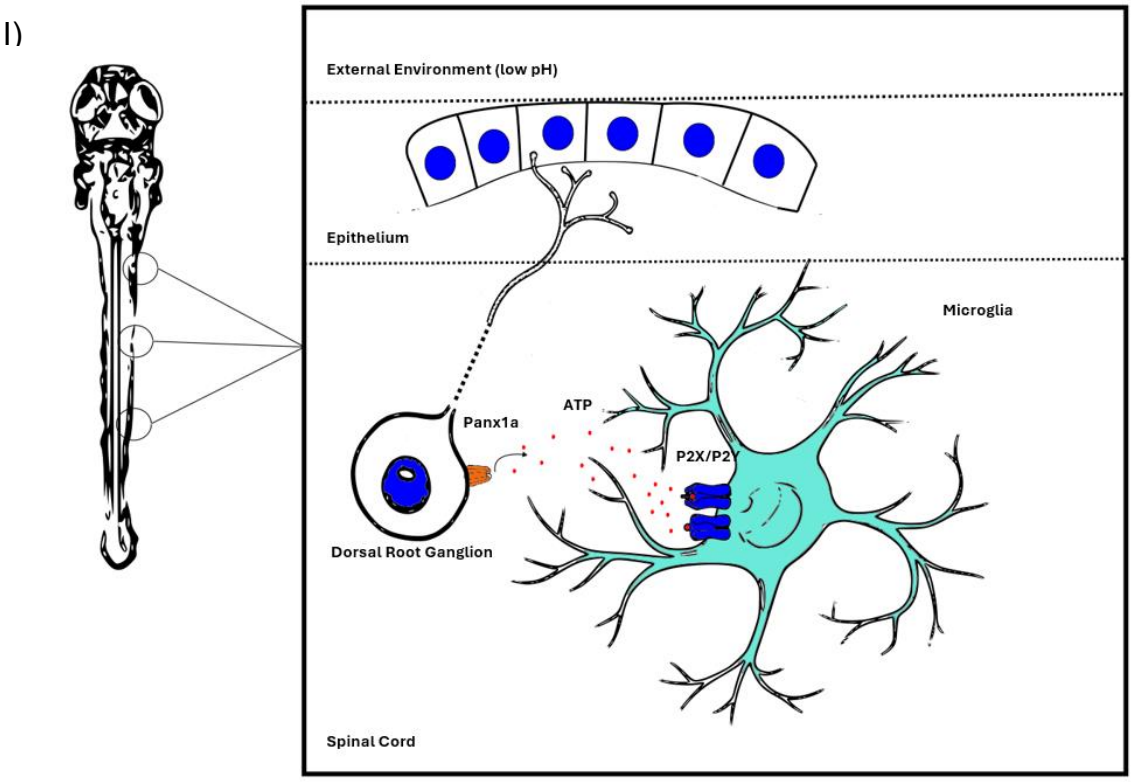

II)

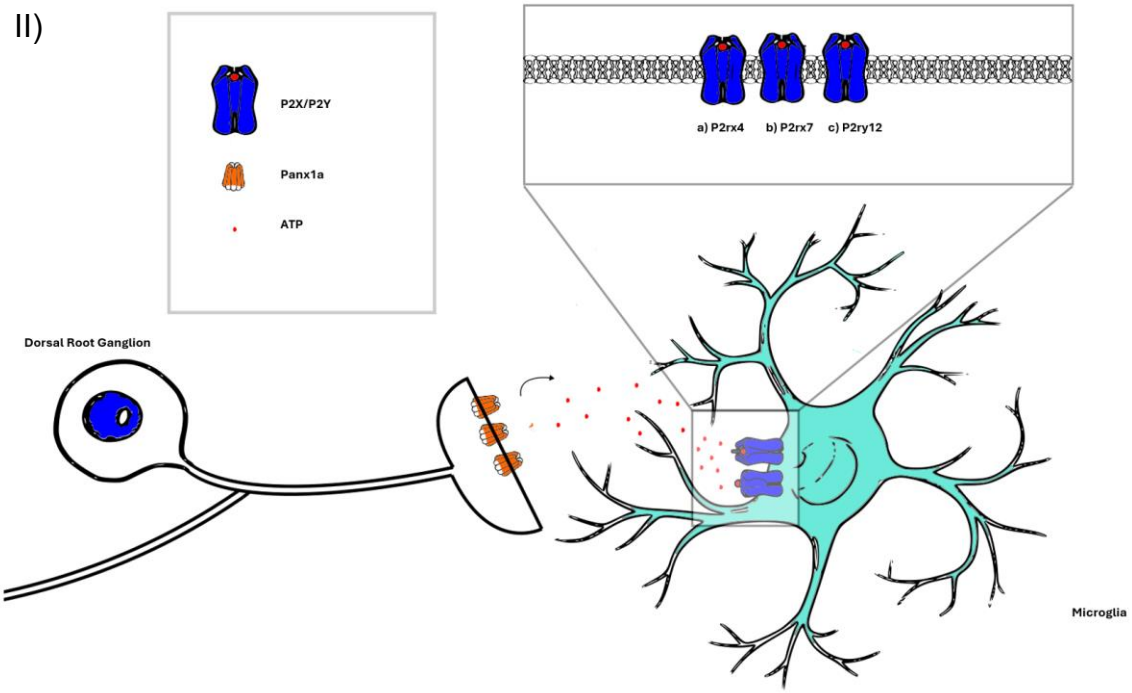

Figure 6: Panx1a modulates microglia activity i) In response to low pH in the environment, the activation of microglia is modulated due to the interaction of Panx1a and P2X/P2Y receptors. The function of the microglia will be specialized to return to homeostatic levels of inflammation in the CNS. **ii)** Panx1a-mediated ATP release modulates the activity of microglia activity. A) P2rx4 is an ATP gated ion channel mediating neuroinflammatory effects of microglia B) P2rx7 are ATP gated ion channels mediating cytokine release and cell death. C) P2ry12 are ATP gated ion channels that mediate motility and migratory function of microglia. Created on Inkscape.

1.13 Hypothesis

The objective of this study is to unveil mechanisms of nociception of zebrafish. Firstly, we want to study the mechanisms of nociception in response to AA treatments, secondly, we want to gain insight into the mechanisms of PANX1 regarding nociception and neuroinflammation. In this current project we treat zebrafish with acetic acid (AA) to trigger nociceptive signaling, we predict that this will lead to nociceptive behavioral effects and activation of neuroinflammatory mechanisms. We hypothesize that we will

see changes in behavior in response to AA treatments in Tupel longfin (TL) zebrafish larvae.

Based on evidence from mice pain models that PANX1 mediates both nociception and neuroinflammation, we hypothesize that the KO and pharmacological blockade of Panx1 will modulate behavioral response to AA treatments. We also hypothesize that ibuprofen - a COX-1 and COX-2 inhibitor - will modulate behavioral response to AA treatments.

We also study the expression of gene markers of memory, pain, and neuroinflammation using qPCR and RNA seq. *C-fos* is a biomarker of nociceptive neuron activity in response to harmful stimuli, we hypothesize that *c-fos* is regulated in response to AA treatments. Purinergic and TRP receptors are mediators of pain and neuroinflammation, we hypothesize that purinergic receptors are regulated in response to AA treatments. Cytokines are proteins released in an immune response; we hypothesize that cytokines are regulated in response to AA treatments.

In this study, we characterize the role of Panx1 in AA-induced nociception and the neuroinflammatory response. We predict that Panx1 plays a role in nociceptive signaling. We hypothesize that Panx1 is modulating mRNA levels of genes associated with nociceptive signaling.

In this study, we characterize the extracellular ATP concentration in response to AA treatments using ATP luminescence assays. We hypothesize that extracellular ATP levels are modulated in response to harmful stimuli, as this was observed in neuropathic mice models (Hanstein et al., 2016).

In conclusion, this study provides evidence that panx1 is mediating behavioral and neuroinflammatory mechanisms in response to AA treatments.

2.0 Materials and Methods

2.1 Animal care

Adult zebrafish were raised in a vivarium at York university following the rules and regulations set by the animal care committee (ACC). The wild type strain known as Tupel long fin (TL), the panx1a KO, and panx1b KO were all used in the following experiments. The KO lines were generated in house via TALEN gene editing method (Safarian et al., 2021). The different genotypes were maintained by the vivarium staff at 28^{o}C. Breeding was handled by Christiane and other Zoidl lab members.

2.2 Maintenance of Zebrafish Larvae

Zebrafish larvae are raised from 0 to 7 days post-fertilization (dpf) in an egg water medium. Cleaning of petri dishes (housing larvae) were performed by Zoidl lab members. When they reach 7 dpf the larvae are discarded in accordance with ACC rules and regulations. Experiments were performed on 6 dpf larvae.

2.3 qPCR

2.3.1 RNA Extraction

RNA extraction was preformed using the RNAeasy plus mini kit (Qiagen). 30 TL or Panx1a KO larvae were collected for each sample. The pain treatment used was the

0.005% acetic acid treatment. The pain treatment was neutralized after 5 mins and the samples were either incubated at 28ºC for the short-term (30 min) or long-term period (115 min) (Figure 7). These samples were then stored in -80ºC.

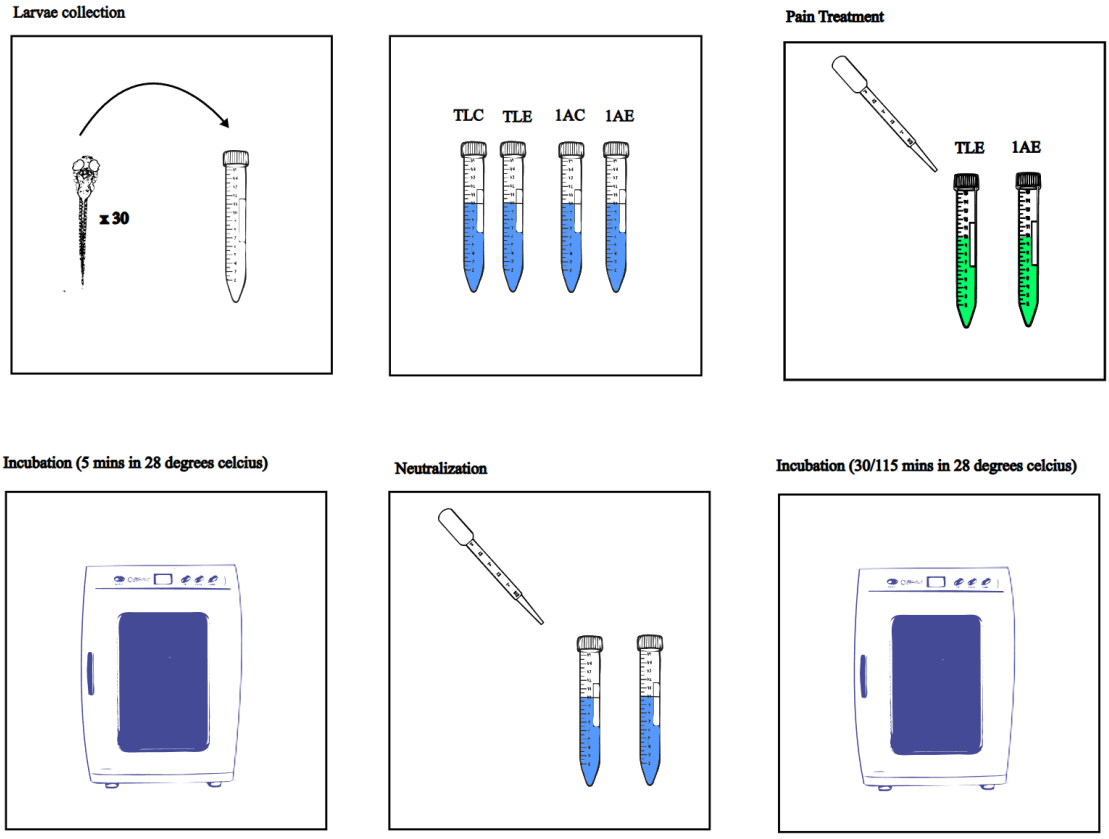

Figure 7: qPCR RNA sample preparation: 30 larvae are collected for each group: TL control (TLC), TL AA treated (TLE), panx1a KO control (1AC) and panx1a KO AA treated (1AE). Pain treatment (0.005% AA) is added to both TLE and 1AE and incubated for 5 mins. The pH is neutralized and the either incubated for 30 or 115 mins. Samples are then collected and frozen in -80ºC. Created on Inkscape.

Table 2: RNA sample name; corresponding pain treatment, genotype and total incubation.

RNA sample name	Pain treatment	Genotype	Total Incubation (minutes)

TLC 35	N/A	TL	35
TLE (5+30)	0.005% acetic acid	TL	35
1AC 35	N/A	Panx1a KO	35
1AE (5+30)	0.005% acetic acid	Panx1a KO	35
TLC 120	N/A	TL	120
TLE (5+115)	0.005% acetic acid	TL	120
1AC 120	N/A	Panx1a KO	120
1AE (5+115)	0.005% acetic acid	Panx1a KO	120

For extraction, metal beads were added to each sample tube (2mL) in addition to 350 uL RLT (cell lysis buffer) and 3.5 uL beta-mercaptoethanol (BME), and the samples were subjected to tissue lysis using a tissue lyser for 3 minutes at 50 Hz. After the samples were centrifuged (13,000 rpm for 2 minutes), and the supernatant was transferred to a fresh 2 mL tube. RNA extraction was performed either using the QIAcube or the RNAeasy Plus Mini Kit protocol for manual extraction, following detailed hand extraction procedures.

RNA samples were assessed for quality using OD readings, and RNA gel electrophoresis was conducted. For the samples to be run by gel electrophoresis, 2 uL of each RNA sample was mixed with formaldehyde (4 µL), RNA water (4 µL) and incubated for 10 mins at 55^{o}C. proceeding the sample prep ethidium bromide (ETBR) + stop mix (2 µL) was added. The gel used was 2% agarose, the samples were then run at 80V for 30 minutes before imaging using an Alpha Imager.

2.3.2 cDNA synthesis

1 µg of RNA was used to make the respective cDNA samples that will proceed to qPCR analysis. cDNA synthesis was performed using the iScript™ Reverse Transcription Supermix. The cDNA synthesis was preformed in the thermocycler following the standard protocol (Table 3).

Table 3: cDNA Synthesis Thermocycler Protocol

Time (min)	Temperature (°C)
5	25
30	42
5	85
indefinite	4

2.3.3 18s PCR

Following cDNA synthesis, quality of cDNA was assessed with 18s RT-PCR. The following experiment was performed using the HotStarTaq DNA Polymerase kit (Qiagen). The reaction mix for each sample contained 10x PCR buffer, forward and reverse primers for 18s, dNTPs, HotStarTaq polymerase, and the respective cDNA in 0.2 mL tubes. The reaction took place in thermocycler using the standard PCR amplification protocol (Table 4).

Table 4: 18s RT-PCR Thermocycler Protocol

Time (min)	Temperature (°C)	
15	95	
0.5	95	x 17
0.5	52	
1	72	
10	72	
Indefinite	4	

After this reaction was complete, gel electrophoresis was performed on the respective samples. 2x stop mix is added to each 18s sample and ran on 2% agarose gel (containing ETBR) at 80V for 30 minutes. The gel is imaged using Alpha Imager and 18s product is verified before proceeding to qPCR.

2.3.4 qPCR primers

Table 5: Gene names and the respective ATCG sequence for forward and reverse primers

Gene name	Forward Primer (5'-3')	Reverse Primer (5'-3')
trpa1a	CCTCTACAAGCAATCCTACCTG	GCCGCCCAGTCCATGTAGTTC
trpa1b	ACCCCTTGAGCCGAAAATAC	GATTGAGGATGAGGTATGTGAGG

Il-6	AGATGACAGTGAAGCTCTTGG	ACATACTTAAGATGCGCTCCG
Il-4	TGAGGACTTTCTTGCTGTTGG	TTTCCCCTTTCCCATTCAGG
IL10	CAAGCGGGATATGGTGAAATG	CGATGTACCTAAAGAGCAAATCAA
IL1b	GTTCAGATCCGCTTGCAATG	TGCTTCATTCTGTTCAGGGC
CFOSAA	AACATCAAGAAGCGAGGCST	CGGAGACTCGCCCTGTGC
CFOSAB	CGATACACTGCAAGCTGAAAC	CGGCGAGGATGAACTCTAAC
CFOSB	GTCAAAGTGGCACGGGCT	GGTCAGCGTTTCATCTCGTG
CFOSL1a	CACAACCCAACAACAACAGAA	GTGCCTATTGAAGGCTGAAGCATC
CFOSL1b	TCAAACCCGCAAGTCACCTC	ATCTATGCTGGTTGTGAATGAC
CFOSL2	GACACTGGTCGTCTGGGAAT	TACTTCTGGTAACTGGAGGCG
p2rx4a	GAGACCAGGACACTTATCAAGG	TCACAGATGACGTTCACCAG
p2ry11	GTTCTTTACATCCTGACCCTCC	ACATAGAGGTTGCTGGTGAAG
p2ry12	TCTTCGGTTTGATCAGCATCG	TCAGGATTACATTTGGGAGCG
p2rx8	TTTCGGCTGGGAGATATTGTG	AGACATAAAGCTGTACTGAGGATG
p2rx7	GTGTCATTTGTGGACGAGGAC	CACTCAACAGAGTCTTCATGCTG
p2rx5	AGTAAATGGAAAGGCTGGGAG	CTCTCGGTAAAAGGAGCTCTT
18s	GAGGTGAAATTCTTGGACCGG	CGAACCTCCGACTTTCGTTCT

The reaction mix for qPCR reaction consisted of RNA water, respective primers and Syber Green PCR mix. The primers used are listed in Table 5. For each cDNA sample 3 experimental replicates were done for the respective primers. The reactions were done on 96 well plates in the BIO-RAD CFX thermocycler. The qPCR machine evaluated the reactions and provided Raw cycle threshold values (Ct). The Ct values are analyzed in REST (2009) analysis software to give the expression ratios of the respective genes. The expression ratios described the gene expression in experimental groups compared to control groups.

2.4 Quantification of Extracellular ATP

Table 6: ATP sample names and the corresponding pain treatments, genotypes, and incubation times

ATP sample name	Pain treatment	Genotype	Total Incubation (minutes)
TLC 5	N/A	TL	5
TLE 5	0.005% acetic acid	TL	5
TLC 60	N/A	TL	60
TLE (5+55)	0.005% acetic acid	TL	60

Samples for ATP assays were created using a 5 min pain treatment followed by incubation period: either 0 or 55 minutes. 30 larvae were collected in 2mL tubes for each sample before freezing and storing in -80^{o}C. Samples were then subjected to tissue lysis and ATP extraction. In each sample tube the following items were added: a metal bead, 4^{o}C in phosphate buffered saline (PBS) and 100 μM ARL and Halt Protease

inhibitor. The samples were lysed at 50 hz for 3 min using the tissue lyser. samples were centrifuged (13,000 rpm for 2 minutes), and the supernatant was transferred to a fresh 1.5 mL tube that was kept at -20^{o}C. The samples were then assessed for extracellular ATP in a 96-well plate using the ATP determination Kit (Life Technologies). Samples were measured in replicates of 4 using the Synergy H4 Hybrid Multi well Plate Reader (Biotek) – The protocol used maintained a temperature of 28^{o}C. ATP concentrations of samples were determined using a standard curve prepared from stock ATP dilutions.

2.5 Tissue fixation, Embedding, Cryosectioning

Table 7: Immunohistochemistry sample names and the corresponding pain treatments, genotypes, and incubation times

Immuno sample name	Pain Treatment	Genotype	Total Incubation (minutes)
TL35	N/A	TL	35
TL(5+30)	0.005% acetic acid	TL	35

Samples were treated for 5 mins with pain treatment then incubated and fixed in 4% paraformaldehyde (PFA) for 5 days at 4^{o}C. Following this fixation period, we drain the PFA and treat with 15% sucrose for 1 day at 4^{o}C. Following this treatment, we drain 15% sucrose and add a new 30% sucrose treatment and incubate it for 1 day at 4^{o}C. Tissue blocks for Cryosectioning were made in a 3d printed cast for OCT medium (VWR clear Frozen Section Compound, cat#95057-838). This medium turned solid at freezing

temperatures caused by dry ice stored in a Styrofoam box (-20^{o}C) and was stored in -80^{o}C prior to Cryosectioning.

Tissue sectioning was done on a cryotome machine (Thermo Scientific Cryotome FSE Cryostat Microtome), sections were 12 µm. The temperature setting are as follows: Cryobar set to -24^{o}C, chamber is set to -24 ^{o}C, and specimen temperature was set to -24^{o}C. The tissue sections were placed on glass slides and stored in -80^{o}C.

2.6 Immunohistochemistry

Prior to starting the 1-day immunohistochemistry protocol, the slides that are going to undergo staining are warmed to room temperature. To get rid of unwanted debris, the tissues were washed with 1xPBS medium (0.1% tween), this wash is done for 5 mins and repeated 3 times. Antibody dilution blocker was added to each tissue section, the slides were placed in a moist chamber to keep the tissue from drying out. The tissue was incubated in this moist chamber for an hour. Following this incubation the tissue is washed (1X PBS) for 5-minute time periods (x3). Primary antibody is then added to the tissue section. After this the slides are placed in 4^{o}C and incubated for 2 hours. After the incubation step the tissue is washed again for another 3x5 mins in 1X PBS (0.01% tween). Then the secondary antibody is added to the tissue sections, and the slides are incubated at room temperature in the dark for 1 hour. Finally, the last wash with 1X PBS (0.01% tween) 3 x 5 mins, and a final wash with RO water to remove impurities. Tissue sections are emersed in 10 µL of DAPI mounting medium and covered with a glass cover slip. The tissue sections were imaged on the LSM 700 laser scanning microscope.

2.7 Assessment of behavior to noxious stimuli

The following drug treatments that were tested were ibuprofen and probenecid. First 30 TL larvae (6 dpf) were collected in 15 mL Eppendorf tube. Depending on the concentration of the drug tested, I added the appropriate amount of stock to reach the desired concentration. Following the drug treatment, the fish were incubated for a total of 1 hour. 20 mins before behavioral assessment the fish were loaded into 48 well plates (200 µL) and placed in the ZebraFish Box (28^{o}C). Baseline recording (5 mins) was done at 30% lux and then pain/control treatment (200 µL) was added and we proceeded with behavioral assessment to noxious stimuli (5 mins) (Figure 8). The ZebraFish Box was used for video quantization of burst level activity and freeze duration, the threshold for burst level activity is activity that exceeded 15 mm/s and threshold for freeze duration was activity that did not exceed 0 mm/s. The data was analyzed in GraphPad Prism software and statistical analysis was done to assess the significance of the data.

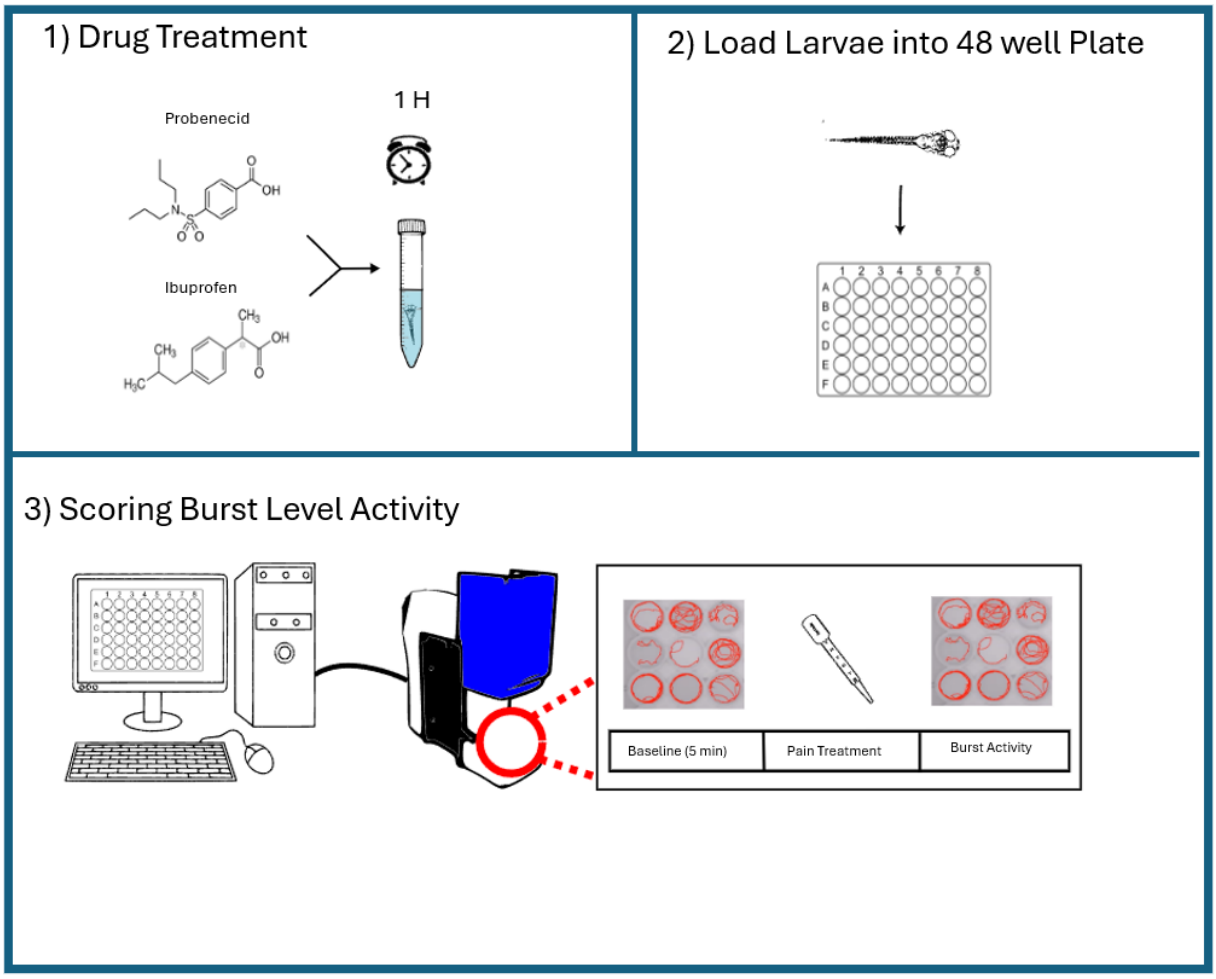

Figure 8: Drug treatments: 1) 30 larvae are treated with either Probenecid (20 µM) or ibuprofen (25 µg/L and 50 µM) for 1 hour prior to experimentation 2) larvae are loaded into a 48 well plate with 200 µL of egg water. 3) the plate is placed into the ZebraBox (viewpoint) and baseline recording is taken. Pain treatment is added (either 0.005% or 0.00125% AA) and placed back into Zebrabox for behavioral assessment. Created on Inkscape.

2.8 Statistical Analysis Behavioral Assays

The behavioral data from ZebraBox™ were extracted and sorted. The data from "FREEZE DUR" and "BURST DUR" were analyzed. The time points of interest: 1s – 150s time period and the 151s – 300s time period. These time periods were analyzed

using Prism Graph Pad 10. For, behavioral assessment we performed the Kolmogorov–Smirnov test to assess the normality of data, then Two-Way ANOVA post hoc Tukey's multiple comparison test. If data did not meet normality requirements, we preformed the Kruskal-Wallis test (non-parametric ANOVA) post hoc Dunn's multiple comparison test.

2.9 Reagents

2.9.1 Molecular Biology Reagents

Procedure	Solutions	Source
ATP Assay	PBS, ARL-67156, Halt Protease inhibitor, D-Luciferin, Luciferase, Dithiothreitol, Adenosine 5′-triphosphate, 20X Reaction Buffer	Sigma-Aldrich, ThermoFisher Scientific, Life Technologies
Tissue lysis and RNA extraction	RLT Plus Lysis Buffer, βME, RW1 Wash Buffer, RPE Wash Buffer, 70% Ethanol, RNase-free water	QIAGEN (RNeasy plus mini kit)
RNA/DNA visualization	Formaldehyde, Agar, 1x TAE buffer, EtBr, 100bp DNA Ladder	ThermoFisher Scientific
cDNA synthesis	5x iScript Reaction Mix, iScript Reverse Transcriptase, Nuclease-free water	Bio-Rad
18s product PCR	HotStarTaq DNA Polymerase, 1x PCR Buffer, dNTPs, 10mM 18s FP and RP solution, Nuclease-free water	QIAGEN (HotStar Taq Pol Kit)
RT-qPCR	Ssofast™ EvaGreen® Supermix	Bio-Rad

2.9.2 Drugs Used in Treatments to Larvae

Reagent	In-text appearance	Source
2-(4-Isobutylphenyl)propanoic acid, Brufen, Motrin, Rebugen, α-Methyl-4-(isobutyl)phenylacetic acid, (±)-2-(4-Isobutylphenyl)propanoic acid	Ibuprofen (IBU)	Sigma Product# I4883
p-(Dipropylsulfamoyl)benzoic acid	Probenecid (PROB)	Sigma Product#P8761

2.9.3 Acetic acid and neutralization treatments to Larvae

Reagent	In-text appearance	Source
Acetic Acid	Acetic Acid (AA)	Sigma Product# 695092
Sodium Hydroxide	Sodium Hydroxide (NaOH)	Sigma Product# 1.60309

2.10 Equipment

2.10.1 Equipment for behavioral analysis

Procedure	Equipment	Source
Locomotor activity retrieval; automatically generated outputs and videos	ZebraBox	ViewPoint Behavior Technology, Lyon, France
Incubation of larvae at 28°C before insertion into ZebraBox	Exo Terra Incubator	Exo Terra, Montreal, Canada

2.10.2 Equipment for ATP assay

Procedure	Equipment	Source
Tissue lysis	TissueLyser LT Adapter, 12-tube	QIAGEN
ATP quantification	Synergy H4 Hybrid Multi-well Plate Reader	Biotek

2.10.3Equipment for molecular qPCR

Procedure	Equipment	Source
Tissue lysis	TissueLyser LT Adapter, 12-tube	QIAGEN
	Sorvall™ Legend™ Micro 21R Microcentrifuge	Thermo Scientific
RNA extraction	QIAcube	QIAGEN
cDNA PCR	Mastercycler® nexus	Eppendorf, Canada
RNA and cDNA visualization	Nanodrop 2000 Photospectrometer	Thermo Scientific
	Mini-Sub Cell GT System	Bio-Rad
	AlphaImager™ HP System	Alpha Innotech
RT-qPCR	CFX96™ Real-Time PCR Detection System	Bio-Rad

2.11 Software

2.11.1 Software for ATP assay

Purpose	Software
Fluorescence Assay	ZEN 2010 (Carl Zeiss Microscopy)
Luminescence Assay	Gen5 Data Analysis Software (BioTek)
Protein Concentration	Nanodrop2000 a280

2.11.2 Software for qPCR

Purpose	Software
Gene sequence retrieval	NCBI – nucleotide
Primer Design	IDT - RealTime qPCR tool
Primer location	SnapGene Viewer 5.3.2
RT-qPCR data acquisition	CFX Manager software™
Relative expression analysis	REST 2009©

2.11.3 Software for behavioral assay

Purpose	Software
Behavioral tracking	ZebraLab (ViewPoint, Life Technology, Lyon, France)
Processing of ZebraLab output	Fast Data Monitor (ViewPoint Biotechnology)
Statistical analysis and figure generation	GraphPad Prism 9.3.1

3.0 Results

3.1 Behavioral assessment of Panx1a KO in response to noxious stimuli

Zebrafish larvae were loaded into 48 well plates (200 µL) and placed in the Zebrafish box (28^{o}C) (viewpoint). The genotypes studied were TL and Panx1a KO (6dpf). Baseline recording is performed for 5 mins at 30% lux. Following this, 200 µL of control (egg water) and AA treatment are added to larvae (AA treatments used: 0.01%,

0.005%, 0.0025%, and 0.00125% acetic acid). The 48-well plate was placed back in the zebrafish box and again recorded for 5 mins. Burst activity (activity >15mm/s) and freeze duration (activity = 0mm/s) were scored by Viewpoint Access software. The data was analyzed in GraphPad Prism software and statistical analysis (2-way ANOVA/Kruskal-Wallis) was done to assess the significance of the data.

3.2 Panx1a KO larvae burst duration activity and freeze duration activity assessment

The subsequent section will present and analyze the behavioral assessment of Panx1a knockout (KO) in response to AA treatments. Studies have demonstrated significant alterations in zebrafish locomotion in response to acetic acid (AA) treatments. Furthermore, these researchers found that treatment with the PANX1 inhibitor probenecid ameliorated these locomotor changes (Gusso et al., 2022). This suggests that blocking pannexin rescued pain behavior. Therefore, we predicted to see this effect in the Panx1a KO and/or Panx1b KO in response to AA treatments. Evidence suggests that Panx1a KO larvae exhibit deficits in nociceptive signaling to AA treatments.

Average burst duration (BDA) - defined as the fraction of time larvae exhibit activity greater than 15mm/s - was assessed in response to AA treatments. Panx1a KO was treated with different AA concentrations (0.01%, 0.005%, 0.0025%, 0.00125%). The results show significant increases in BDA at all concentrations except 0.00125% (Figure 9 D; 1s-150s p-value = 0.2458, 151s – 300s p-value = 0.6499). In contrast, we saw significant increases in BDA in the TL larvae in response to all AA concentrations. At the 0.00125% AA concentration, the results indicated significant increases in BDA at both time points (Figure 9D; 1s-150s p-value = 0.0079, 151s-300s p-value = 0.0018). This

evidence suggests that Panx1a KO larvae have a higher threshold for harmful stimuli to elicit significant changes to BDA.

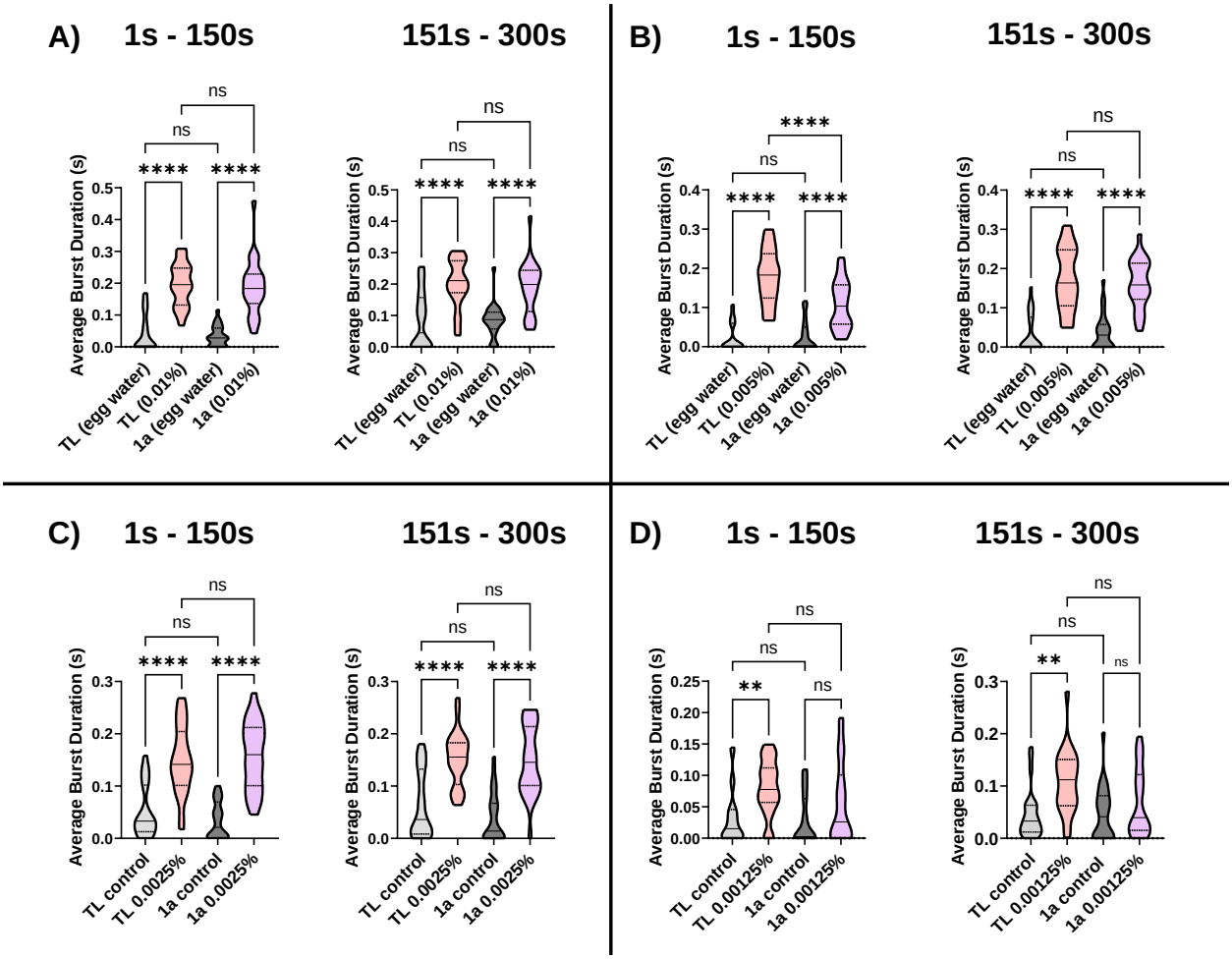

Figure 9: Average burst duration TL and Panx1a KO. The different time points of behavioral assessment: 1st time point (1s-150s) and 2nd time point (151s -300s). The 4 different acetic acid concentrations tested: 0.01%, 0.005%, 0.0025% and 0.00125%. Different genotypes tested: Tupel Longfin (TL) and Panx1a KO (1a). Data was analyzed using Prism Graph Pad, 2-way ANOVA followed by Tukey's post hoc multiple comparison test. Significance values * p<0.05, ** p<0.01, ***p<0.001, and ****p<0.0001. **(a)** N = 24 TL control, n = 24 TL AA treated (0.01%), n = 24 Panx1a KO control, n = 24 Panx1a KO AA treated (0.01%). **(b)** N = 24 TL control, n = 24 TL AA treated (0.005%), n = 24 Panx1a KO control, n = 24 Panx1a KO AA treated (0.005%). **(c)** N = 24 TL control, n = 24 TL AA treated (0.0025%), n = 24 Panx1a KO control, n = 24 Panx1a KO AA treated (0.0025%). **(d)** N = 24 TL control, n = 24 TL AA treated (0.00125%), n = 24 Panx1a KO control, n = 24 Panx1a KO AA treated (0.00125%).

Principal component analysis was performed on AA trials, and we found that Freeze duration activity had the highest PCA score (PC1 = 0.957), indicating that this variable captures most of the data variance. This suggests that Freeze duration activity is the best variable to use to describe behavioral changes to AA treatments. Average freeze duration (FDA) is defined as the fraction of time larvae spend immobile (~0mm/s). Panx1a KO was treated with AA (0.01%, 0.005%, 0.0025%, 0.00125%) at multiple concentrations. Panx1a KO larvae exhibit significant decreases in freeze duration at all concentrations except 0.00125% (Figure 10 D, 1s-150s: p-value = 0.4374, 151s-300s: p-value = 0.9193). In contrast, the TL larvae saw significant modulation of FDA at all concentrations. This suggests that Panx1a has a higher threshold for harmful stimuli, requiring higher AA concentration to significantly modulate FDA compared to TL (Figure 10).

3.3 Panx1b KO larvae burst duration activity assessment

We assessed the behavior of the Panx1b KO in response to AA treatments. We determined that Panx1b also exhibited significant increases in BDA in response to AA treatments. More specifically, at 0.00125% AA treatments, we saw significant increases in BDA (1s-150s: p-value = 0.0007, 151s-300s: p-value = 0.001). We can conclude that the Panx1b KO line exhibits aversive behavior in response to AA treatments. In contrast the Panx1a KO did not experience a significant increase in BDA at 0.00125% AA treatments. This suggests that the effect we are seeing is specific to the Panx1a gene.

This could be attributed to where Panx1a is localized compared to Panx1b.

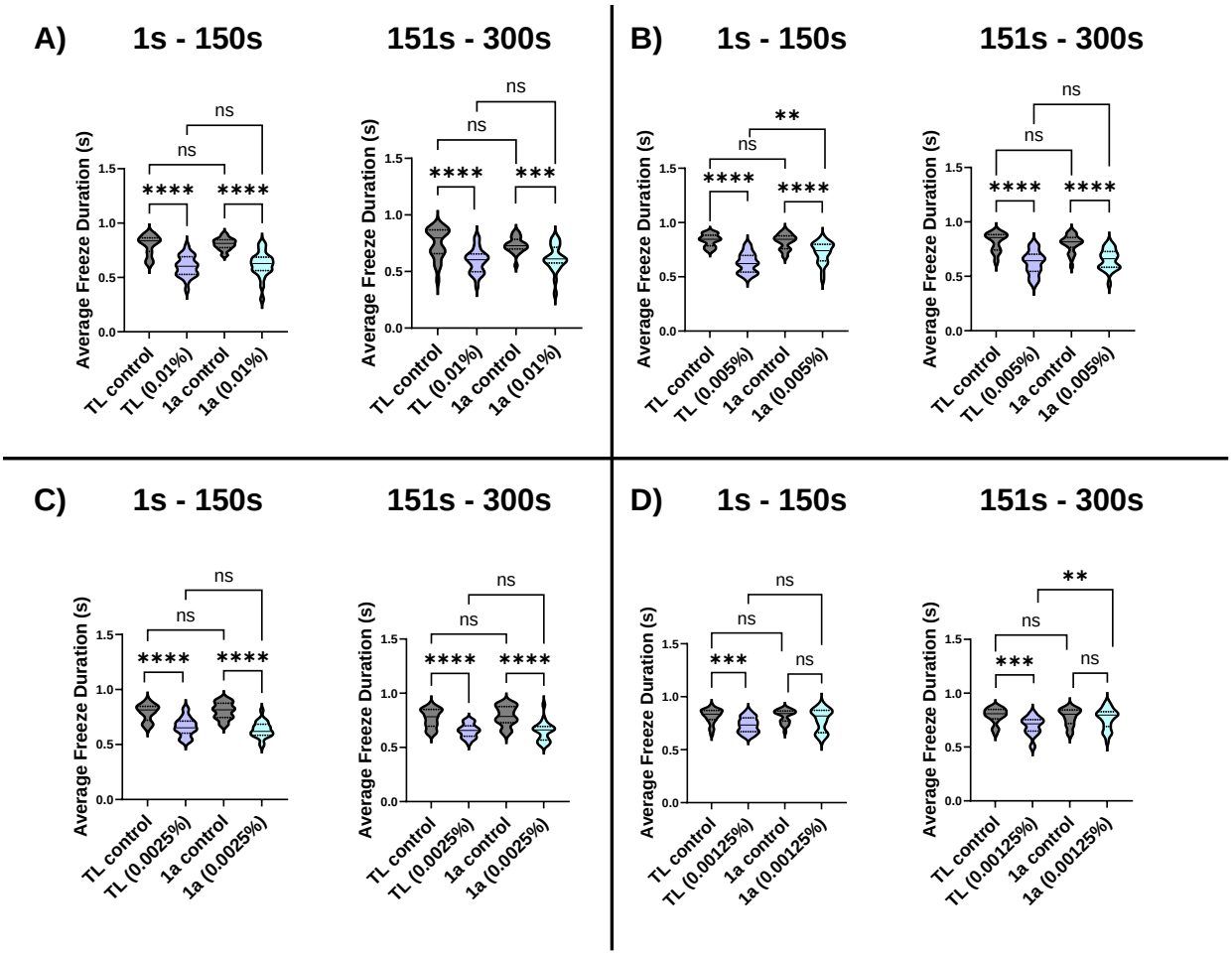

Figure 10: Average freeze duration TL and Panx1a KO. The different time points of behavioral assessment: 1st time point (1s-150s) and 2nd time point (151s -300s). The 4 different acetic acid concentrations tested: 0.01%, 0.005%, 0.0025% and 0.00125%. Different genotypes tested: Tupel Longfin (TL) and Panx1a KO (1a). Data was analyzed using Prism Graph Pad, 2-way ANOVA followed by Tukey's post hoc multiple comparison test. Significance values * p<0.05, ** p<0.01, ***p<0.001, and ****p<0.0001. **(a)** N = 24 TL control, n = 24 TL AA treated (0.01%), n = 24 Panx1a KO control, n = 24 Panx1a KO AA treated (0.01%). **(b)** N = 24 TL control, n = 24 TL AA treated (0.005%), n = 24 Panx1a KO control, n = 24 Panx1a KO AA treated (0.005%). **(c)** N = 24 TL control, n = 24 TL AA treated (0.0025%), n = 24 Panx1a KO control, n = 24 Panx1a KO AA treated (0.0025%). **(d)** N = 24 TL control, n = 24 TL AA treated (0.00125%), n = 24 Panx1a KO control, n = 24 Panx1a KO AA treated (0.00125%).

3.4 Pharmacological block of Pannexin1; burst duration activity assessment

We used probenecid, a well-known pannexin channel blocker to study the effects on behavior in response to AA treatments. Past studies have shown that probenecid rescued nociceptive response in AA-treated larvae (Gusso et al., 2022). Therefore, in this AA model, we predicted to see a rescue of nociceptive response in probenecid-treated larvae.

Larvae were treated with probenecid for 1 hour before treatment. At both AA concentrations, we observed a significant increase in burst level activity for the probenecid-treated larvae (Figure 11 A; 1s – 150: p-value = <0.0001, 151s - 300s: p-value = 0.0002) (Figure 11 B; 1s – 150s: p-value = <0.0001, 151s - 300s: p-value < 0.0001). Another notable observation is the significant decrease in BDA observed in probenecid + AA-treated larvae compared to AA-treated larvae (Figure 11A; 1s-150s: p-value = 0.0631, 151s-300s: p-value = 0.0139) (Figure 11B; 1s-150s: p-value = 0.0265, 151s-300s: p-value = 0.0038). These results suggest that Panx1 mediates BDA in response to AA treatment.

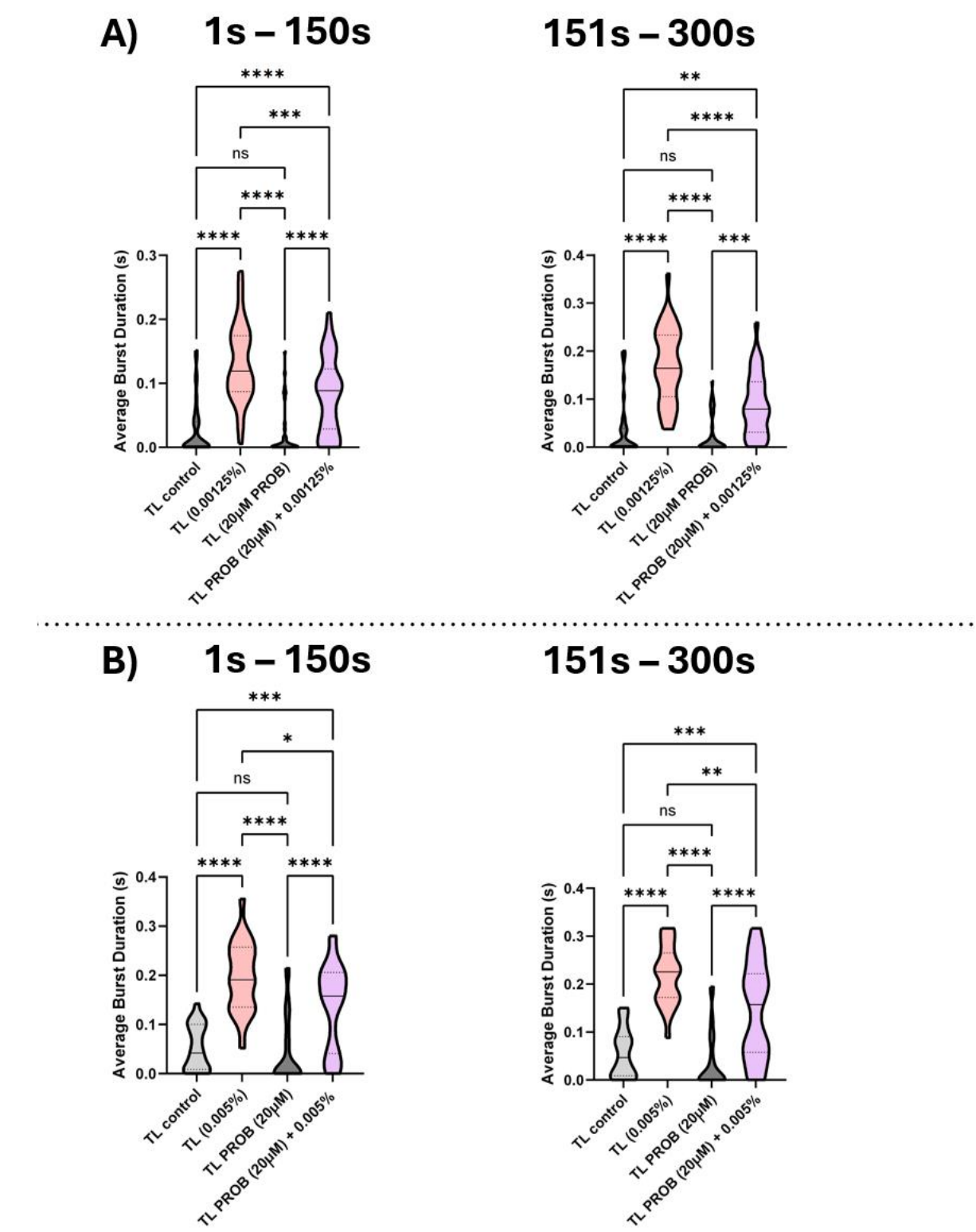

Figure 11: Average burst duration of Probenecid treated (20 μM) TL. Data as shown: the different time points of behavioral assessment: 1st time point (1s-150s) and

2nd time point (151s -300s). The 2 different acetic acid concentrations tested: %, 0.005%, and 0.00125%. TL larvae were treated with 20 μM of probenecid (1 hour) prior to behavioral assessment. Data was analyzed using Prism Graph Pad Significance values * p<0.05, ** p<0.01, ***p<0.001, and ****p<0.0001. **(a)** N = 36 TL control, n = 36 TL AA treated (0.00125%), n = 36 TL PROB, n = 36 TL PROB + AA treatment (0.00125%) Kruskal-Wallis test (non-parametric ANOVA) followed by Dunn's post hoc multiple comparison test. **(b)** N = 24 TL control, n = 24 TL AA treated (0.005%), n = 24 TL PROB, n = 24 TL PROB + AA treatment (0.005%). 2-way ANOVA followed by Tukey's post hoc multiple comparison test.

3.5 Pharmacological block of Pannexin1; freeze duration activity assessment

As stated previously, PCA analysis revealed freeze duration as the best variable to show behavioral changes to AA treatments. Therefore, we assessed FDA in these probenecid drug trials. TL larvae were treated with probenecid for 1 hour before the assessment of FDA. Data show significant modulation of both probenecid-treated and control fish in response to AA treatments. However, it should be noted that there are significant increases in FDA in the AA-treated control compared to AA + probenecid-treated TL (Figure 12 A; 1s – 150: p-value = 0.0044, 151s - 300s: p-value < 0.0001) (Figure 12 B; 1s – 150s: p-value =0.0292, 151s - 300s: 0.0034). The results show that FDA is modulated in response to the pharmacological block of pannexin (Figure 12). This suggests that pannexin is mediating nociceptive behavior in response to AA treatments.

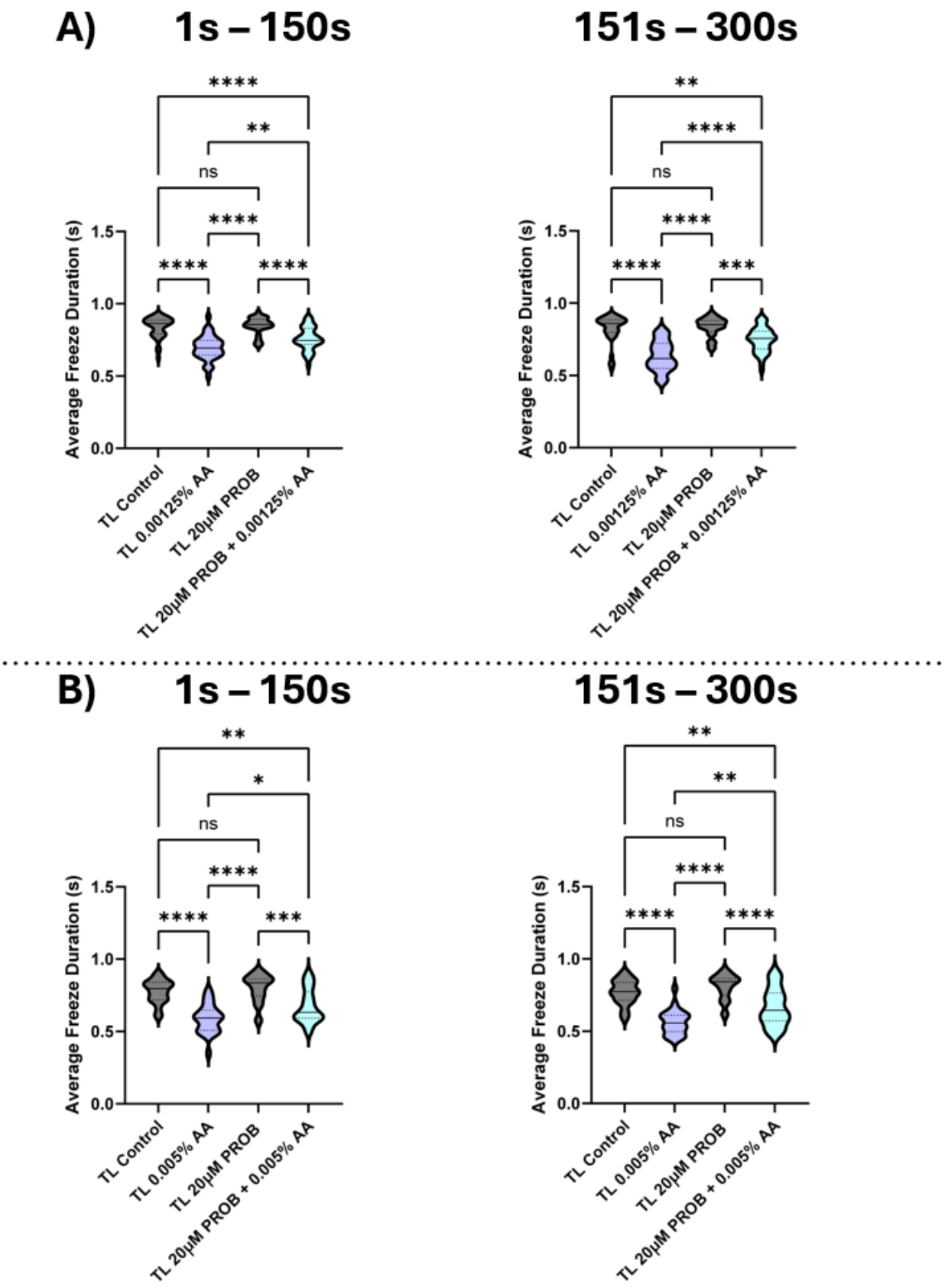
A)
1s – 150s
151s – 300s
Average Freeze Duration (s)
0.0
0.5
1.0
1.5
****
**
ns
****
****
****
**
****
ns
****
****
***
TL Control
TL 0.00125% AA
TL 20μM PROB
TL 20μM PROB + 0.00125% AA
B)
1s – 150s
151s – 300s
Average Freeze Duration (s)
**
*
ns
****
****
***
**
**
ns
****
****
****
TL Control
TL 0.005% AA
TL 20μM PROB
TL 20μM PROB + 0.005% AA

Figure 12: Average freeze duration of probenecid treated (20 uM) TL. Data as shown: the different time points of behavioral assessment: 1st time point (1s-150s) and 2nd time point (151s -300s). The 2 different acetic acid concentrations tested: %, 0.005%, and 0.00125%. TL larvae were treated with 20 μM of probenecid (1 hour) prior to behavioral assessment. Data was analyzed using Prism Graph Pad, 2-way ANOVA followed by Tukey's post hoc multiple comparison test. Significance values * p<0.05, ** p<0.01, ***p<0.001, and ****p<0.0001. **(a)** N = 36 TL control, n = 36 TL AA treated (0.00125%), n = 36 TL PROB, n = 36 TL PROB + AA treatment (0.00125%). **(b)** N = 24 TL control, n = 24 TL AA treated (0.005%), n = 24 TL PROB, n = 24 TL PROB + AA treatment (0.005%).

3.6 Ibuprofen burst duration activity assessment

Ibuprofen is a household anti-inflammatory drug that inhibits the enzyme cyclooxygenase (COX). This enzyme is required to convert arachidonic acid into thromboxanes, prostaglandins, and prostacyclins. The lack of these compounds is believed to provide analgesic effects to the user (Zhang et al., 2020). In this AA model, we predicted to see a rescue of nociceptive behavior in ibuprofen treated larvae. We performed a treatment for 1h and then looked at the effects of AA treatments on burst activity. We have no evidence for analgesic effects of ibuprofen in this AA model.

In our study, we observed significant decreases in BDA in response to ibuprofen treatments (50 μM) in TL larvae. Specifically, for the time point 1s – 150s, there was a significant reduction in BDA in the TL ibuprofen-treated group (50 μM) compared to the control (Figure 13 D, p-value=0.0326). Similarly, for the time point 151s – 300s, the TL ibuprofen-treated group (50 μM) also showed a significant decrease in BDA compared to the control (Figure 13 D; p-value=0.05). These results indicate that ibuprofen significantly reduces the BDA in the treated group compared to the control group. There was no significant change in behavior when larvae were treated with 25 μg/L (Figure 13 A,C). This suggests a dose-dependent effect of ibuprofen on behavior.

Ibuprofen-treated larvae exhibited significant changes in behavior in response to AA (Figure 13A; 151s – 300s p-value=0.0439) (Figure13B; 151s – 300s p-value=0.0426) (Figure 13C; 1s – 150s and 151s – 300s $p<0.0001$ for both) (Figure 13D; 1s – 150s and 151s – 300s $p<0.0001$ for both). These results suggest that ibuprofen does not have an analgesic effect in this AA model.

A)

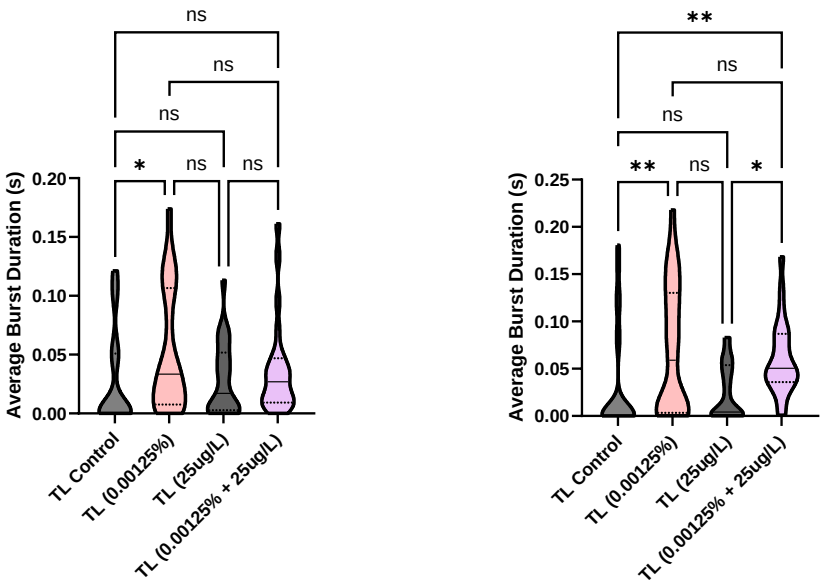
1s - 150s
151s - 300s
Average Burst Duration (s)
0.00
0.05
0.10
0.15
0.20
0.25
ns
*
**
TL Control
TL (0.00125%)
TL (25ug/L)
TL (0.00125% + 25ug/L)

B)

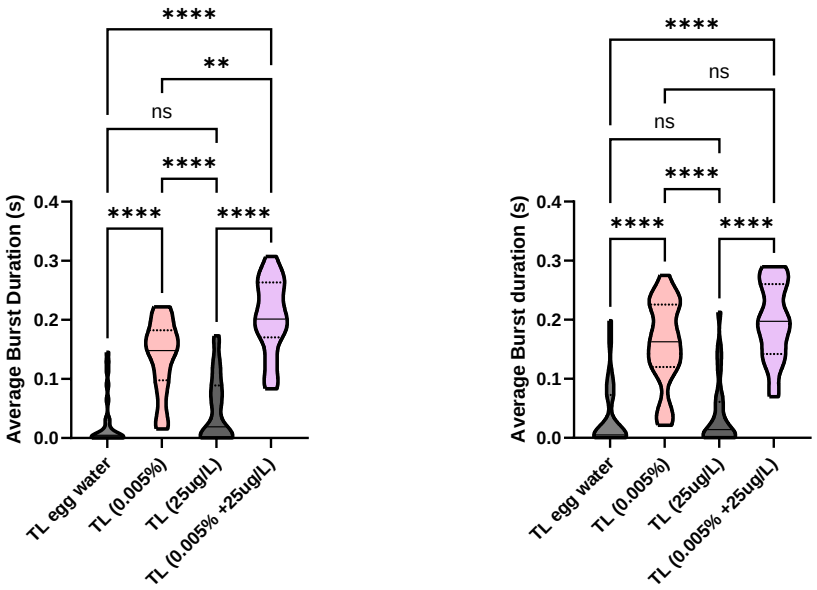
1s - 150s
151s - 300s
Average Burst Duration (s)
Average Burst duration (s)
0.0
0.1
0.2
0.3
0.4
ns
**
****
TL egg water
TL (0.005%)
TL (25ug/L)
TL (0.005% +25ug/L)

C) 1s - 150s

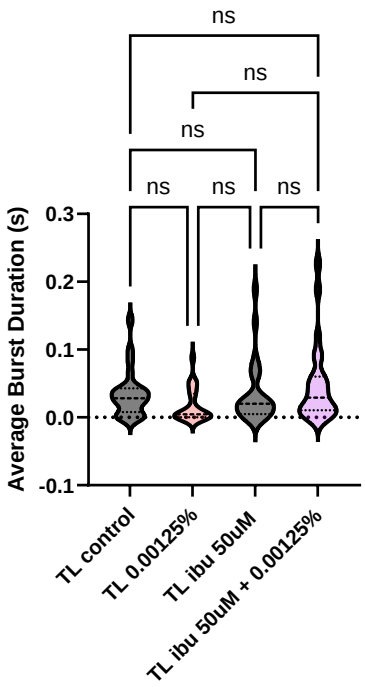

151s - 300s

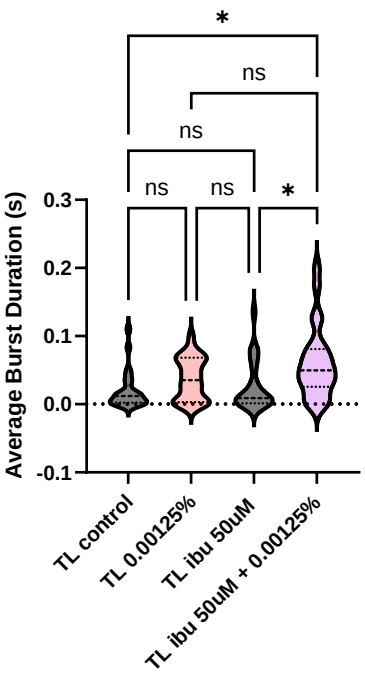

D) 1s - 150s

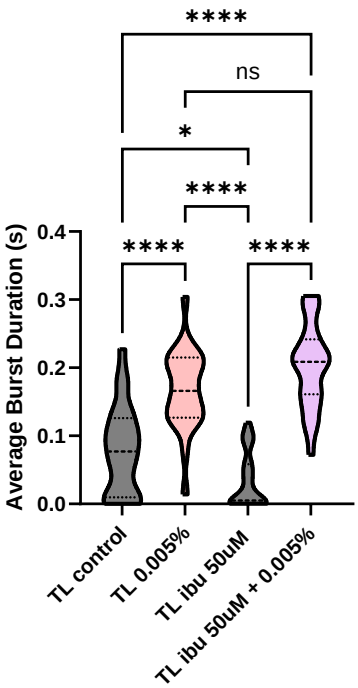

151s - 300s

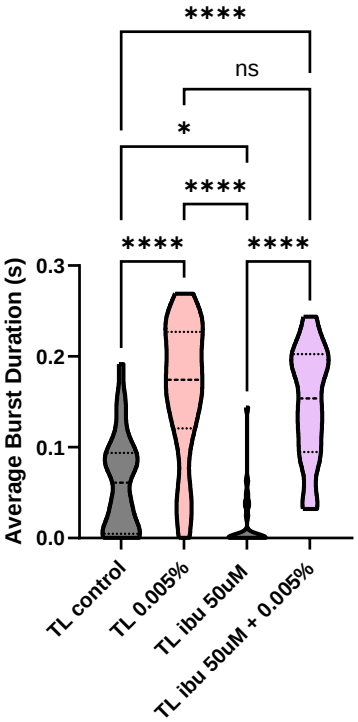

Figure 13: Average burst duration of Ibuprofen treated TL. Data as shown: the different time points of behavioral assessment: 1st time point (1s-149s) and 2nd time point (150s -300s). The 2 different acetic acid concentrations tested: 0.005%, and 0.00125%. TL larvae were treated with 25 µg/L or 50 µM of ibuprofen (1 hour) prior to behavioral assessment. Data was analyzed using Prism Graph Pad, 2-way ANOVA followed by Tukey's post hoc multiple comparison test. Significance values * p<0.05, ** p<0.01, ***p<0.001, and ****p<0.0001. **(a)** N = 24 TL control, n = 24 TL AA treated (0.005%), n = 24 Ibuprofen (25 µg/L), n = 24 AA treated (0.00125%) + Ibuprofen (25 µg/L). **(b)** N = 24 TL control, n = 24 TL AA treated (0.005%), n = 24 Ibuprofen (25 µg/L), n = 24 AA treated (0.00125%) + Ibuprofen (25 µg/L). **(c)** N = 24 TL control, n = 24 TL AA treated (0.00125%), n = 24 Ibuprofen (50 µM), n = 24 AA treated (0.00125%) + Ibuprofen (50 µM). **(d)** N = 24 TL control, n = 24 TL AA treated (0.005%), n = 24 Ibuprofen (50 µM), n = 24 AA treated (0.005%) + Ibuprofen (50 µM).

3.7 Ibuprofen freeze duration activity assessment

As stated previously, PCA analysis revealed freeze duration as the best variable to show behavioral changes to AA treatments. Therefore, we assessed FDA in these ibuprofen drug trials. FDA was assessed after a 1-hour ibuprofen treatment. We saw an increase in FDA activity in response to ibuprofen treatment at 50 µM (Figure 14C; 1s-150s p-value=0.0108, 151s-300s p-value=0.0087). Results suggest that the lower concentration (25µg/L) did not affect FDA (Figure 14B 1s-150s and 151s-300s p-value > 0.999). Ibuprofen treated larvae exhibited significant changes to FDA in response to AA treatments (Figure 14A; 151s – 300s p-value=0.0096) (Figure 14B; 1s-150s and 151s – 300s p-value<0.0001) (Figure 14C; 1s – 149s and 150s – 300s p<0.0001 for both) (Figure 14D; 1s – 150s and 151s – 300s p<0.0001 for both). This suggests that ibuprofen does not affect nociceptive behavior to AA treatments.

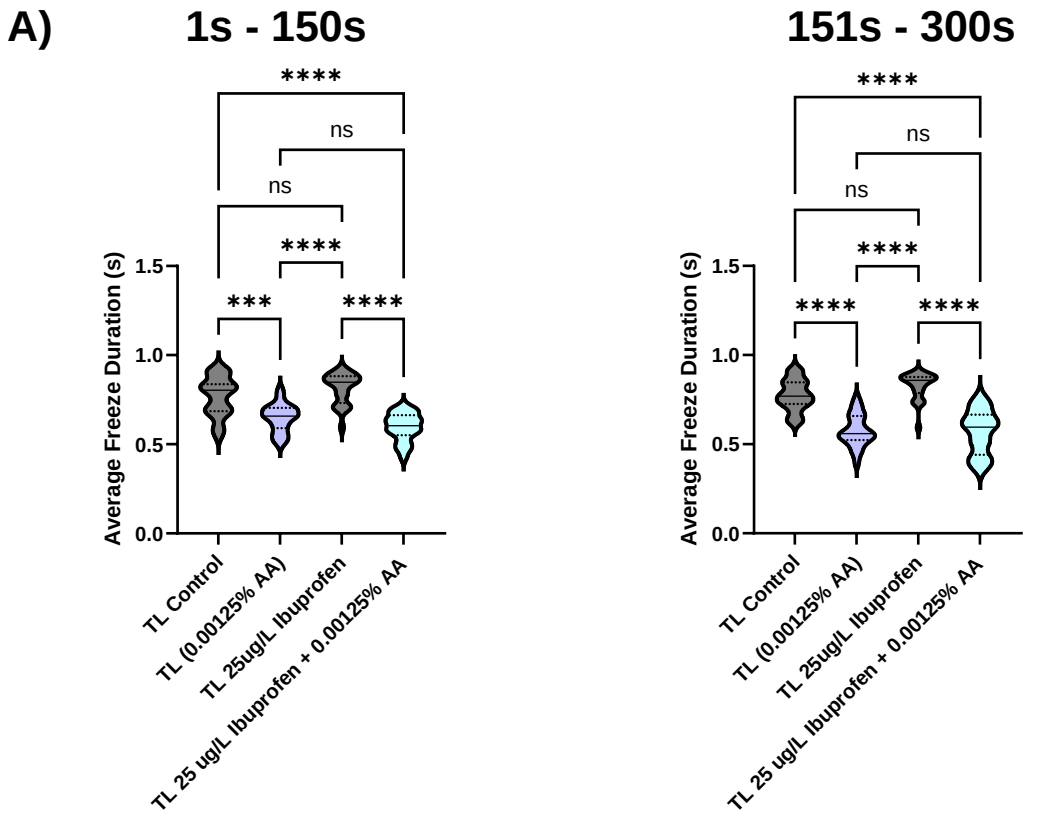
A)
1s - 150s
151s - 300s
Average Freeze Duration (s)
0.0
0.5
1.0
1.5
****
ns
ns
****
***
****
TL Control
TL (0.00125% AA)
TL 25ug/L Ibuprofen
TL 25 ug/L Ibuprofen + 0.00125% AA

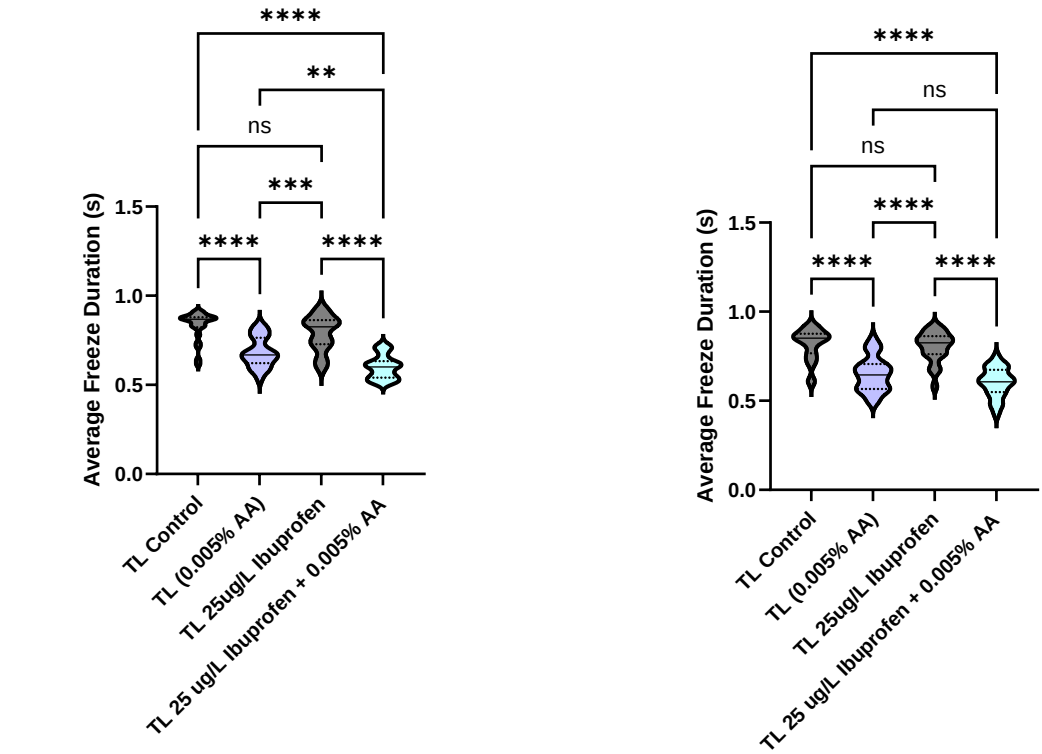
B)
1s - 150s
151s - 300s
Average Freeze Duration (s)
0.0
0.5
1.0
1.5
****
**
ns
***
****
****
TL Control
TL (0.005% AA)
TL 25ug/L Ibuprofen
TL 25 ug/L Ibuprofen + 0.005% AA

C)

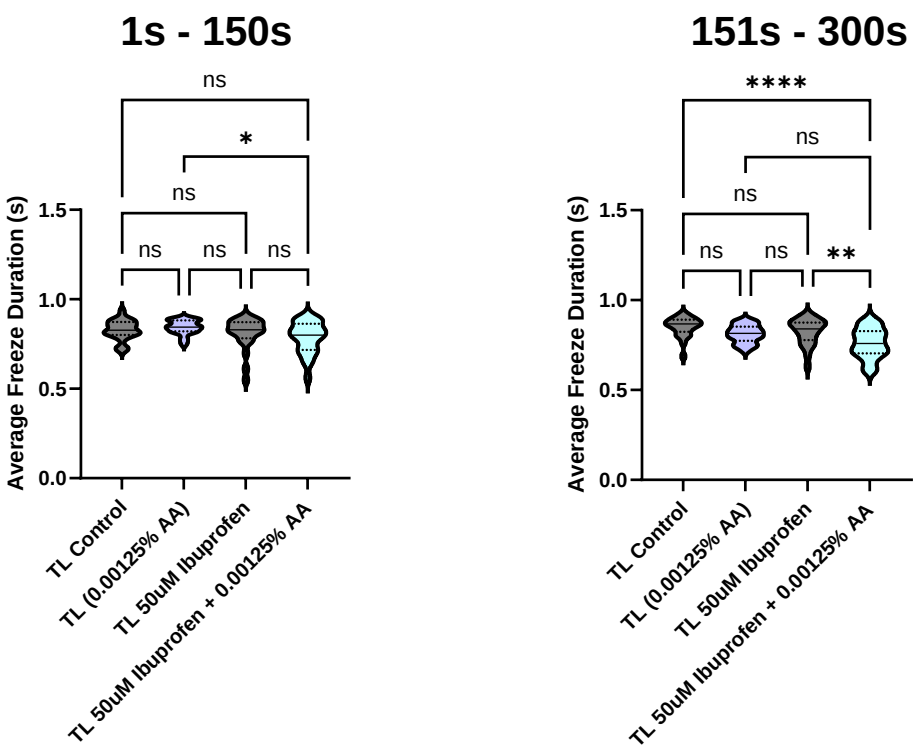
1s - 150s
151s - 300s
Average Freeze Duration (s)
0.0
0.5
1.0
1.5
ns
*
****
**
TL Control
TL (0.00125% AA)
TL 50uM Ibuprofen
TL 50uM Ibuprofen + 0.00125% AA

D)

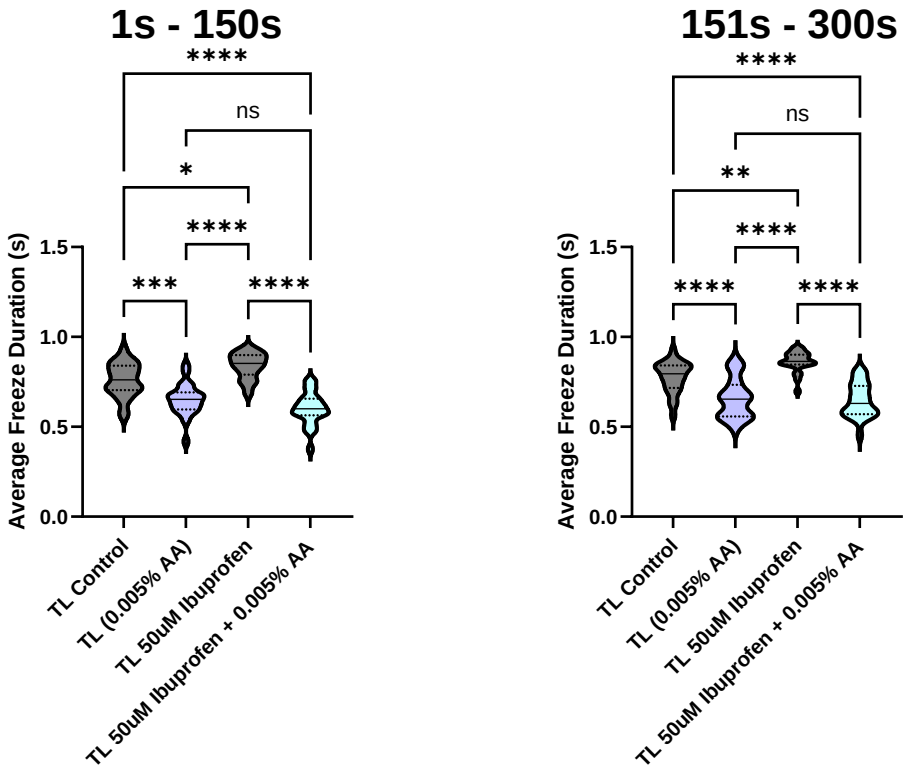
1s - 150s
151s - 300s
Average Freeze Duration (s)
0.0
0.5
1.0
1.5
ns
*
**
***
****
TL Control
TL (0.005% AA)
TL 50uM Ibuprofen
TL 50uM Ibuprofen + 0.005% AA

Figure 14: **Average freeze duration of Ibuprofen treated TL.** Data as shown: the different time points of behavioral assessment: 1st time point (1s-149s) and 2nd time point (150s -300s). The 2 different acetic acid concentrations tested: 0.005%, and 0.00125%. TL larvae were treated with 25 µg/L or 50 µM of ibuprofen (1 hour) prior to behavioral assessment. Data was analyzed using Prism Graph Pad, 2-way ANOVA followed by Tukey's post hoc multiple comparison test. Significance values * p<0.05, ** p<0.01, ***p<0.001, and ****p<0.0001. **(a)** N = 24 TL control, n = 24 TL AA treated (0.005%), n = 24 Ibuprofen (25 µg/L), n = 24 AA treated (0.00125%) + Ibuprofen (25 µg/L). **(b)** N = 24 TL control, n = 24 TL AA treated (0.005%), n = 24 Ibuprofen (25 µg/L), n = 24 AA treated (0.00125%) + Ibuprofen (25 µg/L). **(c)** N = 24 TL control, n = 24 TL AA treated (0.00125%), n = 24 Ibuprofen (50 µM), n = 24 AA treated (0.00125%) + Ibuprofen (50 µM). **(d)** N = 24 TL control, n = 24 TL AA treated (0.005%), n = 24 Ibuprofen (50 µM), n = 24 AA treated (0.005%) + Ibuprofen (50 µM).

3.8 c-fos, purinergic, cytokine, and trp mRNA levels in response to AA treatment (TL control vs TL AA treated)

This study investigated the mRNA transcript levels of genes within the *c-fos* family, known for their role as early response genes, particularly in stressful conditions. c-FOS upregulation has been identified as a biomarker of neural activity and therefore has been implicated in nociception (Jaworski et al., 2018).

Our investigation revealed dynamic changes in expression over time. Notably, *c-fosab, c-fosb,* and *c-fosl1a* exhibited a significant increase in mRNA transcript levels at the 30-minute time point, with expressions of 2.020 (p-value = 0.013), 1.801 (p-value = 0.007), and 2.255 (p-value = 0.002), respectively. However, by the 115-minute time point, these levels decreased to 0.581 (p-value = 0.097), 0.882 (p-value = 0.694), and 0.467 (p-value = 0.239) for *c-fosab, c-fosb*, and *cfosl1a*, respectively. These results suggest temporal regulation of the c-fos family of genes (Figure 15 B, E, F).

To identify any purinergic receptors that are a biomarker of nociception to AA treatment, this study investigated the expression of purinergic receptors in larvae

treated with acetic acid compared to control conditions. The results revealed distinct patterns of expression for various receptors. Firstly, *p2rx4a* exhibited significantly lower mRNA transcript levels at both time points, with a significant decrease at 30 minutes (expression = 0.645, p-value < 0.001) and the trend continuing at 115 minutes (expression = 0.751, p-value = 0.062). Similarly, *p2ry11* showed significantly lower mRNA transcripts at 30 minutes (expression = 0.648, p-value = 0.017), followed by an increase at 115 minutes (expression = 1.579, p-value = 0.156). Furthermore, *p2rx7* displayed lower mRNA transcript levels at 30 minutes (expression = 0.694, p-value = 0.121). These receptors are recognized as ATP-gated ion channels, suggesting regulation in response to acetic acid treatments (Figure 15 A, E, F). This raises questions regarding the role of pannexin-mediated ATP release in this pain model.

To identify any biomarkers of microglia activity and neuroinflammation in response to AA treatments our investigation examined mRNA levels of cytokines, important in both inflammatory and anti-inflammatory mechanisms (Babchenko et al., 2022; Gan et al., 2020). *il-6* exhibited a significant decrease in mRNA transcript levels at the 30-minute time point (expression = 0.623, p-value = 0.049). Similarly, *il-4* showed a significant decrease in mRNA transcripts at 30 minutes (expression = 0.544, p-value < 0.001). *il-10* displayed a significant decrease in mRNA transcript levels at 30 minutes (expression = 0.307, p-value < 0.001), followed by a notable increase at 115 minutes (expression = 1.573, p-value = 0.100) (Figure 15 C,E,F). These findings are evidence of microglia activity response to AA treatments.

Lastly, we investigated the mRNA levels of the trpa1a/b gene. Predicted to be a chemo sensitive channel that mediates neuron excitation in response to harmful stimuli,

like acetic acid (Wang et al., 2012). Our findings showed significant decreases in mRNA transcript levels for *trpa1b,* suggesting downregulation of this pain receptor. Specifically, at the 30-minute time point, Trpa1b expression was significantly reduced (expression = 0.790, p-value = 0.05), with this trend persisting at 115 minutes (expression = 0.643, p-value = 0.023) (Figure 15 D,E,F). These results suggest a possible role in this receptor in our pain model.

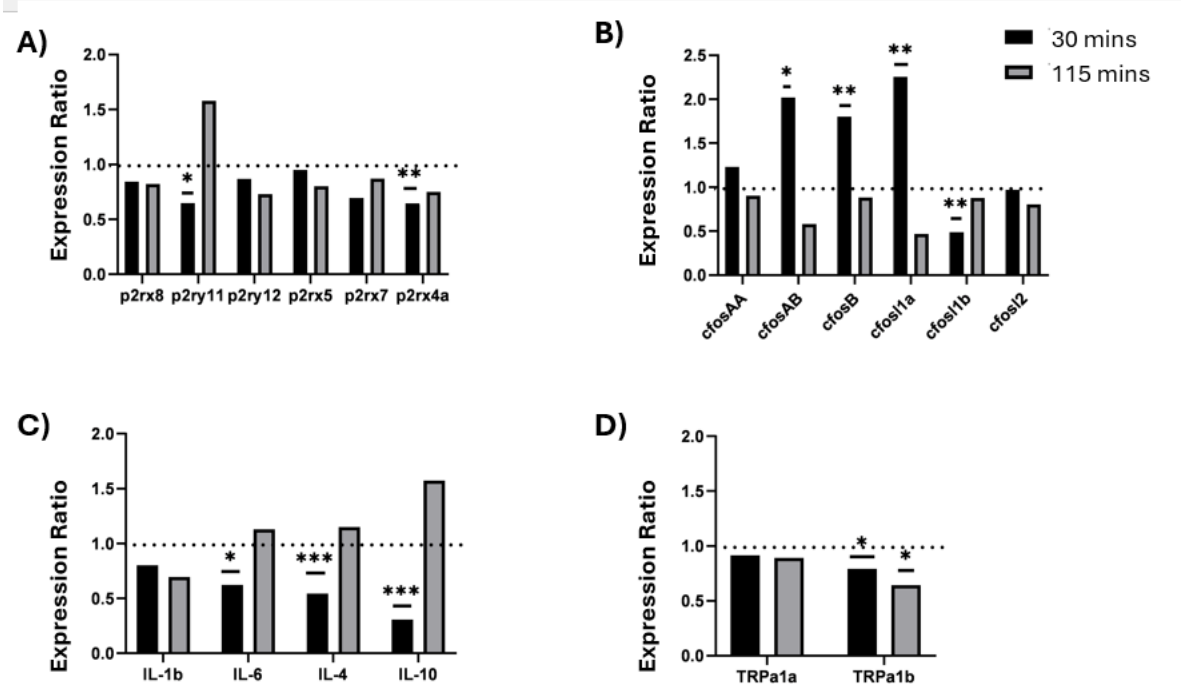

E) **30 minutes post AA treatment**

Gene	Expression	P-Value	Result
p2rx8	0.842	0.364	
p2ry11	0.648	0.017	DOWN
p2ry12	0.869	0.419	
p2rx5	0.95	0.723	
p2rx7	0.694	0.121	
p2rx4a	0.645	0	DOWN
cfosAA	1.231	0.687	
cfosAB	2.02	0.013	UP
cfosB	1.801	0.007	UP
cfosl1a	2.255	0.002	UP
cfosl1b	0.488	0.001	DOWN
cfosl2	0.97	0.893	
IL-1b	0.8	0.461	
IL-6	0.623	0.049	DOWN
IL-4	0.544	0	DOWN
IL-10	0.307	0	DOWN
Trpa1a	0.914	0.501	
Trpa1b	0.79	0.05	DOWN

F) **115 minutes post AA treatment**

Gene	Expression	P-Value	Result
p2rx8	0.822	0.453	
p2ry11	1.579	0.156	
p2ry12	0.729	0.148	
p2rx5	0.801	0.219	
p2rx7	0.871	0.508	
p2rx4a	0.751	0.062	
cfosAA	0.904	0.7	
cfosAB	0.581	0.097	
cfosB	0.882	0.694	
cfosl1a	0.467	0.239	
cfosl1b	0.877	0.549	
cfosl2	0.806	0.472	
IL-1b	0.694	0.399	
IL-6	1.129	0.658	
IL-4	1.151	0.437	
IL-10	1.573	0.1	
Trpa1a	0.893	0.649	
Trpa1b	0.643	0.023	DOWN

Figure 15: qPCR TL control vs TL pain treated. The gene families that were tested for expression in the AA-treated TL: **a)** purinergic, **b)** c-fos, **c)** cytokines, and **d)** TRP

genes. The TL AA-treated larvae were collected at two time points to study differences in mRNA levels after a 5-minute AA treatment: 30 minutes and 115 minutes. Data was analyzed using REST2009, **e) f)** the “expression” values are ratios that describe gene mRNA levels in AA-treated TL larvae compared to TL control larvae. Significance values * $p<0.05$, ** $p<0.01$, ***$p<0.001$, and ****$p<0.0001$. 30-minute time point: N = 3 TL control, n = 3 TL AA treated (0.005%). 115-minute time point: N = 3 TL control, n = 3 TL AA treated (0.005%).

3.9 c-fos, purinergic, cytokine, and TRP mRNA levels in response to AA treatment (TL AA treated vs Panx1a KO AA treated)

Behavioral testing revealed that Panx1a knockout (KO) zebrafish exhibited deficits in nociceptive signaling. To understand the underlying reasons, we studied the previously mentioned pain and neuroinflammation biomarkers using qPCR, comparing Panx1a KO zebrafish treated with AA to TL zebrafish treated with AA. The objective of these experiments was to determine whether the Panx1a gene modulates the mRNA levels of the genes studied in these AA experiments. Therefore, we predicted changes in the regulation of these biomarkers in Panx1a KO zebrafish treated with AA compared to TL zebrafish treated with AA.

This following investigation revealed the regulation of genes in the purinergic and c-fos gene families. Purinergic receptors are ATP ligand-gated ion channels associated with many different functions of neurons. The aspects that are focused on in my project are functions such as cell death, inflammation, immune response (microglia signaling), and neuron remodeling. These experiments reveal insights into the Panx1a gene’s role in these numerous functions.

The analysis of purinergic receptor genes revealed significant regulation of *p2rx4a* and *p2rx7*. *P2rx4a* showed a significant change in the 115-minute time point, and *p2rx4a* exhibited an almost significant increase in mRNA levels, with an expression of 1.566 (p-value = 0.054) (Figure 16 A). *P2rx7* exhibits a significant decrease in mRNA levels at the 35-minute time point, with an expression of 0.422 (p-value = 0.032) (Figure 17). Both genes have been implicated in microglia activity and nociceptive signaling (Inoue & Tsuda, 2021; Long et al., 2018; Monif et al., 2009). This is evidence that Panx1a could be regulating microglia activity and nociceptive signaling in response to AA treatments. Future studies should look at the pharmacological blockade of P2rx4a and P2rx7 in this AA model.

C-Fos is an early response gene that indicates neuron activity and is upstream of the activation of pathways that result in neuron cell remodeling. This gene has been implicated in associative learning of pain (Lin et al., 2018). The data suggests that the Panx1a is regulating the mRNA levels of numerous c-fos genes, this is evidence of Panx1a role in neuron activity and changes in morphology to AA treatments. This may also have higher implications for associative learning. Future studies should look into characterizing Panx1a function in operant conditioning procedures. These studies can provide insights into the role of Panx1a in learning and responding to environmental stressors.

The analysis of c-fos family genes highlights several notable trends. *C-fosAA* shows a significant increase in mRNA levels at the 30-minute time point, with an expression of 0.570 (p-value = 0.021). *C-fosAB* exhibits a significant decrease in mRNA levels at the 30-minute time point, with an expression of 0.404 (p-value = 0.001). *C-fosl2*

shows a significant decrease in mRNA levels at the 30-minute time point, with an expression of 0.65 (p-value = 0.049), but a notable increase at the 115-minute time point, with an expression of 1.172 (p-value = 0.596) (Figure 16 A,D).

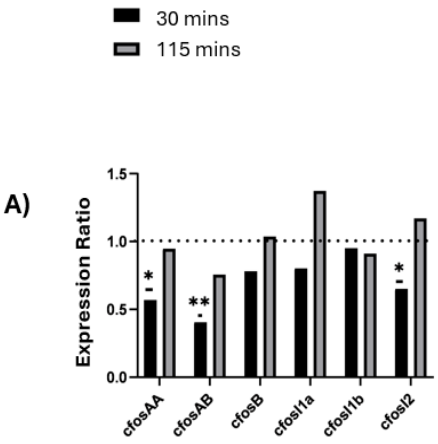

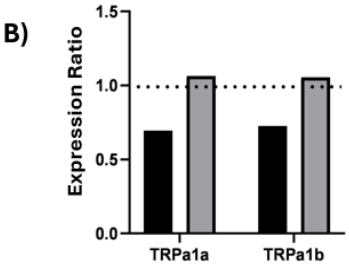

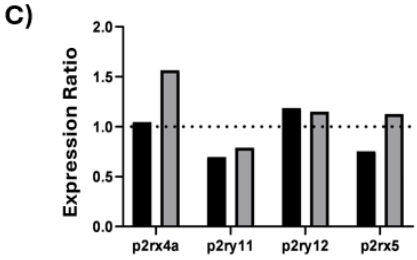

D)

TL AA treated vs Panx1a KO AA treated (30 minutes)

Gene	Expression	P(H1)	Result
p2rx4a	1.048	0.912	
p2ry11	0.698	0.329	
p2ry12	1.188	0.77	
p2rx5	0.754	0.239	
TRPa1a	0.694	0.236	
TRPa1b	0.725	0.317	
cfosAA	0.57	0.021	DOWN
cfosAB	0.404	0.001	DOWN
cfosB	0.78	0.463	
cfosl1a	0.802	0.401	
cfosl1b	0.95	0.92	
cfosl2	0.65	0.049	DOWN

E)

TL AA treated vs Panx1a KO AA treated (115 minutes)

Gene	Expression	P(H1)	Result
p2rx4a	1.566	0.054	
p2ry11	0.791	0.488	
p2ry12	1.151	0.75	
p2rx5	1.127	0.632	
TRPa1a	1.064	0.89	
TRPa1b	1.055	0.776	
cfosAA	0.948	0.862	
cfosAB	0.756	0.485	
cfosB	1.038	0.935	
cfosl1a	1.373	0.571	
cfosl1b	0.912	0.744	
cfosl2	1.172	0.596	

Figure 16: qPCR TL AA treated vs Panx1a KO AA treated. The gene families that were tested for expression in the Panx1a KO AA treated compared to TL AA treated: **a)** CFOS, **b)** TRP and **c)** purinergic receptor genes. The time points at which TL and Panx1a KO larvae were collected to study differences in mRNA levels after AA treatment were 30 minutes and 115 minutes**.** Data was analyzed using REST2009, **d) e)** the "expression" values are ratios that describe gene mRNA levels in AA treated TL larvae Panx1a KO AA treated compared to TL AA treated larvae. Significance values * p<0.05, ** p<0.01, ***p<0.001, and ****p<0.0001. 35-minute time point: n = 3 TL AA treated (0.005%), n = 3 Panx1a KO AA treated (0.005%). 120-minute time point: n = 3 TL AA treated (0.005%), n = 3 Panx1a KO AA treated (0.005%).

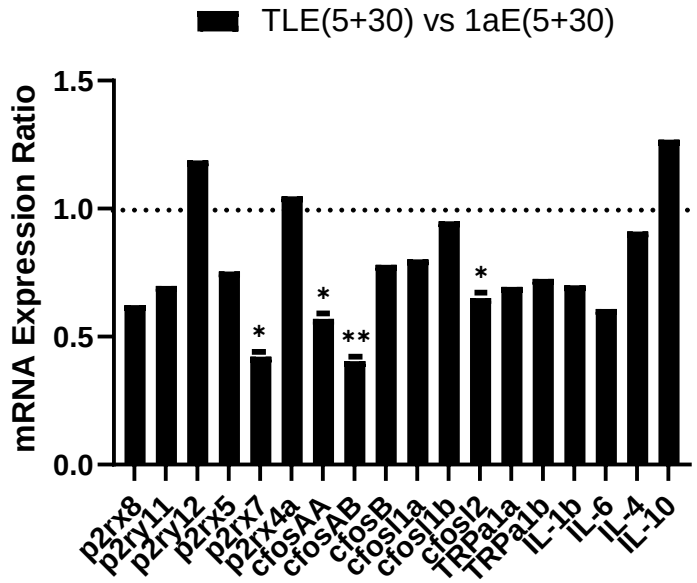

Figure 17: qPCR TL AA treated vs Panx1a KO AA treated. The gene families that were tested for expression in the AA-treated Panx1a KO (1AE). CFOS, purinergic, cytokine, and TRP genes. The time points at which larvae were collected to study differences in mRNA levels post-AA treatment: 35 minutes. Data was analyzed using REST2009, the values are ratios that describe mRNA levels in 1AE compared to TL AA-treated larvae (TLE). Significance values * p<0.05, ** p<0.01, ***p<0.001, and ****p<0.0001. 35-minute time point: n = 3 TL AA treated (0.005%), n = 3 Panx1a KO AA treated (0.005%).

3.10 c-fos mRNA levels in response to AA treatment (Panx1a KO Control vs Panx1a KO Panx1a)

qPCR was conducted on the Panx1a KO AA-treated group, using the untreated Panx1a KO group as the control. Specifically, we examined the mRNA levels of the c-fos family of genes. C-FOS is a biomarker of neuronal activity, and we aimed to characterize its regulation in response to AA treatments to gain insight into Panx1a's role in neuronal activity and nociceptive signaling. Previous studies have shown increased c-FOS immunostaining in response to harmful treatments in mouse models of pain (Harris, 1998; Lin et al., 2018). Given that Panx1 is implicated in nociceptive signaling (Hanstein et al., 2016; Spray & Hanani, 2019), we hypothesized that AA treatments would modulate c-fos upregulation in Panx1a KO AA-treated zebrafish compared to the Panx1a KO control group. Our results provide evidence of Panx1a's role in c-fos regulation in this AA model.

Some of the notable trends observed are as follows: *c-fosAA* (expression = 0.901, p-value = 0.639), *c-fosAB* (expression = 1.218, p-value = 0.457), *c-fosB* (expression = 1.253, p-value = 0.461), and *c-fosl2* (expression = 0.936, p-value = 0.829) show no significant regulation. However, *c-fosl1a* exhibits an upregulation of mRNA levels with an expression of 1.939 (p-value = 0.021), while *c-fosl1b* shows a downregulation of mRNA levels with an expression of 0.652 (p-value = 0.021) (Figure 18). This suggests that Panx1a KO zebrafish are exhibiting c-fos regulation in response to AA treatments. These results differ from the data in TL AA treated versus TL control, suggesting that Panx1a KO zebrafish exhibit deficits in neuron activity and ultimately

nociceptive signaling.

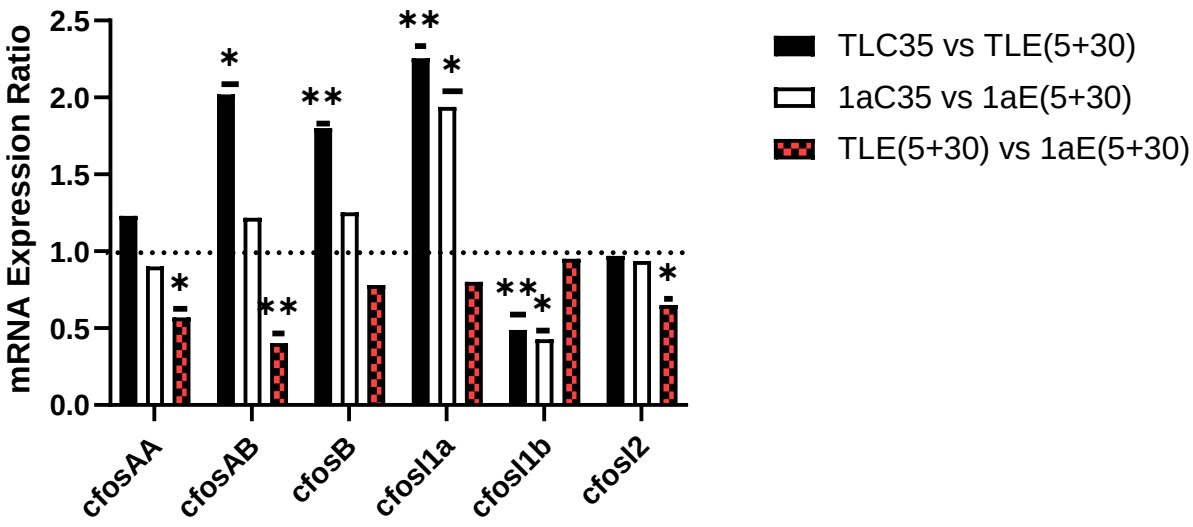

Figure 18: qPCR c-fos expression. mRNA levels of c-fos genes were assessed in 3 different groups. These groups include TL control vs TL AA treated (TLC35 vs TLE 5+30), Panx1a KO control vs Panx1a KO AA treated (1aC35 vs 1aE5+30) and TL AA treated vs Panx1a KO AA treated (TLE 5+30 vs 1aE 5+30). The time point at which these groups were collected: 35 minutes. Data was analyzed using REST2009, the values are ratios that describe mRNA levels in experimental groups vs the respective control groups. Significance values * p<0.05, ** p<0.01, ***p<0.001, and ****p<0.0001. 35-minute time point: n = 3 TL control, n = 3 TL AA treated (0.005%). 35-minute time point: n = 3 Panx1a KO control, n = 3 Panx1a KO AA treated (0.005%). 35-minute time point: n = 3 TL AA treated (0.005%), n = 3 Panx1a KO AA treated (0.005%).

3.11 RNA seq data (TLC vs 1AC)

We mined RNA-seq data from our group (Safarian et al., 2021) to identify potential differences in gene expression between untreated TL zebrafish and untreated Panx1a KO zebrafish for selected genes relevant to this study. The behavioral deficits observed in Panx1a KO zebrafish in response to AA treatments could be due to different baseline expressions of the biomarkers discussed in previous sections.

The genes analyzed were associated with the c-fos, purinergic, TRP, and cytokine families, specifically the genes tested in qPCR. The main question being asked is whether there are any baseline differences in gene expression. We predict that genes implicated in pain and inflammation, identified in both zebrafish and neuropathic mouse models, are differentially expressed, contributing to the deficits in nociceptive signaling.

Notable trends in the expression of key genes in the Panx1a KO include a significant downregulation of *Il4r.1* with a log2 fold change of -3.05 (p-value = 0.00079) and upregulation of *Il4r.2* with a log2 fold change of 7.96 (p-value = 0.002418). *Il6r* showed a downregulation with a log2 fold change of -0.84 (p-value = 0.032798) (Figure 19 B). *P2rx7* exhibited a downregulation with a log2 fold change of -1.13 (p-value = 8.79685E-08), while *p2rx4a* and *p2ry12* showed smaller, non-significant changes with log2 fold changes of -0.25 (p-value = 0.145413) and -0.82 (p-value = 0.301049), respectively (Figure 19 C). These results highlight alterations in gene expression in the Panx1a KO samples. This could be contributing to nociceptive deficits observed in Panx1a KO.

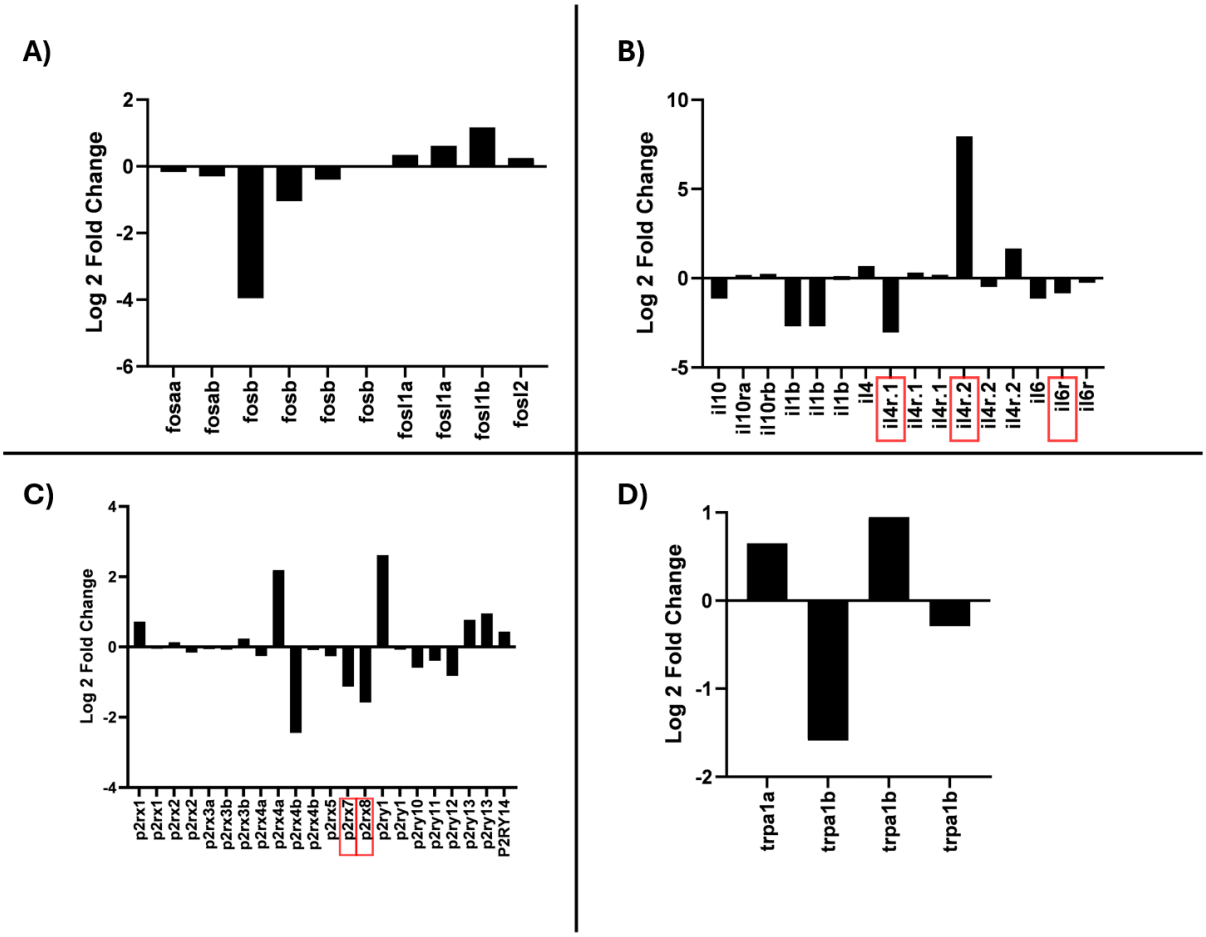

Figure 19: RNA sequencing data (TL vs Panx1a KO): This data describes mRNA expression levels of Panx1a KO compared to TL control larvae. These expression levels indicate differences in expression due to TALEN mediated knock out of the Panx1a gene. Highlighted in red are the genes that are significantly (p-value < 0.05) regulated. **a)** c-fos Family genes **b)** Cytokines and Cytokine receptor family genes **c)** Purinergic receptor family genes **d)** Transient receptor potential channel family (TRP).

3.12 ATP assay

ATP release from PANX1 channels has been noted as a mechanism to initiate inflammatory mechanisms in response to harmful stimuli. Extracellular ATP levels saw an increase in response to pain treatments in mice over 6 months, this suggests that ATP release is mediating nociceptive signaling (Spray and Hanani 2019). We

hypothesize that ATP release is mediating nociceptive signaling in response to AA treatments. We predicted that AA treatments would modulate extracellular ATP levels. Our research looked at defining the ATP release at the 1-hour time point. Our results showed no significant change (p-value=0.27) in ATP levels in TL control (4.4 nM/µg) vs TL AA treated (4.8 nM/µg) (Figure 20). This suggests that ATP levels are not altered due to the AA treatment.

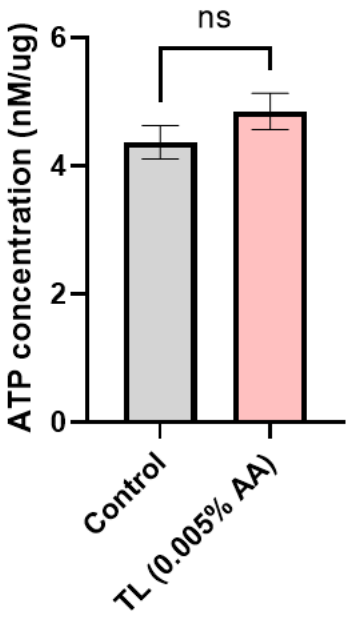

Figure 20: Extracellular ATP levels (nM/µg) of TL control (incubated for 60 minutes) and TL AA treated (5-minute AA treatment followed by 55-minute incubation). Analyzed using non-parametric T-test.

3.13 Immunohistochemistry

Our qPCR showed post 5-minute AA treatments and 30-minute incubation, *panx1a* mRNA levels were significantly down regulated (expression = 0.78, p-value = 0.055). Therefore, we characterized Panx1a protein localization and expression in response to the AA treatment, in hopes to unveil Panx1a mechanism of action in nociceptive signaling. We predicted there would be some modulation of protein expression due to previous results showing modulation of *panx1a* mRNA expression.

We performed immunohistochemistry to study Panx1a protein localization and expression. Following 5 min AA treatment and 30-minute incubation, the localization and expression of Panx1a appears unchanged after AA treatment (Supplementary Figure S53). This suggests that the observed behavioral changes in TL can't be attributed to changes in Panx1a protein expression or localization. This is consistent with the idea that channel activity is the primary contributor to changes to behavior.

4.0 Discussion

4.1 Behavioral changes in response to AA treatments

Panx1 is an ATP-release channel that has been implicated in the nociceptive signaling of mice (Spray & Hanani, 2019; Hanstein et al., 2016). This project uses the AA-treated zebrafish model (AA model) to study how Panx1a mediates pain and neuroinflammation. Our research aims to understand how Panx1 mediates nociception, ultimately leading to the development of targeted therapies for pain management. To achieve this, we use behavioral and molecular assays.

The behavioral assays tested the activity of zebrafish larvae and assessed the response to AA treatments. Burst activity, defined as movements at speeds greater than 15 mm/s, were assessed in Tupel Longfin (TL) and Panx1a knockout (KO) zebrafish larvae treated with varying concentrations of AA. The Panx1a KO larvae exhibited a higher threshold for BDA increases than the TL larvae (Figure 9D). The same trend was observed when assessing FDA, which is detected as immobile activity (Figure 10D). This suggests that Panx1a KO larvae, require a greater concentration of AA, to elicit the same level of modulation to burst/freeze activity as seen in TL larvae, indicating that Panx1a plays a crucial role in mediating the behavioral response of zebrafish to AA.

In contrast, Panx1b KO larvae behaved very similarly to the TL fish in response to AA treatments. When treated with 0.00125% AA, Panx1b KO larvae exhibited a significant increase in BDA. This suggests that Panx1a, depending on its localization, mediates nociceptive signaling, while Panx1b does not. Panx1a is expressed ubiquitously, whereas Panx1b is primarily found in the retina, where it is expressed on astrocytes. The behavioral effect of the AA treatment on the Panx1b KO needs to be further explored (Safarian et al., 2021;Safarian et al., 2020). Future studies should look into bridging our understanding of astrocytes role in nociception.

Panx1a is expressed in microglia and sensory neurons (DRG and TG) (Xing et al., 2024), behavioral data provides evidence that Panx1a mediates the nociceptive signaling in response to AA treatments. Mice models have revealed Panx1 to be localized to postsynaptic densities with NMDA receptors, this suggest Panx1 may be implicated in the activation of these receptors (Zoidl et al., 2007, Bravo et al., 2022).

This mechanism is not well understood in zebrafish in the context of our AA model. Future studies should focus on elucidating the mechanisms underlying Panx1a's modulation of NMDA receptor activity and its role in nociceptive signaling. Pharmacological blockade of NMDA receptors could give us insight to this mechanism.

4.2 Pharmacological Insights

We characterized the behavioral response to pharmacological treatments: probenecid, a PANX1 channel blocker, and ibuprofen, a COX-1 and COX-2 inhibitor. We also assessed how these treatments would affect behavior in AA-treated larvae.

4.2.1 Probenecid

Probenecid is a well-known pannexin channel blocker and has been shown to reduce pain responses in the orofacial pain model of mice (Fejes-Szabó et al., 2015). The rationale behind using probenecid in this AA model is based on its demonstrated ability to inhibit ATP release via PANX1 channels (Fejes-Szabó et al., 2015; Hainz et al., 2016). This suggests that PANX1-mediated ATP release influences neuronal excitation in nociceptive signaling. Consequently, it is expected that larvae treated with probenecid will show a reduced nociceptive response to AA treatments.

We saw significant changes in the behavior of dual-treated (probenecid and AA-treated) fish compared to fish treated with AA (Figure 11 A, B & 12 A, B). This suggests that blocking Panx1 channels results in significantly different responses to AA treatments. This is evidence that pannexin is mediating nociceptive signaling pathways in response to AA treatments. This is similar to the effects we observed in Panx1a KO

larvae and aligns with previous studies that demonstrate rescue of behavioral changes following probenecid treatments (Gusso et al., 2022).

4.2.2 Ibuprofen

Ibuprofen is classified as a nonsteroidal anti-inflammatory drug (NSAID) and works by inhibiting cyclooxygenase (COX) enzymes. Ibuprofen specifically inhibits COX-1 and COX-2, which are responsible for converting arachidonic acid into prostaglandins (Mazaleuskaya et al., 2015). Prostaglandins are mediators of pain, inflammation, and fever. Therefore, we predicted that ibuprofen would alleviate behavioral changes due to AA treatments.

We observed some notable effects. Firstly, we saw a dose-dependent effect of ibuprofen on activity. At a concentration of 50 μM, ibuprofen-treated larvae showed a significant behavior change (BDA/FDA) (Figures 13 D & 14 C). However, at a lower concentration of 25 μg/L, activity was not significantly altered in response to ibuprofen treatments (Figures 13 A, C & 14 B, D). The rationale for using the 25 μg/L concentration is based on previous studies showing that larvae treated with this dose exhibited decreased heart rates (Zhang et al., 2020). We hypothesized that this concentration would also affect behavior. The 50 μM concentration of ibuprofen was chosen because it was the highest dose that did not result in larval mortality.

Secondly, at lower concentrations of ibuprofen (25 μg/L), no rescue of pain behavior was observed in the AA model. Also, ibuprofen-treated fish (50 μM) did not show any improvement in behavioral effects induced by AA. We conclude that ibuprofen does not alleviate pain symptoms in zebrafish larvae in response to AA treatments. This

raises questions about the mechanism of pain detection in AA treatments. Ibuprofen is an anti-inflammatory drug that targets the inhibition of COX-1 and COX-2 enzymes. These results suggest that Panx1a plays a more significant role in nociceptive signaling than the inflammation pathways mediated by COX-1 and COX-2.

4.2.3 Pharmacological findings

In summary, blocking pannexin channels rescues the behavioral changes to AA treatments. These results in conjunction with the Panx1a KO behavioral assessment conclude that pannexin is mediating behavioral response to AA treatments. These results are consistent with the findings in neuropathic mice, following targeted inhibition of Panx1 (Hanstein et al., 2016; Spray & Hanani, 2019).

Other observations that can be inferred from the data: the effects of ibuprofen on burst and freeze activities are dose dependent. Higher concentrations (50 μM) have a more pronounced impact, indicating that sufficient dosing is necessary to observe significant behavioral changes. Secondly, the data definitively shows that inhibiting the COX-1 and COX-2 pathways of inflammation does not rescue changes in behavior induced by AA treatments. These results suggest that Panx1a plays a more significant role in nociceptive signaling, in response to AA treatments, than the pathways of inflammation induced by COX-1 and COX-2. Therefore, research and development of more specific drugs targeting pannexin could lead to novel therapeutic strategies for pain management.

4.3 c-fos expression

4.3.1 *c-fos* regulation in response to AA treatments

C-fos genes are early response genes that have been known to be regulated in response to harmful stimuli and environmental stressors in mice models (Jaworski et al., 2018; Lin et al., 2018). C-FOS upregulation is recognized as a biomarker of neural activity and, consequently, serves as an indicator of the activity within nociceptive neural networks. (Harris, 1998). In this model, we study the expression of *c-fos* genes in response to AA treatments.

Following AA treatments TL larvae exhibited significant changes in *c-fos* mRNA levels; we observed significant upregulation of *c-fosab*, *c-fosb*, and *c-fosl1a* in the first 35 min after AA treatments. Following this upregulation, we observe a crash in mRNA levels at the 120-minute time point. This data suggests a temporal regulation of *c-fos* genes in response to AA treatments (Figure 15 B). This is consistent with previous findings showing that c-FOS immunostaining levels peaked at the 30-60 minute period post stress treatment in mice pain models (Lin et al., 2018). This data suggests that AA treatments modulate nociceptive neuron activity.

These qPCR results are not conclusive in determining whether c-Fos protein levels are upregulated in response to AA treatments, as increased mRNA levels do not necessarily translate to higher protein expression. However, this study does conclude that *c-fos* mRNA levels are increased post-AA treatments. Future studies should focus on characterizing c-Fos protein expression in response to AA treatments to support these findings.

4.3.2 *c-fos* expression in Panx1a KO in response to AA treatments

To build on the results of the TL larvae, we tested *c-fos* expression in Panx1a KO larvae in response to AA treatments. Functional neuropathic mice models have shown the c-FOS immunoreactivity significantly increased in the dorsal column 7 days following neuropathic pain induction, this effect was ameliorated due to the pharmacological blockade of PANX1 (Mousseau et al., 2018). Considering that c-FOS is a marker of neuron activity, this suggests that the blockade of Panx-1 significantly modulated neuron activity in response to neuropathic treatments. This has not been explored in zebrafish or the context of a Panx1a KO model.

The AA-treated Panx1a KO saw upregulation of *c-fosl1a* and significant downregulation of *c-fosl1b* (Figure 18). Both of these trends were observed in the TL control vs TL AA treated. Unlike the TL, we did not see any upregulation of *c-fosab* and *c-fosb*. Notably, the AA concentration used was on the higher end (0.005% AA), eliciting significant behavioral changes in Panx1a KO. These results suggest that 0.005% AA treatments also elicit *c-fos* regulation. Panx1a KO larvae did not show significant changes in BDA/FDA in response to 0.00125% AA treatments. Future studies should investigate *c-fos* expression levels in response to a lower AA concentration (0.00125%) to address gaps in knowledge about Panx1a's role in *c-fos* regulation. Based on behavioral data, we predict that Panx1a KO larvae will exhibit modulated *c-fos* expression in response to lower AA treatments.

Although we do see some regulation of *c-fos* family genes, it doesn't reflect what we see in the TL. Mice studies have shown that inhibition of c-FOS resulted in memory deficits (Lin et al., 2018). It is not known whether Panx1a KO larvae will exhibit deficits in learning harmful stimuli. Future studies should look at operant conditioning protocols

and study the behavior of the TL and Panx1a KO genotypes. This could reveal insights into Panx1a's role in learning harmful stimuli. Due to differing *c-fos* expression levels, we hypothesize that Panx1a KO will show differences in learning the association of harmful stimuli with environmental cues.

4.3.3 Panx1a mediates expression levels of *c-fos* family genes in response to AA treatments

This study attempted to uncover the mechanisms implicated in the nociceptive deficits observed in Panx1a KO larvae and probenecid-treated larvae. To study Panx1a's role in nociceptive neuron activity, we investigated the levels of *c-fos* mRNA in Panx1a KO AA treated compared to TL AA treated. The data showed significant downregulation of *c-fosaa*, c-*fosab*, and *c-fosl2* (Figure 18). Considering there is no evidence of significant changes in baseline regulation of these genes in the RNA seq data (Figure 19), this suggests that the AA treatments are eliciting differences in *c-fos* expression in TL compared to Panx1a KO genotypes. Therefore, we have evidence that the Panx1a KO has altered nociceptive neuron activity in response to AA treatments.

What is Panx1a's possible role in nociceptive signaling mechanisms? Mice pain studies have implicated the upregulation of c-FOS by NMDA receptor activity in response to harmful treatments (Chapman et al., 1995.) and functional neuropathic mice models have shown that NMDA activation in nociceptive signaling is dependent on PANX1 activation (Bravo et al., 2022). This could suggest that c-fos activation is dependent on Panx1a + NMDA activity in nociceptive signaling pathways in this zebrafish AA model. Therefore, future studies should investigate the pharmacological

modulation of NMDA receptor activity. This could give insight into mechanisms of nociceptive signaling mediated by Panx1a.

4.4 Biomarkers of pain and neuroinflammation

This project aimed to identify any regulation of biomarkers associated with pain and neuroinflammation in response to AA treatments. The main question trying to be answered is whether any of the genes that are associated with pain and neuroinflammation are implicated in this AA model. Another question explored is whether Panx1a is mediating the expression levels of any genes of interest. This could explain the behavioral deficits observed in Panx1a KO larvae in response to AA treatments. The genes of interest associated with pain and neuroinflammation include the purinergic receptor family, cytokines, and *trpa1a/b*.

4.4.1 Purinergic receptors of interest

Purinergic receptors bind the ATP ligand, and extracellular ATP communicates harmful environmental conditions on a cellular level (Munoz et al., 2021). Purinergic receptors play a role in the modulation of synaptic plasticity and can modulate nociceptive signaling. This gene family was studied because purinergic receptors are predicted to be implicated in nociceptive signaling and the immune response to harmful stimuli (S. Li et al., 2014; Rodríguez et al., 2008). We hypothesized that AA treatments would regulate the expression of purinergic receptor genes. These qPCR results reveal the involvement of purinergic receptors in nociceptive signaling and the immune response to AA treatments.

P2rx4a

The *p2rx4a* gene has not been explored in the context of zebrafish CNS. This gene is an ohnologue of the human *P2RX4* gene, therefore these results could give us insight into the function of said gene. This gene has been associated with neuropathic pain (Inoue et al., 2012), and studies have suggested that activation of this receptor results in pain symptoms (Inoue & Tsuda, 2021; Long et al., 2018; W. jun Zhang et al., 2020).

The literature shows that in response to neuropathology, P2RX4 is upregulated, primarily in the microglia (Montilla et al., 2020). Studies in mice, utilizing the nitroglycerin (NTG) model for chronic migraine, demonstrated increased mechano-sensitivity and upregulation of P2rx4 protein expression.

In this current model, the *p2rx4a* gene is downregulated in TL AA treated compared to TL control (Figure 15 A). Our data also revealed that *p2rx4a* is upregulated in the Panx1a KO AA treated compared to TL AA treated (Figure 16 C). This suggests that Panx1a mediates the expression levels of *p2rx4a*, this could implicate the *p2rx4a* gene in the nociceptive deficits observed in Panx1a KO larvae. qPCR has its limitations, as it is not always clear whether changes in mRNA regulation correspond to changes in protein expression. Therefore, future studies should focus on characterizing P2rx4a protein expression in response to AA treatments. This could provide valuable insights into the role of P2rx4a in this AA model.

Is there a possible role of P2rx4a and microglia in nociceptive signaling, in response to AA treatments? Past studies in mice have shown that blockade of P2rx4

activity led to deficits in nociceptive signaling (Long et al., 2018; W. jun Zhang et al., 2020). Treatment with 5-BDBD (P2RX4 antagonist) prevented NTG-induced mechano-sensitivity, indicating a potential therapeutic target (Long et al.,2018). The interaction between Panx1a and P2rx4a is not well understood and could provide insight into nociception in the current AA model. The pharmacological blockade of P2rx4a could provide insight into its possible involvement in behavioral changes induced by AA treatments.

P2rx7

P2RX7 is an ATP ligand-gated cation channel that is heavily implicated in chronic pain models of mice (Spray & Hanani, 2019). After binding ATP this channel allows for the influx of calcium and consequently the depolarization of the neuron. P2RX7 activation initiates a positive feedback loop, leading to increased PANX1-mediated ATP release. Downstream to this signaling, neuroinflammatory mechanisms are activated, proteins such as NLRP3 inflammasome are activated and the production of pro-inflammatory cytokines is upregulated (Jiang et al., 2017).

The current findings give us some insight into the function of P2rx7 in this AA model. Although insignificant we noted a downregulation of the *p2rx7* expression in TL AA-treated compared to TL control (Figure 15 A). This could suggest that P2rx7 has a role in the nociceptive signaling of AA treatments. Although there is no evidence for this, past studies have shown inhibition of P2rx7 did not affect the changes induced by AA. Researchers suggested this was due to the concentrations of the drug tested (Gusso et al., 2022).

The literature suggests that P2rx7 activity is dependent on high extracellular ATP levels (Adinolfi et al., 2018; Burnstock & Knight, 2018; Miteva et al., 2020). It is important to note, that there is no evidence of high extracellular ATP in response to AA treatments in this study (Figure 20). Evidence from results is not conclusive, whether or not P2rx7 has a role in nociception to AA treatments.

This project investigated whether Panx1a is mediating the expression of *p2rx7*. We observed significant downregulation of *p2rx7* in the Panx1a KO AA-treated group compared to the TL AA-treated group. This suggests that Panx1a is involved in regulating *p2rx7* expression levels (Figure 17). RNA seq data also shows a significant down expression of *p2rx7* in the Panx1a KO compared to the control. This could suggest that Panx1a is mediating the activation of P2rx7 (Figure 19). As previously stated, qPCR has its limitations, and future studies should investigate the protein expression of P2rx7 in this AA model.

Not much is known about how p2rx7, expressed on microglia, mediates nociceptive signaling. Targeted inhibition of p2rx7 in neuropathic mice models caused deficits in nociceptive signaling (Bhattacharya & Biber, 2016; Dalgarno et al., 2018; Honore et al., 2006). We cannot conclude based on previous AA models (Gusso et al., 2022), and our results, that *p2rx7* is not implicated in mediating nociceptive signaling. Future studies should look into the pharmacological blockade of P2rx7 in this AA model to address gaps in knowledge.

In conclusion, the purinergic genes of interest in this model: *p2rx4a* and *p2rx7* are implicated in modulating microglia activity. The role of microglia in modulating nociceptive signaling pathways remains unclear. Further investigation is needed to

understand the function of purinergic receptors, particularly through pharmacological blockade. Behavioral assays could provide valuable insights into how microglia influence nociceptive signaling in this AA model.

4.4.2 Cytokines of interest

Cytokines are prime biomarkers of pain and inflammation and more specifically microglia activity. Past studies have shown that cytokines are regulated in response to harmful treatments, suggesting increased microglia activity under these conditions. (Babchenko et al., 2022; Gan et al., 2020). We hypothesize that AA treatments will elicit microglia activity. Therefore, we predicted these cytokines to be regulated in this AA model.

M1 microglia are associated with pro-inflammatory responses. They secrete a variety of cytokines and chemokines that promote inflammation and are typically involved in the initial response to injury or infection. In this project we study the mRNA levels of pro-inflammatory cytokines: Interleukin-1 beta (IL-1β) and Interleukin-6 (IL-6) (Arruda et al., 1998; Gruol, 2015; Karavis et al., 2023).

M2 microglia are associated with anti-inflammatory and tissue repair processes. They secrete cytokines and growth factors that promote tissue repair, resolution of inflammation, and restoration of homeostasis. In this project, we study the mRNA levels of anti-inflammatory cytokines: Interleukin-4 (IL-4) and Interleukin-10 (IL-10) (Bottiglione et al., 2020; Shemer et al., 2020).

Previous studies have shown the secretion of these cytokines in neuroinflammatory models, more specifically a zebrafish brain lesion model (Gan et al.,

2020). The objective was to study whether AA treatments are eliciting an immune response, mediated by microglia. We hypothesized that there would be some regulation of pro-inflammatory and anti-inflammatory cytokines in response to AA treatments. Our results showed that to be the case, although, no evidence in our qPCR results suggested any modulation of cytokine levels was mediated by Panx1a. RNA-seq data, on the other hand, showed down expression of *il-4r* and *il-6r* in Panx1a KO compared to TL. This evidence may suggest that Panx1a KO exhibits a modulated immune response to AA treatments.

Significant downregulation of *il-6* was observed in TL AA treated compared to TL control (Figure 15 C). In the context of the CNS, Il-6 is secreted by glial cells and neurons. It has been reported to be upregulated in response to damage to the CNS (Arruda et al., 1998). In the context of zebrafish, the function is not well understood, but it is predicted to activate microglia (Babchenko et al., 2022; Rodríguez et al., 2008). In conclusion, the modulation of *il-6* expression levels is evidence that AA treatments may be modulating microglia activity.

Il-4 signaling is critical in inhibiting pro-inflammatory signaling in zebrafish gill (Bottiglione et al., 2020). The role of Il-4 in the CNS homeostasis of zebrafish is not well understood, although it is predicted to have neuroprotective effects in the CNS. Vogelaar et al. (2018) utilized the experimental autoimmune encephalomyelitis (EAE) model in mice, which mimics aspects of multiple sclerosis (MS), to investigate the therapeutic potential of interleukin-4 (Il-4) in neuroinflammation. They found that Il-4 treatment during the chronic phase of EAE significantly improved clinical outcomes and

axonal morphology. Il-4 exerted its beneficial effects through direct neuronal signaling promoting cytoskeletal remodeling and axonal repair (Vogelaar et al., 2018).

A significant downregulation of *il-4* was observed in TL AA treated compared to TL control (Figure 15 C). In conclusion, *il-4* expression levels are regulated in response to AA treatments, and this suggests that AA treatments are modulating an immune response. RNA seq data showed low basal expression of *il-4r* in the Panx1a KO, this raises questions about how these neuroprotective mechanisms are affected (Figure 19 B).

Significant downregulation of *Il-10* was observed in TL AA treated compared to TL control. *Il-10* is shown to mediate inflammation in zebrafish gills, Il-10 deficient fish exhibited prolonged inflammation in response to irritants (Bottiglione et al., 2020). It is predicted to have an anti-inflammatory effect on the CNS, studies have shown that Il-10 does modulate microglial function, exerting anti-inflammatory effects (Shemer et al., 2020). In conclusion, significant downregulation of *il-10* in response to AA treatments is evidence that microglia activity may be modulated in response to AA treatments.

In conclusion, this data suggests that AA treatments are modulating the gene expression levels of multiple cytokines involved in regulating the homeostasis of the CNS. This evidence could suggest that microglia activity is modulated, as they are the resident macrophages of the CNS responsible for maintaining homeostasis. There is no evidence of Panx1a regulating the expression levels of any cytokines studied, although RNA seq results show decreased expression of *il-4r* and *il-6r* (Figure 19 B), this may be evidence of a deficiency in homeostatic response to external stressors. Future studies

should investigate microglia activity in Panx1a KO, immunological staining could give us insights into how Panx1a mediates the activity of microglia.

4.4.3 Panx1a

In this current study we observed significant downregulation of *panx1a* mRNA in TL AA treated compared to TL control. Past mice studies have shown significant modulation of *Panx1* mRNA and PANX1 protein levels in response to neuropathic pain treatments (Hanstein et al., 2016; Xing et al., 2024; Y. Zhang et al., 2015). Therefore, after qPCR experiments, we looked to characterize Panx1a protein expression and localization in response to AA treatments. We observed no change to Panx1a protein expression of localization in response to AA treatments. This data suggests that behavioral changes to AA treatments are not due to differential expression or localization of Panx1a. This is consistent with the theory that Panx1a opening/closing is modulating acute nociceptive signalling. As previously stated, microglia express Panx1a and this data could also suggest that microglia activity is modulated in response to AA treatments.

4.4.4 Trpa1b

In this current study, we observed downregulation of *trpa1b* in TL AA treated compared to TL control. This gene has been closely associated with the detection of chemical irritants (Ko et al., 2019). We hypothesized regulation of the *trpa1a/b* gene in response to AA treatments. The results provide evidence of regulation of *trpa1b* in response to AA treatments, although there is no evidence of Panx1a mediation of *trpa1b* expression levels. Its role in this pain model can be further investigated through

pharmacological blockade. This gene could play a critical role in nociception in peripheral organs of zebrafish larvae in response to AA treatments.

4.5 Future directions

P2rx7 is an ATP ligand-gated cation channel that is heavily implicated in chronic pain models of mice (Spray & Hanani, 2019). After binding ATP this channel allows for the influx of calcium and consequently the depolarization of the neuron. Not much is known about this mechanism in terms of nociceptive signaling. Positive feedback signaling activation of P2rx7 and Panx1a could be mediating acute nociceptive signaling through modulation of NMDA activity at the sensory synapse. Future studies should focus on elucidating the mechanisms underlying Panx1a's modulation of NMDA receptor activity and its role in nociceptive signaling. Pharmacological blockade of NMDA receptors could give us insight.

It is important to note, that we have no evidence of increased extracellular ATP response to AA treatments. Although not significant, *p2rx7* expression was downregulated in TL AA treated compared to TL control. To add to this, we have evidence of Panx1a modulating *p2rx7* expression levels. This could explain the deficits in nociceptive signaling observed with the Panx1a KO and pharmacological blockade of Panx1. Therefore, future studies should look at the pharmacological blockade of P2xr7 receptors to study its role in nociception in response to AA treatments. qPCR methods are limited, expression levels don’t necessarily translate to protein expression. Therefore, we should investigate, the protein expression of p2rx7 to study if it is implicated in this AA model.

An aspect that should be further investigated is the role of P2rx4 in nociception, evidence suggests that *p2rx4a* were downregulated in response to AA treatments. Functional mice models have shown that P2rx4 is associated with the activation of microglia and neuropathic pain (Long et al., 2018). This evidence suggests the role of microglia could be mediating nociceptive signaling to harmful stimuli. Future behavioral studies should look at treating zebrafish larvae with a P2rx4 channel blocker in this AA model. Again, due to qPCR limitations, we should investigate the protein expression of P2rx4a to study its implications in this AA model.

Currently, the data shows that genes associated with the immune response and more specifically, microglia activity are regulated in this AA model. Not much is understood about the mechanisms underlying nociceptive signaling and how it is modulated by microglia activity. The P2rx4a and P2rx7 receptors should be further studied to address some of the gaps in knowledge. As stated previously, literature provides ample evidence that Panx1 expressed in microglia can mediate nociceptive signaling in neuropathic mice (Hanstein et al., 2016; Mousseau et al., 2018). Future immunological staining studies should look at characterizing microglial activity in our AA model.

4.6 Conclusion

In this project we induced nociceptive signaling using AA treatments to study nociceptive responses in zebrafish. Our findings have been consistent with those from neuropathic mice models, showing that targeted inhibition of Panx1 causes deficits in nociceptive signaling. This suggests that zebrafish are a viable model to study

nociceptive signaling. This study has demonstrated that zebrafish offer several advantages for research, potential for high-throughput drug screening, the ability to apply drugs non-invasively, and a 70% conservation of proteins and genes with mammals. Pain and nociception are well conserved, as they are critical for an organism's survival. Studying pain in zebrafish offers us new possibilities for drug discovery. Based on our results, we propose developing specific drugs targeting pannexin for pain management therapies.

Based on behavioral data, Panx1a mediates behavioral changes in response to AA treatments. Pharmacological data show that blockade of Panx1 with probenecid leads to deficiencies in nociceptive signaling in response to AA treatments, further implicating Panx1a in nociceptive signaling. We determined temporal regulation of *c-fos* genes in response to AA treatments and evidence shows Panx1a is mediating *c-fos* expression levels. Considering that *c-fos* is an indicator of neuron activity, it suggests that Panx1a is mediating neuron activity in response to AA treatments. This study also revealed that *p2rx7* and *p2rx4a* mRNA levels are modulated by Panx1a. The mammalian ohnologues are implicated in microglia and nociceptive signaling and therefore P2rx7 and P2rx4a could be implicated in this zebrafish AA model.

In conclusion, this zebrafish AA model has proven to be effective in studying Panx1a’s role nociception, paving the way for new opportunities in zebrafish research, particularly in the field of drug discovery.

5.0 References

Adinolfi, E., Giuliani, A. L., De Marchi, E., Pegoraro, A., Orioli, E., & Di Virgilio, F. (2018). The P2X7 receptor: A main player in inflammation. In *Biochemical Pharmacology* (Vol. 151, pp. 234–244). Elsevier Inc. https://doi.org/10.1016/j.bcp.2017.12.021

Allouche, S., Noble, F., & Marie, N. (2014). Opioid receptor desensitization: Mechanisms and its link to tolerance. In *Frontiers in Pharmacology* (Vol. 5, Issue DEC). Frontiers Media S.A. https://doi.org/10.3389/fphar.2014.00280

Arruda, J. L., Colburn, R. W., Rickman, A. J., Rutkowski, M. D., & Deleo, J. A. (1998). Interactive report Increase of interleukin-6 mRNA in the spinal cord following peripheral nerve injury in the rat: potential role of IL-6 in neuropathic pain 1. In *Molecular Brain Research* (Vol. 62).

Babchenko, V. Y., Belova, A. S., Bashirzade, A. A., Tikhonova, M. A., Demin, K. A., Zabegalov, K. N., Petersen, E. V., Kalueff, A. V., & Amstislavskaya, T. G. (2022). Traumatic Brain Injury Models in Zebrafish (Danio rerio). *Neuroscience and Behavioral Physiology*, *52*(3), 405–414. https://doi.org/10.1007/s11055-022-01254-y

Bautista, D. M., Pellegrino, M., & Tsunozaki, M. (2013). TRPA1: A gatekeeper for inflammation. In *Annual Review of Physiology* (Vol. 75, pp. 181–200). https://doi.org/10.1146/annurev-physiol-030212-183811

Baxter, M., Eltom, S., Dekkak, B., Yew-Booth, L., Dubuis, E. D., Maher, S. A., Belvisi, M. G., & Birrell, M. A. (2014). Role of transient receptor potential and pannexin channels in cigarette smoke-triggered ATP release in the lung. *Thorax*, *69*(12), 1080–1089. https://doi.org/10.1136/thoraxjnl-2014-205467

Bhattacharya, A., & Biber, K. (2016). The microglial ATP-gated ion channel P2X7 as a CNS drug target. In *GLIA* (Vol. 64, Issue 10, pp. 1772–1787). John Wiley and Sons Inc. https://doi.org/10.1002/glia.23001

Bond, S. R., Wang, N., Leybaert, L., & Naus, C. C. (2012a). Pannexin 1 ohnologs in the teleost lineage. *Journal of Membrane Biology*, *245*(8), 483–493. https://doi.org/10.1007/s00232-012-9497-4

Bond, S. R., Wang, N., Leybaert, L., & Naus, C. C. (2012b). Pannexin 1 ohnologs in the teleost lineage. *Journal of Membrane Biology*, *245*(8), 483–493. https://doi.org/10.1007/s00232-012-9497-4

Bottiglione, F., Dee, C. T., Lea, R., Zeef, L. A. H., Badrock, A. P., Wane, M., Bugeon, L., Dallman, M. J., Allen, J. E., & Hurlstone, A. F. L. (2020). Zebrafish IL-4–like Cytokines and IL-10 Suppress Inflammation but Only IL-10 Is Essential for Gill Homeostasis. *The Journal of Immunology*, *205*(4), 994–1008. https://doi.org/10.4049/jimmunol.2000372

Bourne, S., Machado, A. G., & Nagel, S. J. (2014). Basic anatomy and physiology of pain pathways. In *Neurosurgery Clinics of North America* (Vol. 25, Issue 4, pp. 629–638). W.B. Saunders. https://doi.org/10.1016/j.nec.2014.06.001

Bravo, D., Zepeda-Morales, K., Maturana, C. J., Retamal, J. S., Hernández, A., Pelissier, T., Barra, R., Sáez-Briones, P., Burgos, H., & Constandil, L. (2022). NMDA and P2X7 Receptors Require Pannexin 1 Activation to Initiate and Maintain Nociceptive Signaling in the Spinal Cord of Neuropathic Rats. *International Journal of Molecular Sciences*, *23*(12), 6705. https://doi.org/10.3390/ijms23126705

Burma, N. E., Bonin, R. P., Leduc-Pessah, H., Baimel, C., Cairncross, Z. F., Mousseau, M., Shankara, J. V., Stemkowski, P. L., Baimoukhametova, D., Bains, J. S., Antle, M. C., Zamponi, G. W., Cahill, C. M., Borgland, S. L., De Koninck, Y., & Trang, T. (2017). Blocking microglial pannexin-1 channels alleviates morphine withdrawal in rodents. *Nature Medicine*, *23*(3), 355–360. https://doi.org/10.1038/nm.4281

Burnstock, G. (2013). Purinergic mechanisms and pain - An update. In *European Journal of Pharmacology* (Vol. 716, Issues 1–3, pp. 24–40). Elsevier B.V. https://doi.org/10.1016/j.ejphar.2013.01.078

Burnstock, G., & Knight, G. E. (2018). The potential of P2X7 receptors as a therapeutic target, including inflammation and tumour progression. In *Purinergic Signalling* (Vol. 14, Issue 1). Springer Netherlands. https://doi.org/10.1007/s11302-017-9593-0

Campagno, K. E., & Mitchell, C. H. (2021). The P2X7 Receptor in Microglial Cells Modulates the Endolysosomal Axis, Autophagy, and Phagocytosis. In *Frontiers in Cellular Neuroscience* (Vol. 15). Frontiers Media S.A. https://doi.org/10.3389/fncel.2021.645244

Campbell, J. N., & Meyer, R. A. (2006). Mechanisms of Neuropathic Pain. In *Neuron* (Vol. 52, Issue 1, pp. 77–92). https://doi.org/10.1016/j.neuron.2006.09.021

Chapman, V., Honore, P., Buritova, J., & Besson, J.-M. (n.d.). *The contribution of NMDA receptor activation to spinal c-Fos expression in a model of inflammatory pain*.

Costigan, M., Scholz, J., & Woolf, C. J. (2009). Neuropathic pain: A maladaptive response of the nervous system to damage. In *Annual Review of Neuroscience* (Vol. 32, pp. 1–32). https://doi.org/10.1146/annurev.neuro.051508.135531

Dalgarno, R., Leduc-Pessah, H., Pilapil, A., Kwok, C. H. T., & Trang, T. (2018). Intrathecal delivery of a palmitoylated peptide targeting Y382-384 within the P2X7 receptor alleviates neuropathic pain. *Molecular Pain*, *14*. https://doi.org/10.1177/1744806918795793

Fejes-Szabó, A., Bohár, Z., Nagy-Grócz, G., Vámos, E., Tar, L., Pődör, B., Tajti, J., Toldi, J., Vécsei, L., & Párdutz, Á. (2015). Send Orders for Reprints to reprints@benthamscience.ae Effect of Probenecid on the Pain-Related Behaviour and Morphological Markers in Orofacial Formalin Test of the Rat. In *CNS & Neurological Disorders-Drug Targets* (Vol. 14).

Gallo, F. T., Katche, C., Morici, J. F., Medina, J. H., & Weisstaub, N. V. (2018). Immediate early genes, memory and psychiatric disorders: Focus on c-Fos, Egr1 and Arc. In *Frontiers in Behavioral Neuroscience* (Vol. 12). Frontiers Media S.A. https://doi.org/10.3389/fnbeh.2018.00079

Gan, D., Wu, S., Chen, B., & Zhang, J. (2020). Application of the Zebrafish Traumatic Brain Injury Model in Assessing Cerebral Inflammation. *Zebrafish*, *17*(2), 73–82. https://doi.org/10.1089/zeb.2019.1793

Gilmore, S. A. (n.d.). *Proliferation of Non-neuronal Cells in Spinal Cords of Irradiated, Immature Rats Following Transection of the Sciatic Nerve*.

Gilron, I., Baron, R., & Jensen, T. (2015). Neuropathic pain: Principles of diagnosis and treatment. *Mayo Clinic Proceedings*, *90*(4), 532–545. https://doi.org/10.1016/j.mayocp.2015.01.018

Gruol, D. L. (2015). IL-6 regulation of synaptic function in the CNS. *Neuropharmacology*, *96*(PA), 42–54. https://doi.org/10.1016/j.neuropharm.2014.10.023

Gusso, D., Cruz, F. F., Fritsch, P. M., Gobbo, M. O., Morrone, F. B., & Bonan, C. D. (2022). Pannexin channel 1, P2×7 receptors, and Dimethyl Sulfoxide mediate pain responses in zebrafish. *Behavioural Brain Research*, *423*. https://doi.org/10.1016/j.bbr.2022.113786

Hainz, N., Wolf, S., Tschernig, T., & Meier, C. (2016). Probenecid Application Prevents Clinical Symptoms and Inflammation in Experimental Autoimmune

Encephalomyelitis. *Inflammation*, *39*(1), 123–128. https://doi.org/10.1007/s10753-015-0230-1

Hanstein, R., Hanani, M., Scemes, E., & Spray, D. C. (2016). Glial pannexin1 contributes to tactile hypersensitivity in a mouse model of orofacial pain. *Scientific Reports*, *6*. https://doi.org/10.1038/srep38266

Harris, J. A. (1998). *Using c-fos as a Neural Marker of Pain*.

Haynes, S. E., Hollopeter, G., Yang, G., Kurpius, D., Dailey, M. E., Gan, W. B., & Julius, D. (2006). The P2Y12 receptor regulates microglial activation by extracellular nucleotides. *Nature Neuroscience*, *9*(12), 1512–1519. https://doi.org/10.1038/nn1805

Honore, P., Donnelly-Roberts, D., Namovic, M. T., Hsieh, G., Zhu, C. Z., Mikusa, J. P., Hernandez, G., Zhong, C., Gauvin, D. M., Chandran, P., Harris, R., Medrano, A. P., Carroll, W., Marsh, K., Sullivan, J. P., Faltynek, C. R., & Jarvis, M. F. (2006). A-740003 [N-(1-{[(cyanoimino)(5-quinolinylamino) methyl]amino}-2,2- dimethylpropyl)-2-(3,4-dimethoxyphenyl)acetamide], a novel and selective P2X7 receptor antagonist, dose-dependently reduces neuropathic pain in the rat. *Journal of Pharmacology and Experimental Therapeutics*, *319*(3), 1376–1385. https://doi.org/10.1124/jpet.106.111559

Illes, P., Rubini, P., Ulrich, H., Zhao, Y., & Tang, Y. (2020). Regulation of Microglial Functions by Purinergic Mechanisms in the Healthy and Diseased CNS. In *Cells* (Vol. 9, Issue 5). NLM (Medline). https://doi.org/10.3390/cells9051108

Inoue, K., & Tsuda, M. (2021). Nociceptive signaling mediated by P2X3, P2X4 and P2X7 receptors. In *Biochemical Pharmacology* (Vol. 187). Elsevier Inc. https://doi.org/10.1016/j.bcp.2020.114309

Jaworski, J., Kalita, K., & Knapska, E. (2018). C-Fos and neuronal plasticity: The aftermath of kaczmarek's theory. In *Acta Neurobiologiae Experimentalis* (Vol. 78, Issue 4, pp. 287–296). Nencki Institute of Experimental Biology. https://doi.org/10.21307/ane-2018-027

Jiang, S., Zhang, Y., Zheng, J. H., Li, X., Yao, Y. L., Wu, Y. L., Song, S. Z., Sun, P., Nan, J. X., & Lian, L. H. (2017). Potentiation of hepatic stellate cell activation by extracellular ATP is dependent on P2X7R-mediated NLRP3 inflammasome activation. *Pharmacological Research*, *117*, 82–93. https://doi.org/10.1016/j.phrs.2016.11.040

Julius, D. (2013). TRP channels and pain. In *Annual Review of Cell and Developmental Biology* (Vol. 29, pp. 355–384). https://doi.org/10.1146/annurev-cellbio-101011-155833

Karavis, M. Y., Siafaka, I., Vadalouca, A., & Georgoudis, G. (2023). Role of microglia in neuropathic pain. *Cureus*. https://doi.org/10.7759/cureus.43555

Ko, M. J., Ganzen, L. C., Coskun, E., Mukadam, A. A., Leung, Y. F., & van Rijn, R. M. (2019). A critical evaluation of TRPA1-mediated locomotor behavior in zebrafish as a screening tool for novel anti-nociceptive drug discovery. *Scientific Reports*, *9*(1). https://doi.org/10.1038/s41598-019-38852-9

Koizumi, S., Ohsawa, K., Inoue, K., & Kohsaka, S. (2013). Purinergic receptors in microglia: Functional modal shifts of microglia mediated by P2 and P1 receptors. *GLIA*, *61*(1), 47–54. https://doi.org/10.1002/glia.22358

Kosten, T. R., & George, T. P. (n.d.). *R E S E A R C H R E V I E W S-T H E N E U R O B I O L O G Y O F O P I O I D D E P E N D E N C E • 1 3 The Neurobiology of Opioid Dependence: Implications for Treatment*.

Kurtenbach, S., Prochnow, N., Kurtenbach, S., Klooster, J., Zoidl, C., Dermietzel, R., Kamermans, M., & Zoidl, G. (2013). Pannexin1 Channel Proteins in the Zebrafish Retina Have Shared and Unique Properties. *PLoS ONE*, *8*(10). https://doi.org/10.1371/journal.pone.0077722

Lee, S. H., Shi, X. Q., Fan, A., West, B., & Zhang, J. (2018). Targeting macrophage and microglia activation with colony stimulating factor 1 receptor inhibitor is an effective strategy to treat injury-triggered neuropathic pain. *Molecular Pain*, *14*. https://doi.org/10.1177/1744806918764979

Li, S., Li, X., Chen, X., Geng, X., & Sun, J. (2014). ATP release channel Pannexin1 is a novel immune response gene in Japanese flounder Paralichthys olivaceus. *Fish and Shellfish Immunology*, *40*(1), 164–173. https://doi.org/10.1016/j.fsi.2014.06.034

Lin, X., Itoga, C. A., Taha, S., Li, M. H., Chen, R., Sami, K., Berton, F., Francesconi, W., & Xu, X. (2018). c-Fos mapping of brain regions activated by multi-modal and electric foot shock stress. *Neurobiology of Stress*, *8*, 92–102. https://doi.org/10.1016/j.ynstr.2018.02.001

Long, T., He, W., Pan, Q., Zhang, S., Zhang, Y., Liu, C., Liu, Q., Qin, G., Chen, L., & Zhou, J. (2018). Microglia P2X4 receptor contributes to central sensitization

following recurrent nitroglycerin stimulation. *Journal of Neuroinflammation*, *15*(1). https://doi.org/10.1186/s12974-018-1285-3

Mazaleuskaya, L. L., Theken, K. N., Gong, L., Thorn, C. F., Fitzgerald, G. A., Altman, R. B., & Klein, T. E. (2015). PharmGKB summary: Ibuprofen pathways. *Pharmacogenetics and Genomics*, *25*(2), 96–106. https://doi.org/10.1097/FPC.0000000000000113

Medrano, M. P., Bejarano, C. A., Battista, A. G., Venera, G. D., Bernabeu, R. O., & Faillace, M. P. (2017). Injury-induced purinergic signalling molecules upregulate pluripotency gene expression and mitotic activity of progenitor cells in the zebrafish retina. *Purinergic Signalling*, *13*(4), 443–465. https://doi.org/10.1007/s11302-017-9572-5

Michalski, K., Syrjanen, J. L., Henze, E., Kumpf, J., Furukawa, H., & Kawate, T. (2020). The Cryo-EM structure of a pannexin 1 reveals unique motifs for ion selection and inhibition. *ELife*, *9*. https://doi.org/10.7554/eLife.54670

Miteva, A., Gaydukov, A., & Balezina, O. (2020). Interaction between calcium chelators and the activity of P2X7 receptors in mouse motor synapses. *International Journal of Molecular Sciences*, *21*(6). https://doi.org/10.3390/ijms21062034

Monif, M., Reid, C. A., Powell, K. L., Smart, M. L., & Williams, D. A. (2009). The P2X7 receptor drives microglial activation and proliferation: A trophic role for P2X7R pore. *Journal of Neuroscience*, *29*(12), 3781–3791. https://doi.org/10.1523/JNEUROSCI.5512-08.2009

Montilla, A., Mata, G. P., Matute, C., & Domercq, M. (2020). Contribution of p2x4 receptors to cns function and pathophysiology. *International Journal of Molecular Sciences*, *21*(15), 1–16. https://doi.org/10.3390/ijms21155562

Morillas, A. G., Besson, V. C., & Lerouet, D. (2021). Microglia and neuroinflammation: What place for p2ry12? In *International Journal of Molecular Sciences* (Vol. 22, Issue 4, pp. 1–16). MDPI AG. https://doi.org/10.3390/ijms22041636

Mousseau, M., Burma, N. E., Lee, K. Y., Leduc-Pessah, H., Kwok, C. H. T., Reid, A. R., O'brien, M., Sagalajev, B., Stratton, J. A., Patrick, N., Stemkowski, P. L., Biernaskie, J., Zamponi, G. W., Salo, P., Mcdougall, J. J., Prescott, S. A., Matyas, J. R., & Trang, T. (2018). Microglial pannexin-1 channel activation is a spinal determinant of joint pain. In *Sci. Adv* (Vol. 4). https://www.science.org

Muñoz, M. F., Griffith, T. N., & Contreras, J. E. (2021). Mechanisms of ATP release in pain: role of pannexin and connexin channels. In *Purinergic Signalling* (Vol. 17, Issue 4, pp. 549–561). Springer Science and Business Media B.V. https://doi.org/10.1007/s11302-021-09822-6

Oda, M., Kurogi, M., Kubo, Y., & Saitoh, O. (2016). Sensitivities of two zebrafish TRPA1 paralogs to chemical and thermal stimuli analyzed in heterologous expression systems. *Chemical Senses*, *41*(3), 261–272. https://doi.org/10.1093/chemse/bjv091

Penuela, S., Gehi, R., & Laird, D. W. (2013). The biochemistry and function of pannexin channels. In *Biochimica et Biophysica Acta - Biomembranes* (Vol. 1828, Issue 1, pp. 15–22). https://doi.org/10.1016/j.bbamem.2012.01.017

Prober, D. A., Zimmerman, S., Myers, B. R., McDermott, B. M., Kim, S. H., Caron, S., Rihel, J., Solnica-Krezel, L., Julius, D., Hudspeth, A. J., & Schier, A. F. (2008). Zebrafish TRPA1 channels are required for chemosensation but not for thermosensation or mechanosensory hair cell function. *Journal of Neuroscience*, *28*(40), 10102–10110. https://doi.org/10.1523/JNEUROSCI.2740-08.2008

Qiu, F., Wang, J., Spray, D. C., Scemes, E., & Dahl, G. (2011). Two non-vesicular ATP release pathways in the mouse erythrocyte membrane. *FEBS Letters*, *585*(21), 3430–3435. https://doi.org/10.1016/j.febslet.2011.09.033

Ransford, G. A., Fregien, N., Qiu, F., Dahl, G., Conner, G. E., & Salathe, M. (2009). Pannexin 1 contributes to ATP release in airway epithelia. *American Journal of Respiratory Cell and Molecular Biology*, *41*(5), 525–534. https://doi.org/10.1165/rcmb.2008-0367OC

Reoyl Seo, D., Kim, S. Y., Kim, K. Y., Lee, H. G., Moon, J. H., Lee, J. S., Lee, S. H., Kim, S. U., Lee, Y. B., & Program, N. G. (2008). Cross talk between P2 purinergic receptors modulates extracellular ATP-mediated interleukin-10 production in rat microglial cells. In *EXPERIMENTAL and MOLECULAR MEDICINE* (Vol. 40, Issue 1).

Rodríguez, I., Novoa, B., & Figueras, A. (2008). Immune response of zebrafish (Danio rerio) against a newly isolated bacterial pathogen Aeromonas hydrophila. *Fish and Shellfish Immunology*, *25*(3), 239–249. https://doi.org/10.1016/j.fsi.2008.05.002

Safarian, N., Houshangi-tabrizi, S., Zoidl, C., & Zoidl, G. R. (2021). Panx1b modulates the luminance response and direction of locomotion in the zebrafish. *International Journal of Molecular Sciences*, *22*(21). https://doi.org/10.3390/ijms222111750

Safarian, N., Whyte-Fagundes, P., Zoidl, C., Grigull, J., & Zoidl, G. (2020). Visuomotor deficiency in panx1a knockout zebrafish is linked to dopaminergic signaling. *Scientific Reports*, *10*(1). https://doi.org/10.1038/s41598-020-66378-y

Scemes, E., Spray, D. C., & Meda, P. (2009). Connexins, pannexins, innexins: Novel roles of “hemi-channels.” In *Pflugers Archiv European Journal of Physiology* (Vol. 457, Issue 6, pp. 1207–1226). https://doi.org/10.1007/s00424-008-0591-5

Scemes, E., Suadicani, S. O., Dahl, G., & Spray, D. C. (2007). Connexin and pannexin mediated cell-cell communication. *Neuron Glia Biology*, *3*(3), 199–208. https://doi.org/10.1017/S1740925X08000069

Shemer, A., Scheyltjens, I., Frumer, G. R., Kim, J. S., Grozovski, J., Ayanaw, S., Dassa, B., Van Hove, H., Chappell-Maor, L., Boura-Halfon, S., Leshkowitz, D., Mueller, W., Maggio, N., Movahedi, K., & Jung, S. (2020). Interleukin-10 Prevents Pathological Microglia Hyperactivation following Peripheral Endotoxin Challenge. *Immunity*, *53*(5), 1033-1049.e7. https://doi.org/10.1016/j.immuni.2020.09.018

Silverman, W., Locovei, S., & Dahl, G. (2008). Probenecid, a gout remedy, inhibits pannexin 1 channels. *American Journal of Physiology - Cell Physiology*, *295*(3). https://doi.org/10.1152/ajpcell.00227.2008

Silverman, W. R., de Rivero Vaccari, J. P., Locovei, S., Qiu, F., Carlsson, S. K., Scemes, E., Keane, R. W., & Dahl, G. (2009). The pannexin 1 channel activates the inflammasome in neurons and astrocytes. *Journal of Biological Chemistry*, *284*(27), 18143–18151. https://doi.org/10.1074/jbc.M109.004804

Sneddon, L. U. (2002). *Anatomical and Electrophysiological Analysis of the Trigeminal Nerve in a Teleost Fish, Oncorhynchus mykiss*. https://www.wellbeingintlstudiesrepository.org/acwp_vsm

Sneddon, L. U. (2003). *Trigeminal Somatosensory Innervation of the Head of a Teleost Fish with Particular Reference to Nociception*. https://www.wellbeingintlstudiesrepository.org/acwp_vsm

Sneddon, L. U. (2015). Pain in aquatic animals. In *Journal of Experimental Biology* (Vol. 218, Issue 7, pp. 967–976). Company of Biologists Ltd. https://doi.org/10.1242/jeb.088823

Sneddon, L. U. (2019). Evolution of nociception and pain: Evidence from fish models. In *Philosophical Transactions of the Royal Society B: Biological Sciences* (Vol. 374, Issue 1785). Royal Society Publishing. https://doi.org/10.1098/rstb.2019.0290

Spray, D. C., & Hanani, M. (2019). Gap junctions, pannexins and pain. In *Neuroscience Letters* (Vol. 695, pp. 46–52). Elsevier Ireland Ltd. https://doi.org/10.1016/j.neulet.2017.06.035

Tsuda, M. (1959). Review Microglia-Mediated Regulation of Neuropathic Pain: Molecular and Cellular Mechanisms. In *Biol. Pharm. Bull* (Vol. 42, Issue 12).

Vogelaar, C. F., Mandal, S., Lerch, S., Birkner, K., Birkenstock, J., Bühler, U., Schnatz, A., Raine, C. S., Bittner, S., Vogt, J., Kipnis, J., Nitsch, R., & Zipp, F. (2018). Fast direct neuronal signaling via the IL-4 receptor as therapeutic target in neuroinflammation. In *Sci. Transl. Med* (Vol. 10). http://stm.sciencemag.org/

Wang, Y. Y., Chang, R. B., Allgood, S. D., Silver, W. L., & Liman, E. R. (2011). A TRPA1-dependent mechanism for the pungent sensationof weak acids. *Journal of General Physiology*, *137*(6), 493–505. https://doi.org/10.1085/jgp.201110615

Weber, E. S. (2011). Fish analgesia: Pain, stress, fear aversion, or nociception? In *Veterinary Clinics of North America - Exotic Animal Practice* (Vol. 14, Issue 1, pp. 21–32). https://doi.org/10.1016/j.cvex.2010.09.002

Weilinger, N. L., Lohman, A. W., Rakai, B. D., Ma, E. M. M., Bialecki, J., Maslieieva, V., Rilea, T., Bandet, M. V., Ikuta, N. T., Scott, L., Colicos, M. A., Teskey, G. C., Winship, I. R., & Thompson, R. J. (2016). Metabotropic NMDA receptor signaling couples Src family kinases to pannexin-1 during excitotoxicity. *Nature Neuroscience*, *19*(3), 432–442. https://doi.org/10.1038/nn.4236

Whyte-Fagundes, P., Taskina, D., Safarian, N., Zoidl, C., Carlen, P. L., Donaldson, L. W., & Zoidl, G. R. (2022). Panx1 channels promote both anti- and pro-seizure-like activities in the zebrafish via p2rx7 receptors and ATP signaling. *Communications Biology*, *5*(1). https://doi.org/10.1038/s42003-022-03356-2

Williams, J. (n.d.). *Basic opioid pharmacology*.

Xing, Q., Cibelli, A., Yang, G. L., Dohare, P., Li, Q. H., Scemes, E., Guan, F. X., & Spray, D. C. (2024). Neuronal Panx1 drives peripheral sensitization in experimental plantar inflammatory pain. *Military Medical Research*, *11*(1), 27. https://doi.org/10.1186/s40779-024-00525-8

Yeung, A. K., Patil, C. S., & Jackson, M. F. (2020). Pannexin-1 in the CNS: Emerging concepts in health and disease. In *Journal of Neurochemistry* (Vol. 154, Issue 5, pp. 468–485). Blackwell Publishing Ltd. https://doi.org/10.1111/jnc.15004

Zhang, W. jun, Luo, H. liang, & Zhu, Z. ming. (2020). The role of P2X4 receptors in chronic pain: A potential pharmacological target. In *Biomedicine and Pharmacotherapy* (Vol. 129). Elsevier Masson SAS. https://doi.org/10.1016/j.biopha.2020.110447

Zhang, Y., Laumet, G., Chen, S. R., Hittelman, W. N., & Pan, H. L. (2015). Pannexin-1 up-regulation in the dorsal root ganglion contributes to neuropathic pain development. *Journal of Biological Chemistry*, *290*(23), 14647–14655. https://doi.org/10.1074/jbc.M115.650218

Zoidl, G., Petrasch-Parwez, E., Ray, A., Meier, C., Bunse, S., Habbes, H. W., Dahl, G., & Dermietzel, R. (2007). Localization of the pannexin1 protein at postsynaptic sites in the cerebral cortex and hippocampus. *Neuroscience*, *146*(1), 9–16. https://doi.org/10.1016/j.neuroscience.2007.01.061

6.0 Supplementary Figures

6.1 Behavioral

6.1.1 Average burst level activity vs AA concentration

TL AA treatment vs Average Burst Level Activity

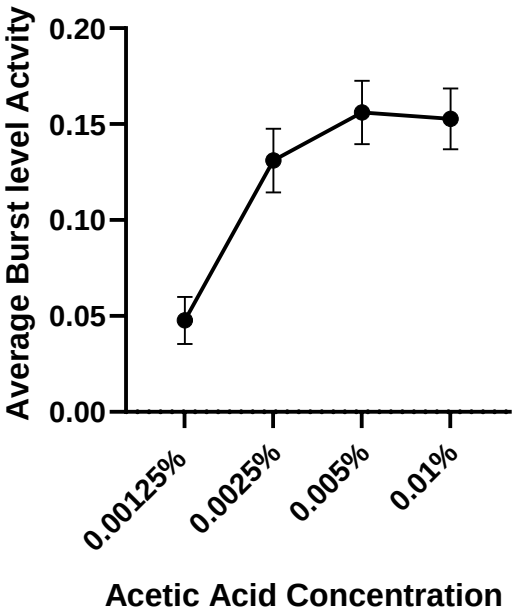

Supplementary figure S1: Acetic acid concentration vs Average burst level activity. Time point 1s – 150s.

6.1.2 AA concentration and corresponding pH

Supplementary figure S2: Concentration of Acetic Acid and corresponding pH Normalized behavioral response to AA treatments.

Concentration	pH
0.01%	3.8
0.005%	4.1
0.0025%	4.6
0.00125%	5.6

6.1.3 Burst level activity TL and Panx1a KO

Supplementary figure S3: Time point 1s – 150s. Two-way ANOVA followed by Tukey's post hoc multiple comparisons tests. “Mean Diff” shows difference of means tested. “Adjusted P-value” shows the p-value of the comparison test for significance. Genotypes used TL and panx1a KO. AA concentration 0.01%.

Tukey's multiple comparisons test	Mean Diff.	95.00% CI of diff.	Summary	Adjusted P Value
TL (egg water) vs. TL (0.01%)	-0.1527	-0.1988 to -0.1066	****	<0.0001
TL (egg water) vs. 1a (egg water)	0.008167	-0.03792 to 0.05426	ns	0.9661
TL (egg water) vs. 1a (0.01%)	-0.1451	-0.1912 to -0.09902	****	<0.0001
TL (0.01%) vs. 1a (egg water)	0.1609	0.1148 to 0.2070	****	<0.0001
TL (0.01%) vs. 1a (0.01%)	0.007611	-0.03848 to 0.05370	ns	0.9723
1a (egg water) vs. 1a (0.01%)	-0.1533	-0.1994 to -0.1072	****	<0.0001

Supplementary figure S4: Time point 151s - 300s. Two-way ANOVA followed by Tukey's post hoc multiple comparisons tests. “Mean Diff” shows difference of means tested. “Adjusted P-value” shows the p-value of the comparison test for significance. Genotypes used TL and panx1a KO. AA concentration 0.01%.

Tukey's multiple comparisons test	Mean Diff.	95.00% CI of diff.	Summary	Adjusted P Value

TL (egg water) vs. TL (0.01%)	-0.1192	-0.1773 to -0.06121	****	<0.0001
TL (egg water) vs. 1a (egg water)	-0.001288	-0.05932 to 0.05675	ns	>0.9999
TL (egg water) vs. 1a (0.01%)	-0.108	-0.1660 to -0.04997	****	<0.0001
TL (0.01%) vs. 1a (egg water)	0.118	0.05992 to 0.1760	****	<0.0001
TL (0.01%) vs. 1a (0.01%)	0.01124	-0.04680 to 0.06927	ns	0.9565
1a (egg water) vs. 1a (0.01%)	-0.1067	-0.1648 to -0.04868	****	<0.0001

Supplementary figure S5: Time point 1s – 150s. Two-way ANOVA followed by Tukey's post hoc multiple comparisons tests. “Mean Diff” shows difference of means tested. “Adjusted P-value” shows the p-value of the comparison test for significance. Genotypes used TL and panx1a KO. AA concentration 0.005%.

Tukey's multiple comparisons test	Mean Diff.	95.00% CI of diff.	Summary	Adjusted P Value
TL (egg water) vs. TL (0.005%)	-0.1561	-0.1941 to -0.1181	****	<0.0001
TL (egg water) vs. 1a (egg water)	-0.004861	-0.04285 to 0.03313	ns	0.9867
TL (egg water) vs. 1a (0.005%)	-0.08453	-0.1225 to -0.04654	****	<0.0001
TL (0.005%) vs. 1a (egg water)	0.1512	0.1132 to 0.1892	****	<0.0001
TL (0.005%) vs. 1a (0.005%)	0.07156	0.03356 to 0.1095	****	<0.0001
1a (egg water) vs. 1a (0.005%)	-0.07967	-0.1177 to -0.04167	****	<0.0001

Supplementary figure S6: Time point 151s – 300s. Two-way ANOVA followed by Tukey's post hoc multiple comparisons tests. “Mean Diff” shows difference of means tested. “Adjusted P-value” shows the p-value of the comparison test for significance. Genotypes used TL and panx1a KO. AA concentration 0.005%.

Tukey's multiple comparisons test	Mean Diff.	95.00% CI of diff.	Summary	Adjusted P Value
TL (egg water) vs. TL (0.005%)	-0.1386	-0.1831 to -0.09412	****	<0.0001
TL (egg water) vs. 1a (egg water)	-0.004691	-0.04920 to 0.03982	ns	0.9925
TL (egg water) vs. 1a (0.005%)	-0.1261	-0.1706 to -0.08159	****	<0.0001

TL (0.005%) vs. 1a (egg water)	0.1339	0.08943 to 0.1785	****	<0.0001
TL (0.005%) vs. 1a (0.005%)	0.01253	-0.03198 to 0.05704	ns	0.8802
1a (egg water) vs. 1a (0.005%)	-0.1214	-0.1659 to -0.07690	****	<0.0001

Supplementary figure S7: Time point 1s – 150s. Two-way ANOVA followed by Tukey's post hoc multiple comparisons tests. “Mean Diff” shows difference of means tested. Genotypes used TL and panx1a KO. “Adjusted P-value” shows the p-value of the comparison test for significance. AA concentration 0.0025%.

Tukey's multiple comparisons test	Mean Diff.	95.00% CI of diff.	Summary	Adjusted P Value
TL control vs. TL 0.0025%	-0.09797	-0.1393 to -0.05663	****	<0.0001
TL control vs. 1a control	0.0185	-0.02284 to 0.05984	ns	0.6426
TL control vs. 1a 0.0025%	-0.1061	-0.1475 to -0.06480	****	<0.0001
TL 0.0025% vs. 1a control	0.1165	0.07513 to 0.1578	****	<0.0001
TL 0.0025% vs. 1a 0.0025%	-0.008167	-0.04951 to 0.03318	ns	0.954
1a control vs. 1a 0.0025%	-0.1246	-0.1660 to -0.08330	****	<0.0001

Supplementary figure S8: Time point 151s – 300s. Two-way ANOVA followed by Tukey's post hoc multiple comparisons tests. “Mean Diff” shows difference of means tested. Genotypes used TL and panx1a KO. “Adjusted P-value” shows the p-value of the comparison test for significance. AA concentration 0.0025%.

Tukey's multiple comparisons test	Mean Diff.	95.00% CI of diff.	Summary	Adjusted P Value
TL control vs. TL 0.0025%	-0.08731	-0.1299 to -0.04476	****	<0.0001
TL control vs. 1a control	0.02525	-0.01730 to 0.06780	ns	0.4068
TL control vs. 1a 0.0025%	-0.08364	-0.1262 to -0.04109	****	<0.0001
TL 0.0025% vs. 1a control	0.1126	0.07000 to 0.1551	****	<0.0001

TL 0.0025% vs. 1a 0.0025%	0.00367	-0.03888 to 0.04622	ns	0.9958
1a control vs. 1a 0.0025%	-0.1089	-0.1514 to -0.06633	****	<0.0001

Supplementary figure S9: Time point 1s – 150s. Two-way ANOVA followed by Tukey's post hoc multiple comparisons tests. “Mean Diff” shows difference of means tested. “Adjusted P-value” shows the p-value of the comparison test for significance. Genotypes used TL and panx1a KO. AA concentration 0.00125%.

Tukey's multiple comparisons test	Mean Diff.	95.00% CI of diff.	Summary	Adjusted P Value
TL control vs. TL 0.00125%	-0.04768	-0.08561 to -0.009748	**	0.0079
TL control vs. 1a control	0.0033	-0.03463 to 0.04123	ns	0.9957
TL control vs. 1a 0.00125%	-0.0238	-0.06173 to 0.01413	ns	0.357
TL 0.00125% vs. 1a control	0.05098	0.01305 to 0.08891	**	0.004
TL 0.00125% vs. 1a 0.00125%	0.02388	-0.01405 to 0.06181	ns	0.3539
1a control vs. 1a 0.00125%	-0.0271	-0.06503 to 0.01083	ns	0.2458

Supplementary figure S10: Time point 151s – 300s. Two-way ANOVA followed by Tukey's post hoc multiple comparisons tests. “Mean Diff” shows difference of means tested. “Adjusted P-value” shows the p-value of the comparison test for significance. Genotypes used TL and panx1a KO. AA concentration 0.00125%.

Tukey's multiple comparisons test	Mean Diff.	95.00% CI of diff.	Summary	Adjusted P Value
TL control vs. TL 0.00125%	-0.06322	-0.1073 to -0.01918	**	0.0018
TL control vs. 1a control	-0.00207	-0.04610 to 0.04196	ns	0.9993
TL control vs. 1a 0.00125%	-0.02158	-0.06561 to 0.02245	ns	0.5722
TL 0.00125% vs. 1a control	0.06115	0.01712 to 0.1052	**	0.0027
TL 0.00125% vs. 1a 0.00125%	0.04164	-0.002394 to 0.08567	ns	0.0705
1a control vs. 1a 0.00125%	-0.01951	-0.06354 to 0.02452	ns	0.6499

6.1.4 Freeze Duration TL Panx1a KO

Supplementary Figure S11: Time point 1s – 150s. Two-way ANOVA followed by Tukey's post hoc multiple comparisons tests. “Mean Diff” shows the difference of means tested. “Adjusted P-value” shows the p-value of the comparison test for significance. Genotypes used: TL and panx1a KO. AA concentration: 0.01%.

Comparison	Mean Diff	95% CI of Diff	Summary	Adjusted P Value
TL control vs. TL (0.01%)	0.1998	0.1343 to 0.2654	****	<0.0001
TL control vs. 1a control	-0.006705	-0.07226 to 0.05885	ns	0.9931
TL control vs. 1a (0.01%)	0.1841	0.1185 to 0.2496	****	<0.0001
TL (0.01%) vs. 1a control	-0.2065	-0.2721 to -0.1410	****	<0.0001
TL (0.01%) vs. 1a (0.01%)	-0.01576	-0.08131 to 0.04980	ns	0.9211
1a control vs. 1a (0.01%)	0.1908	0.1252 to 0.2563	****	<0.0001

Supplementary Figure S12: Time point 151s – 300s. Two-way ANOVA followed by Tukey's post hoc multiple comparisons tests. “Mean Diff” shows the difference of means tested. “Adjusted P-value” shows the p-value of the comparison test for significance. Genotypes used: TL and panx1a KO. AA concentration: 0.01%.

Comparison	Mean Diff	95% CI of Diff	Summary	Adjusted P Value
TL control vs. TL (0.01%)	0.1559	0.07831 to 0.2335	****	<0.0001
TL control vs. 1a control	0.01483	-0.06275 to 0.09241	ns	0.958
TL control vs. 1a (0.01%)	0.132	0.05445 to 0.2096	***	0.0002
TL (0.01%) vs. 1a control	-0.1411	-0.2186 to -0.06348	****	<0.0001
TL (0.01%) vs. 1a (0.01%)	-0.02386	-0.1014 to 0.05372	ns	0.8496
1a control vs. 1a (0.01%)	0.1172	0.03961 to 0.1948	***	0.001

Supplementary Figure S13: Time point 1s – 150s. Two-way ANOVA followed by Tukey's post hoc multiple comparisons tests. “Mean Diff” shows the difference of means tested. “Adjusted P-value” shows the p-value of the comparison test for significance. Genotypes used: TL and panx1a KO. AA concentration: 0.005%.

Comparison	Mean Diff	95% CI of Diff	Summary	Adjusted P Value
TL control vs. TL (0.005%)	0.2087	0.1503 to 0.2671	****	<0.0001
TL control vs. 1a control	0.01131	-0.04710 to 0.06971	ns	0.9565
TL control vs. 1a (0.005%)	0.1138	0.05540 to 0.1722	****	<0.0001
TL (0.005%) vs. 1a control	-0.1974	-0.2558 to -0.1390	****	<0.0001
TL (0.005%) vs. 1a (0.005%)	-0.09486	-0.1533 to -0.03646	***	0.0003
1a control vs. 1a (0.005%)	0.1025	0.04410 to 0.1609	***	0.0001

Supplementary Figure S14: Time point 151s – 300s. Two-way ANOVA followed by Tukey's post hoc multiple comparisons tests. “Mean Diff” shows the difference of means

tested. “Adjusted P-value” shows the p-value of the comparison test for significance. Genotypes used: TL and panx1a KO. AA concentration: 0.005%.

Comparison	Mean Diff	95% CI of Diff	Summary	Adjusted P Value
TL control vs. TL (0.005%)	0.194	0.1245 to 0.2634	****	<0.0001
TL control vs. 1a control	0.01678	-0.05266 to 0.08621	ns	0.92
TL control vs. 1a (0.005%)	0.1653	0.09585 to 0.2347	****	<0.0001
TL (0.005%) vs. 1a control	-0.1772	-0.2466 to -0.1077	****	<0.0001
TL (0.005%) vs. 1a (0.005%)	-0.02867	-0.09810 to 0.04076	ns	0.6986
1a control vs. 1a (0.005%)	0.1485	0.07908 to 0.2179	****	<0.0001

Supplementary Figure S15: Time point 1s – 150s. Two-way ANOVA followed by Tukey's post hoc multiple comparisons tests. “Mean Diff” shows the difference of means tested. “Adjusted P-value” shows the p-value of the comparison test for significance. Genotypes used: TL and panx1a KO. AA concentration: 0.0025%.

Comparison	Mean Diff	95% CI of Diff	Summary	Adjusted P Value
TL control vs. TL (0.0025%)	0.1309	0.07167 to 0.1901	****	<0.0001
TL control vs. 1a control	-0.01664	-0.07583 to 0.04255	ns	0.8805
TL control vs. 1a (0.0025%)	0.1571	0.09789 to 0.2163	****	<0.0001
TL (0.0025%) vs. 1a control	-0.1475	-0.2067 to -0.08831	****	<0.0001
TL (0.0025%) vs. 1a (0.0025%)	0.02622	-0.03297 to 0.08541	ns	0.6499
1a control vs. 1a (0.0025%)	0.1737	0.1145 to 0.2329	****	<0.0001

Supplementary Figure S16: Time point 151s – 300s. Two-way ANOVA followed by Tukey's post hoc multiple comparisons tests. “Mean Diff” shows the difference of means tested. “Adjusted P-value” shows the p-value of the comparison test for significance. Genotypes used: TL and panx1a KO. AA concentration: 0.0025%.

Comparison	Mean Diff	95% CI of Diff	Summary	Adjusted P Value
TL control vs. TL (0.0025%)	0.1178	0.05543 to 0.1802	****	<0.0001
TL control vs. 1a control	-0.0207	-0.08309 to 0.04170	ns	0.8186
TL control vs. 1a (0.0025%)	0.125	0.06258 to 0.1874	****	<0.0001
TL (0.0025%) vs. 1a control	-0.1385	-0.2009 to -0.07613	****	<0.0001
TL (0.0025%) vs. 1a (0.0025%)	0.007147	-0.05524 to 0.06954	ns	0.9904
1a control vs. 1a (0.0025%)	0.1457	0.08328 to 0.2081	****	<0.0001

Supplementary Figure S17: Time point 1s – 150s. Two-way ANOVA followed by Tukey's post hoc multiple comparisons tests. “Mean Diff” shows the difference of means tested. “Adjusted P-value” shows the p-value of the comparison test for significance. Genotypes used: TL and panx1a KO. AA concentration: 0.00125%.

Comparison	Mean Diff	95% CI of Diff	Summary	Adjusted P Value
TL control vs. TL (0.00125%)	0.08503	0.02398 to 0.1461	**	0.0026
TL control vs. 1a control	0.001222	-0.05982 to 0.06227	ns	>0.9999

TL control vs. 1a (0.00125%)	0.03622	-0.02482 to 0.09727	ns	0.4068
TL (0.00125%) vs. 1a control	-0.08381	-0.1449 to -0.02276	**	0.0031
TL (0.00125%) vs. 1a (0.00125%)	-0.04881	-0.1098 to 0.01224	ns	0.1618
1a control vs. 1a (0.00125%)	0.035	-0.02604 to 0.09604	ns	0.4374

Supplementary Figure S18: Time point 151s – 300s. Two-way ANOVA followed by Tukey's post hoc multiple comparisons tests. “Mean Diff” shows the difference of means tested. “Adjusted P-value” shows the p-value of the comparison test for significance. Genotypes used: TL and panx1a KO. AA concentration: 0.00125%.

Comparison	Mean Diff	95% CI of Diff	Summary	Adjusted P Value
TL control vs. TL (0.00125%)	0.09619	0.03186 to 0.1605	**	0.0011
TL control vs. 1a control	0.01247	-0.05186 to 0.07680	ns	0.9563
TL control vs. 1a (0.00125%)	0.02806	-0.03627 to 0.09239	ns	0.661
TL (0.00125%) vs. 1a control	-0.08372	-0.1481 to -0.01939	**	0.0056
TL (0.00125%) vs. 1a (0.00125%)	-0.06813	-0.1325 to -0.003798	*	0.0338
1a control vs. 1a (0.00125%)	0.01559	-0.04874 to 0.07992	ns	0.9193

6.1.5 Panx1b Average Burst duration

Supplementary Figure S19: Time point 1s – 150s. Two-way ANOVA followed by Tukey's post hoc multiple comparisons tests. “Mean Diff” shows the difference of means tested. “Adjusted P-value” shows the p-value of the comparison test for significance. Genotypes used: TL and Panx1b KO. AA concentration: 0.00125%.

Comparison	Mean Diff	95% CI of Diff	Summary	Adjusted P Value
TL (control) vs. TL (0.00125% AA)	-0.008296	-0.06246 to 0.04586	ns	0.977
TL (control) vs. Panx1b KO (control)	-0.01315	-0.06731 to 0.04101	ns	0.9169
TL (control) vs. Panx1b KO (0.00125%)	-0.09752	-0.1517 to -0.04336	****	<0.0001
TL (0.00125% AA) vs. Panx1b KO (control)	-0.004852	-0.05901 to 0.04931	ns	0.9952
TL (0.00125% AA) vs. Panx1b KO (0.00125%)	-0.08922	-0.1434 to -0.03506	***	0.0003
Panx1b KO (control) vs. Panx1b KO (0.00125%)	-0.08437	-0.1385 to -0.03021	***	0.0007

Supplementary Figure S20: Time point 151s – 300s. Two-way ANOVA followed by Tukey's post hoc multiple comparisons tests. “Mean Diff” shows the difference of means

tested. “Adjusted P-value” shows the p-value of the comparison test for significance. Genotypes used: TL and Panx1b KO. AA concentration: 0.00125%.

Comparison	Mean Diff	95% CI of Diff	Summary	Adjusted P Value
TL (control) vs. TL (0.00125% AA)	-0.05011	-0.1157 to 0.01545	ns	0.1906
TL (control) vs. Panx1b KO (control)	-0.01081	-0.07637 to 0.05475	ns	0.9716
TL (control) vs. Panx1b KO (0.00125%)	-0.1107	-0.1762 to -0.04511	***	0.0002
TL (0.00125% AA) vs. Panx1b KO (control)	0.0393	-0.02626 to 0.1049	ns	0.3923
TL (0.00125% AA) vs. Panx1b KO (0.00125%)	-0.06056	-0.1261 to 0.005004	ns	0.0799
Panx1b KO (control) vs. Panx1b KO (0.00125%)	-0.09985	-0.1654 to -0.03429	***	0.001

6.1.6 PROB burst level activity

Supplementary Figure S21: Time point 1s – 150s. Kruskal-Wallis followed by Dunn's multiple comparisons tests. “Mean rank diff.” shows the difference of ranks tested. “Adjusted P-value” shows the p-value of the comparison test for significance. Genotypes used: TL and panx1a KO. AA concentration: 0.00125%.

Comparison	Mean rank diff.	Significant?	Summary	Adjusted P Value
TL control vs. TL (0.00125%)	-64.51	Yes	****	<0.0001
TL control vs. TL (20 µM PROB)	1.556	No	ns	>0.9999
TL control vs. TL PROB (20 µM) + 0.00125%	-39.54	Yes	***	0.0003
TL (0.00125%) vs. TL (20 µM PROB)	66.07	Yes	****	<0.0001
TL (0.00125%) vs. TL PROB (20 µM) + 0.00125%	24.97	No	ns	0.0631
TL (20uM PROB) vs. TL PROB (20 µM) + 0.00125%	-41.1	Yes	***	0.0002

Supplementary Figure S22: Time point 151s – 300s. Kruskal-Wallis followed by Dunn's multiple comparisons tests. “Mean rank diff.” shows the difference of ranks tested. “Adjusted P-value” shows the p-value of the comparison test for significance. Genotypes used: TL and panx1a KO. AA concentration: 0.00125%.

Comparison	Mean rank diff.	Significant?	Summary	Adjusted P Value
TL control vs. TL (0.00125%)	-67.07	Yes	****	<0.0001
TL control vs. TL (20 µM PROB)	4.722	No	ns	>0.9999

TL control vs. TL PROB (20 µM) + 0.00125%	-37.26	Yes	***	0.0008
TL (0.00125%) vs. TL (20 µM PROB)	71.79	Yes	****	<0.0001
TL (0.00125%) vs. TL PROB (20 µM) + 0.00125%`	29.81	Yes	*	0.0139
TL (20uM PROB) vs. TL PROB (20 µM) + 0.00125%	-41.99	Yes	***	0.0001

Supplementary Figure S23: Time point 1s – 150s. Two-way ANOVA followed by Tukey's post hoc multiple comparisons tests. “Mean Diff” shows the difference of means tested. “Adjusted P-value” shows the p-value of the comparison test for significance. Genotypes used: TL and panx1a KO. AA concentration: 0.005%.

Comparison	Mean Diff	95% CI of Diff	Summary	Adjusted P Value
TL control vs. TL (0.005%)	-0.1438	-0.1971 to -0.09062	****	<0.0001
TL control vs. TL PROB (20 µM)	0.009256	-0.04397 to 0.06249	ns	0.9679
TL control vs. TL PROB (20 µM) + 0.005%	-0.0856	-0.1388 to -0.03237	***	0.0004
TL (0.005%) vs. TL PROB (20 µM)	0.1531	0.09987 to 0.2063	****	<0.0001
TL (0.005%) vs. TL PROB (20 µM) + 0.005%	0.05825	0.005019 to 0.1115	*	0.0265
TL PROB (20uM) vs. TL PROB (20uM) + 0.005%	-0.09485	-0.1481 to -0.04162	****	<0.0001

Supplementary Figure S24: Time point 151s – 300s. Two-way ANOVA followed by Tukey's post hoc multiple comparisons tests. “Mean Diff” shows the difference of means tested. “Adjusted P-value” shows the p-value of the comparison test for significance. Genotypes used: TL and panx1a KO. AA concentration: 0.005%.

Comparison	Mean Diff	95% CI of Diff	Summary	Adjusted P Value
TL control vs. TL (0.005%)	-0.1608	-0.2152 to -0.1064	****	<0.0001
TL control vs. TL PROB (20 µM)	0.01965	-0.03475 to 0.07404	ns	0.7774
TL control vs. TL PROB (20 µM) + 0.005%	-0.08747	-0.1419 to -0.03308	***	0.0004
TL (0.005%) vs. TL PROB (20 µM)	0.1804	0.1260 to 0.2348	****	<0.0001
TL (0.005%) vs. TL PROB (20 µM) + 0.005%	0.07329	0.01890 to 0.1277	**	0.0038
TL PROB (20uM) vs. TL PROB (20 µM) + 0.005%	-0.1071	-0.1615 to -0.05273	****	<0.0001

6.1.7 PROB freeze duration activity

Supplementary Figure S25: Time point 1s – 150s. Two-way ANOVA followed by Tukey's post hoc multiple comparisons tests. “Mean Diff” shows the difference of means tested. “Adjusted P-value” shows the p-value of the comparison test for significance. Genotypes used: TL and panx1a KO. AA concentration: 0.00125%.

Comparison	Mean Diff	95% CI of Diff	Summary	Adjusted P Value
TL Control vs. TL 0.00125% AA	0.1429	0.09670 to 0.1892	****	<0.0001
TL Control vs. TL 20uM PROB	-0.00854	-0.05476 to 0.03769	ns	0.9629
TL Control vs. TL 20uM PROB + 0.00125% AA	0.08185	0.03563 to 0.1281	****	<0.0001
TL 0.00125% AA vs. TL 20uM PROB	-0.1515	-0.1977 to -0.1052	****	<0.0001
TL 0.00125% AA vs. TL 20uM PROB + 0.00125% AA	-0.06107	-0.1073 to -0.01485	**	0.0044
TL 20uM PROB vs. TL 20uM PROB + 0.00125% AA	0.09039	0.04416 to 0.1366	****	<0.0001

Supplementary Figure S26: Time point 151s – 300s. Two-way ANOVA followed by Tukey's post hoc multiple comparisons tests. “Mean Diff” shows the difference of means tested. “Adjusted P-value” shows the p-value of the comparison test for significance. Genotypes used: TL and panx1a KO. AA concentration: 0.00125%.

Comparison	Mean Diff	95% CI of Diff	Summary	Adjusted P Value
TL Control vs. TL 0.00125% AA	0.1899	0.1356 to 0.2442	****	<0.0001
TL Control vs. TL 20uM PROB	-0.00988	-0.06419 to 0.04443	ns	0.9645
TL Control vs. TL 20uM PROB + 0.00125% AA	0.07938	0.02507 to 0.1337	**	0.0013
TL 0.00125% AA vs. TL 20uM PROB	-0.1998	-0.2541 to -0.1455	****	<0.0001
TL 0.00125% AA vs. TL 20uM PROB + 0.00125% AA	-0.1106	-0.1649 to -0.05625	****	<0.0001
TL 20uM PROB vs. TL 20uM PROB + 0.00125% AA	0.08926	0.03495 to 0.1436	***	0.0002

Supplementary Figure S27: Time point 1s – 150s. Two-way ANOVA followed by Tukey's post hoc multiple comparisons tests. “Mean Diff” shows the difference of means tested. “Adjusted P-value” shows the p-value of the comparison test for significance. Genotypes used: TL and panx1a KO. AA concentration: 0.005%.

Comparison	Mean Diff	95% CI of Diff	Summary	Adjusted P Value

TL Control vs. TL 0.005% AA	0.1904	0.1110 to 0.2697	****	<0.0001
TL Control vs. TL 20uM PROB	-0.02181	-0.1011 to 0.05753	ns	0.8873
TL Control vs. TL 20uM PROB + 0.005% AA	0.1047	0.02533 to 0.1840	**	0.0048
TL 0.005% AA vs. TL 20uM PROB	-0.2122	-0.2915 to -0.1328	****	<0.0001
TL 0.005% AA vs. TL 20uM PROB + 0.005% AA	-0.08569	-0.1650 to -0.006361	*	0.0292
TL 20uM PROB vs. TL 20uM PROB + 0.005% AA	0.1265	0.04714 to 0.2058	***	0.0005

Supplementary Figure S28: Time point 151s – 300s. Two-way ANOVA followed by Tukey's post hoc multiple comparisons tests. “Mean Diff” shows the difference of means tested. “Adjusted P-value” shows the p-value of the comparison test for significance. Genotypes used: TL and panx1a KO. AA concentration: 0.005%.

Comparison	Mean Diff	95% CI of Diff	Summary	Adjusted P Value
TL Control vs. TL 0.005% AA	0.2086	0.1332 to 0.2840	****	<0.0001
TL Control vs. TL 20uM PROB	-0.03755	-0.1130 to 0.03788	ns	0.5593
TL Control vs. TL 20uM PROB + 0.005% AA	0.1058	0.03035 to 0.1812	**	0.0024
TL 0.005% AA vs. TL 20uM PROB	-0.2462	-0.3216 to -0.1707	****	<0.0001
TL 0.005% AA vs. TL 20uM PROB + 0.005% AA	-0.1028	-0.1783 to -0.02739	**	0.0034
TL 20uM PROB vs. TL 20uM PROB + 0.005% AA	0.1433	0.06791 to 0.2188	****	<0.0001

6.1.8 Ibuprofen burst level activity

Supplementary Figure S29: Time point 1s – 150s. Kruskal-Wallis followed by Dunn's multiple comparisons tests. “Mean rank diff.” shows the difference of ranks tested. “Adjusted P-value” shows the p-value of the comparison test for significance. Genotypes used: TL and panx1a KO. AA concentration: 0.00125%.

Comparison	Mean rank diff.	Significant?	Summary	Adjusted P Value
TL Control vs. TL (0.00125%)	-22.67	Yes	*	0.0282
TL Control vs. TL (25ug/L)	-10.96	No	ns	>0.9999
TL Control vs. TL (0.00125% + 25ug/L)	-17.71	No	ns	0.1632
TL (0.00125%) vs. TL (25ug/L)	11.71	No	ns	0.8653
TL (0.00125%) vs. TL (0.00125% + 25ug/L)	4.958	No	ns	>0.9999

TL (25ug/L) vs. TL (0.00125% + 25ug/L)	-6.75	No	ns	>0.9999

Supplementary Figure S30: Time point 151s – 300s. Kruskal-Wallis followed by Dunn's multiple comparisons tests. “Mean rank diff.” shows the difference of ranks tested. “Adjusted P-value” shows the p-value of the comparison test for significance. Genotypes used: TL and panx1a KO. AA concentration: 0.00125%.

Comparison	Mean rank diff.	Significant?	Summary	Adjusted P Value
TL Control vs. TL (0.00125%)	-25.85	Yes	**	0.0073
TL Control vs. TL (25ug/L)	-7.104	No	ns	>0.9999
TL Control vs. TL (0.00125% + 25ug/L)	-28.54	Yes	**	0.0021
TL (0.00125%) vs. TL (25ug/L)	18.75	No	ns	0.1138
TL (0.00125%) vs. TL (0.00125% + 25ug/L)	-2.688	No	ns	>0.9999
TL (25ug/L) vs. TL (0.00125% + 25ug/L)	-21.44	Yes	*	0.0439

Supplementary Figure S31: Time point 1s – 150s. Two-way ANOVA followed by Tukey's post hoc multiple comparisons tests. “Mean Diff” shows the difference of means tested. “Adjusted P-value” shows the p-value of the comparison test for significance. Genotypes used: TL and panx1a KO. AA concentration: 0.005%.

Comparison	Mean Diff	95% CI of Diff	Summary	Adjusted P Value
TL egg water vs. TL (0.005%)	-0.11	-0.1551 to -0.06492	****	<0.0001
TL egg water vs. TL (25ug/L)	-0.02142	-0.06652 to 0.02369	ns	0.5975
TL egg water vs. TL (0.005% +25ug/L)	-0.1771	-0.2222 to -0.1320	****	<0.0001
TL (0.005%) vs. TL (25ug/L)	0.08861	0.04351 to 0.1337	****	<0.0001
TL (0.005%) vs. TL (0.005% +25ug/L)	-0.06711	-0.1122 to -0.02201	**	0.0012
TL (25ug/L) vs. TL (0.005% +25ug/L)	-0.1557	-0.2008 to -0.1106	****	<0.0001

Supplementary Figure S32: Time point 151s – 300s. Two-way ANOVA followed by Tukey's post hoc multiple comparisons tests. “Mean Diff” shows the difference of means tested. “Adjusted P-value” shows the p-value of the comparison test for significance. Genotypes used: TL and panx1a KO. AA concentration: 0.005%.

Comparison	Mean Diff	95% CI of Diff	Summary	Adjusted P Value
TL egg water vs. TL (0.005%)	-0.1224	-0.1711 to -0.07363	****	<0.0001

TL egg water vs. TL (25ug/L)	-0.00458	-0.05330 to 0.04414	ns	0.9946
TL egg water vs. TL (0.005% +25ug/L)	-0.1611	-0.2098 to -0.1124	****	<0.0001
TL (0.005%) vs. TL (25ug/L)	0.1178	0.06905 to 0.1665	****	<0.0001
TL (0.005%) vs. TL (0.005% +25ug/L)	-0.03877	-0.08749 to 0.009951	ns	0.1649
TL (25ug/L) vs. TL (0.005% +25ug/L)	-0.1565	-0.2053 to -0.1078	****	<0.0001

Supplementary Figure S33: Time point 1s – 150s. Kruskal-Wallis followed by Dunn's multiple comparisons tests. “Mean rank diff.” shows the difference of ranks tested. “Adjusted P-value” shows the p-value of the comparison test for significance. Genotypes used: TL and panx1a KO. AA concentration: 0.00125%.

Comparison	Mean rank diff.	Significant?	Summary	Adjusted P Value
TL control vs. TL 0.00125%	17.69	No	ns	0.1654
TL control vs. TL ibu 50uM	3.938	No	ns	>0.9999
TL control vs. TL ibu 50uM + 0.00125%	-2.625	No	ns	>0.9999
TL 0.00125% vs. TL ibu 50uM	-13.75	No	ns	0.5204
TL 0.00125% vs. TL ibu 50uM + 0.00125%	-20.31	No	ns	0.0684
TL ibu 50uM vs. TL ibu 50uM + 0.00125%	-6.563	No	ns	>0.9999

Supplementary Figure S34: Time point 151s – 300s. Kruskal-Wallis followed by Dunn's multiple comparisons tests. “Mean rank diff.” shows the difference of ranks tested. “Adjusted P-value” shows the p-value of the comparison test for significance. Genotypes used: TL and panx1a KO. AA concentration: 0.00125%.

Comparison	Mean rank diff.	Significant?	Summary	Adjusted P Value
TL control vs. TL 0.00125%	-13.83	No	ns	0.5102
TL control vs. TL ibu 50uM	-2.688	No	ns	>0.9999
TL control vs. TL ibu 50uM + 0.00125%	-24.31	Yes	*	0.0148
TL 0.00125% vs. TL ibu 50uM	11.15	No	ns	0.9915
TL 0.00125% vs. TL ibu 50uM + 0.00125%	-10.48	No	ns	>0.9999
TL ibu 50uM vs. TL ibu 50uM + 0.00125%	-21.63	Yes	*	0.0426

Supplementary Figure S35: Time point 1s – 150s. Two-way ANOVA followed by Tukey's post hoc multiple comparisons tests. “Mean Diff” shows the difference of means tested. “Adjusted P-value” shows the p-value of the comparison test for significance. Genotypes used: TL and panx1a KO. AA concentration: 0.005%.

Comparison	Mean Diff	95% CI of Diff	Summary	Adjusted P Value
TL control vs. TL 0.005%	-0.08906	-0.1328 to -0.04530	****	<0.0001
TL control vs. TL ibu 50uM	0.04656	0.002805 to 0.09031	*	0.0326
TL control vs. TL ibu 50uM + 0.005%	-0.1228	-0.1666 to -0.07908	****	<0.0001
TL 0.005% vs. TL ibu 50uM	0.1356	0.09186 to 0.1794	****	<0.0001
TL 0.005% vs. TL ibu 50uM + 0.005%	-0.03378	-0.07753 to 0.009973	ns	0.1862
TL ibu 50uM vs. TL ibu 50uM + 0.005%	-0.1694	-0.2131 to -0.1256	****	<0.0001

Supplementary Figure S36: Time point 151s – 300s. Two-way ANOVA followed by Tukey's post hoc multiple comparisons tests. “Mean Diff” shows the difference of means tested. “Adjusted P-value” shows the p-value of the comparison test for significance. Genotypes used: TL and panx1a KO. AA concentration: 0.005%.

Comparison	Mean Diff	95% CI of Diff	Summary	Adjusted P Value
TL control vs. TL 0.005%	-0.1006	-0.1469 to -0.05436	****	<0.0001
TL control vs. TL ibu 50uM	0.04627	1.042e-006 to 0.09255	*	0.05
TL control vs. TL ibu 50uM + 0.005%	-0.08642	-0.1327 to -0.04015	****	<0.0001
TL 0.005% vs. TL ibu 50uM	0.1469	0.1006 to 0.1932	****	<0.0001
TL 0.005% vs. TL ibu 50uM + 0.005%	0.01421	-0.03206 to 0.06048	ns	0.8502
TL ibu 50uM vs. TL ibu 50uM + 0.005%	-0.1327	-0.1790 to -0.08642	****	<0.0001

6.1.9 Ibuprofen freeze duration activity

Supplementary Figure S37: Time point 1s – 150s. Two-way ANOVA followed by Tukey's post hoc multiple comparisons tests. “Mean Diff” shows the difference of means tested. “Adjusted P-value” shows the p-value of the comparison test for significance.

Comparison	Mean Diff	95% CI of Diff	Summary	Adjusted P Value
TL Control vs. TL (0.00125% AA)	0.1206	0.05121 to 0.1899	***	0.0001
TL Control vs. TL 25ug/L Ibuprofen	-0.04542	-0.1148 to 0.02393	ns	0.3191
TL Control vs. TL 25ug/L Ibuprofen + 0.00125% AA	0.1728	0.1034 to 0.2421	****	<0.0001
TL (0.00125% AA) vs. TL 25ug/L Ibuprofen	-0.166	-0.2353 to -0.09663	****	<0.0001
TL (0.00125% AA) vs. TL 25ug/L Ibuprofen + 0.00125% AA	0.05219	-0.01715 to 0.1215	ns	0.2049

TL 25ug/L Ibuprofen vs. TL 25ug/L Ibuprofen + 0.00125% AA	0.2182	0.1488 to 0.2875	****	<0.0001

Supplementary Figure S38: Time point 151s – 300s. Two-way ANOVA followed by Tukey's post hoc multiple comparisons tests. “Mean Diff” shows the difference of means tested. “Adjusted P-value” shows the p-value of the comparison test for significance.

Comparison	Mean Diff	95% CI of Diff	Summary	Adjusted P Value
TL Control vs. TL (0.00125% AA)	0.199	0.1242 to 0.2737	****	<0.0001
TL Control vs. TL 25ug/L Ibuprofen	-0.05317	-0.1279 to 0.02158	ns	0.2493
TL Control vs. TL 25ug/L Ibuprofen + 0.00125% AA	0.2044	0.1296 to 0.2791	****	<0.0001
TL (0.00125% AA) vs. TL 25ug/L Ibuprofen	-0.2522	-0.3269 to -0.1774	****	<0.0001
TL (0.00125% AA) vs. TL 25ug/L Ibuprofen + 0.00125% AA	0.005381	-0.06938 to 0.08014	ns	0.9976
TL 25ug/L Ibuprofen vs. TL 25ug/L Ibuprofen + 0.00125% AA	0.2575	0.1828 to 0.3323	****	<0.0001

Supplementary Figure S39: Time point 1s – 150s. Two-way ANOVA followed by Tukey's post hoc multiple comparisons tests. “Mean Diff” shows the difference of means tested. “Adjusted P-value” shows the p-value of the comparison test for significance.

Comparison	Mean Diff	95% CI of Diff	Summary	Adjusted P Value
TL Control vs. TL (0.005% AA)	0.1506	0.08407 to 0.2172	****	<0.0001
TL Control vs. TL 25ug/L Ibuprofen	0.04469	-0.02184 to 0.1112	ns	0.2972
TL Control vs. TL 25ug/L Ibuprofen + 0.005% AA	0.2351	0.1685 to 0.3016	****	<0.0001
TL (0.005% AA) vs. TL 25ug/L Ibuprofen	-0.1059	-0.1725 to -0.03938	***	0.0005
TL (0.005% AA) vs. TL 25ug/L Ibuprofen + 0.005% AA	0.08444	0.01791 to 0.1510	**	0.0072
TL 25ug/L Ibuprofen vs. TL 25ug/L Ibuprofen + 0.005% AA	0.1904	0.1238 to 0.2569	****	<0.0001

Supplementary Figure S40: Time point 151s – 300s. Two-way ANOVA followed by Tukey's post hoc multiple comparisons tests. “Mean Diff” shows the difference of means tested. “Adjusted P-value” shows the p-value of the comparison test for significance.

Comparison	Mean Diff	95% CI of Diff	Summary	Adjusted P Value
TL Control vs. TL (0.005% AA)	0.1701	0.1012 to 0.2390	****	<0.0001

TL Control vs. TL 25ug/L Ibuprofen	0.01462	-0.05427 to 0.08352	ns	0.9438
TL Control vs. TL 25ug/L Ibuprofen + 0.005% AA	0.2153	0.1465 to 0.2842	****	<0.0001
TL (0.005% AA) vs. TL 25ug/L Ibuprofen	-0.1555	-0.2244 to -0.08660	****	<0.0001
TL (0.005% AA) vs. TL 25ug/L Ibuprofen + 0.005% AA	0.04523	-0.02366 to 0.1141	ns	0.3171
TL 25ug/L Ibuprofen vs. TL 25ug/L Ibuprofen + 0.005% AA	0.2007	0.1318 to 0.2696	****	<0.0001

Supplementary Figure S41: Time point 1s – 150s. Two-way ANOVA followed by Tukey's post hoc multiple comparisons tests. “Mean Diff” shows the difference of means tested. “Adjusted P-value” shows the p-value of the comparison test for significance.

Comparison	Mean Diff	95% CI of Diff	Summary	Adjusted P Value
TL Control vs. TL (0.00125% AA)	-0.01481	-0.06828 to 0.03867	ns	0.8852
TL Control vs. TL 50uM Ibuprofen	0.01697	-0.03650 to 0.07045	ns	0.8373
TL Control vs. TL 50uM Ibuprofen + 0.00125% AA	0.04194	-0.01153 to 0.09542	ns	0.1749
TL (0.00125% AA) vs. TL 50uM Ibuprofen	0.03178	-0.02170 to 0.08525	ns	0.4055
TL (0.00125% AA) vs. TL 50uM Ibuprofen + 0.00125% AA	0.05675	0.003275 to 0.1102	*	0.0333
TL 50uM Ibuprofen vs. TL 50uM Ibuprofen + 0.00125% AA	0.02497	-0.02850 to 0.07845	ns	0.6104

Supplementary Figure S42: Time point 151s – 300s. Two-way ANOVA followed by Tukey's post hoc multiple comparisons tests. “Mean Diff” shows the difference of means tested. “Adjusted P-value” shows the p-value of the comparison test for significance.

Comparison	Mean Diff	95% CI of Diff	Summary	Adjusted P Value
TL Control vs. TL (0.00125% AA)	0.0408	-0.01137 to 0.09297	ns	0.177
TL Control vs. TL 50uM Ibuprofen	0.02768	-0.02448 to 0.07985	ns	0.5055
TL Control vs. TL 50uM Ibuprofen + 0.00125% AA	0.09197	0.03980 to 0.1441	****	<0.0001
TL (0.00125% AA) vs. TL 50uM Ibuprofen	-0.01311	-0.06528 to 0.03906	ns	0.911
TL (0.00125% AA) vs. TL 50uM Ibuprofen + 0.00125% AA	0.05118	-0.0009925 to 0.1033	ns	0.0565
TL 50uM Ibuprofen vs. TL 50uM Ibuprofen + 0.00125% AA	0.06429	0.01212 to 0.1165	**	0.0096

Supplementary Figure S43: Time point 1s – 150s. Two-way ANOVA followed by Tukey's post hoc multiple comparisons tests. “Mean Diff” shows the difference of means tested. “Adjusted P-value” shows the p-value of the comparison test for significance.

Comparison	Mean Diff	95% CI of Diff	Summary	Adjusted P Value
TL Control vs. TL (0.005% AA)	0.1092	0.04403 to 0.1745	***	0.0002
TL Control vs. TL 50uM Ibuprofen	-0.07936	-0.1446 to -0.01414	*	0.0108
TL Control vs. TL 50uM Ibuprofen + 0.005% AA	0.1607	0.09547 to 0.2259	****	<0.0001
TL (0.005% AA) vs. TL 50uM Ibuprofen	-0.1886	-0.2538 to -0.1234	****	<0.0001
TL (0.005% AA) vs. TL 50uM Ibuprofen + 0.005% AA	0.05144	-0.01378 to 0.1167	ns	0.171
TL 50uM Ibuprofen vs. TL 50uM Ibuprofen + 0.005% AA	0.2401	0.1748 to 0.3053	****	<0.0001

Supplementary Figure S44: Time point 151s – 300s. Two-way ANOVA followed by Tukey's post hoc multiple comparisons tests. “Mean Diff” shows the difference of means tested. “Adjusted P-value” shows the p-value of the comparison test for significance.

Comparison	Mean Diff	95% CI of Diff	Summary	Adjusted P Value
TL Control vs. TL (0.005% AA)	0.1199	0.05176 to 0.1880	****	<0.0001
TL Control vs. TL 50uM Ibuprofen	-0.08485	-0.1530 to -0.01675	**	0.0087
TL Control vs. TL 50uM Ibuprofen + 0.005% AA	0.1301	0.06203 to 0.1982	****	<0.0001
TL (0.005% AA) vs. TL 50uM Ibuprofen	-0.2047	-0.2728 to -0.1366	****	<0.0001
TL (0.005% AA) vs. TL 50uM Ibuprofen + 0.005% AA	0.01026	-0.05784 to 0.07837	ns	0.9787
TL 50uM Ibuprofen vs. TL 50uM Ibuprofen + 0.005% AA	0.215	0.1469 to 0.2831	****	<0.0001

6.1.10 Principal Component Analysis Behavioral Assays

Supplementary Figure S45: This table presents the loadings of each variable on the first two principal components (PC1 and PC2) from the PCA analysis.

Var	PC1	PC2
frect	-0.745672877508942	0.622080151769056
fredur	0.95772624409403	0.157356387043019
midct	-0.871161808908256	0.365626049557496
middur	-0.811327582312519	0.207327277239099
burct	-0.783335609715838	-0.386396794489461
burdur	-0.762508311057196	-0.539366726481051

zerct	-0.745666121433675	0.622093541560254
zerdur	0.957726244094198	0.15735638704316
actinteg	-0.839312859031556	-0.475524110919363

6.2 qPCR

6.2.1 TLC35 vs TLE(5+30)

Supplementary Figure S46. Expression ratios, a comparison between TL Control (35 minute incubated) (TLC35) vs TL AA treated (35 minute incubated) (TLE (5+30)). Expression levels and statistical analysis preformed with REST 2009 software (Qiagen). P(H1) is the P-value. Std. Error is the standard error. 95% C.I is the 95% confidence interval. Result shows whether the gene is significantly regulated.

Gene	Expression	Std. Error	95% C.I.	P(H1)	Result
panx1a	0.771	0.545 - 1.110	0.401 - 1.495	0.055	
p2rx8	0.842	0.498 - 1.390	0.358 - 2.099	0.364	
p2ry11	0.648	0.418 - 0.985	0.293 - 1.485	0.017	DOWN
p2ry12	0.869	0.519 - 1.430	0.344 - 2.014	0.419	
p2rx5	0.95	0.621 - 1.511	0.457 - 1.905	0.723	
p2rx7	0.694	0.336 - 1.591	0.238 - 2.042	0.121	
p2rx4a	0.645	0.484 - 0.847	0.363 - 1.173	0	DOWN
cfosAA	1.231	0.515 - 2.062	0.279 - 17.388	0.687	
cfosAB	2.02	0.976 - 4.640	0.629 - 7.013	0.013	UP
cfosB	1.801	1.022 - 3.562	0.651 - 5.098	0.007	UP
cfosl1a	2.255	1.195 - 4.549	0.790 - 9.190	0.002	UP
cfosl1b	0.488	0.284 - 0.841	0.172 - 1.206	0.001	DOWN
cfosl2	0.97	0.506 - 1.965	0.323 - 2.990	0.893	
panx1b	0.729	0.386 - 1.373	0.252 - 1.972	0.141	
IL-1b	0.8	0.387 - 2.191	0.163 - 3.732	0.461	
IL-6	0.623	0.336 - 1.184	0.247 - 2.085	0.049	DOWN
IL-4	0.544	0.365 - 0.815	0.285 - 0.979	0	DOWN

IL-10	0.307	0.210 - 0.651	0.018 - 1.197	0	DOWN
Trpa1a	0.914	0.612 - 1.378	0.441 - 1.765	0.501	
Trpa1b	0.79	0.580 - 1.106	0.448 - 1.474	0.05	DOWN

6.2.2 TLC120 vs TLE(5+115)

Supplementary Figure S47. Expression ratios, a comparison between TL Control (120 minute incubated) (TLC120) vs TL AA treated (120 minute incubated) (TLE (5+115)). Expression levels and statistical analysis preformed with REST 2009 software (Qiagen). P(H1) is the P-value. Std. Error is the standard error. 95% C.I is the 95% confidence interval. Result shows whether the gene is significantly regulated.

Gene	Expression	Std. Error	95% C.I.	P(H1)	Result
p2rx8	0.822	0.419 - 2.042	0.188 - 2.732	0.453	
p2ry11	1.579	0.744 - 3.651	0.415 - 7.781	0.156	
p2ry12	0.729	0.419 - 1.355	0.261 - 2.129	0.148	
p2rx5	0.801	0.499 - 1.234	0.321 - 1.905	0.219	
p2rx7	0.871	0.513 - 1.499	0.325 - 2.828	0.508	
p2rx4a	0.751	0.496 - 1.127	0.358 - 1.765	0.062	
cfosAA	0.904	0.426 - 1.947	0.233 - 3.227	0.7	
cfosAB	0.581	0.219 - 1.451	0.114 - 2.042	0.097	
cfosB	0.882	0.339 - 2.438	0.177 - 4.199	0.694	
cfosl1a	0.467	0.109 - 3.475	0.026 - 17.877	0.239	
cfosl1b	0.877	0.469 - 1.582	0.270 - 2.676	0.549	
cfosl2	0.806	0.341 - 1.839	0.168 - 3.364	0.472	
IL-1b	0.694	0.193 - 2.114	0.067 - 6.063	0.399	
IL-6	1.129	0.444 - 2.206	0.328 - 4.112	0.658	
IL-4	1.151	0.714 - 1.833	0.514 - 3.340	0.437	
IL-10	1.573	0.719 - 3.461	0.415 - 6.277	0.1	
TRPa1a	0.893	0.427 - 1.911	0.259 - 3.411	0.649	
TRPa1b	0.643	0.385 - 1.074	0.233 - 1.434	0.023	DOWN

6.2.3 1AC35 vs 1AE(5+30)

Supplementary Figure S48. Expression ratios, a comparison between panx1a KO Control (35 minute incubated) (1AC35) vs panx1a AA treated (35 minute incubated)(1AE(5+30)). Expression levels and statistical analysis preformed with REST 2009 software (Qiagen). P(H1) is the P-value. Std. Error is the standard error. 95% C.I is the 95% confidence interval. Result shows whether the gene is significantly regulated.

Gene	Type	Reaction Efficiency	Expression	Std. Error	95% C.I.	P(H1)	Result
cfosAA	TRG	1	0.901	0.510 - 1.622	0.291 - 3.204	0.639	
cfosAB	TRG	1	1.218	0.584 - 2.392	0.204 - 3.864	0.457	
cfosB	TRG	1	1.253	0.534 - 3.070	0.253 - 4.691	0.461	
cfosl1a	TRG	1	1.939	1.000 - 4.236	0.532 - 5.579	0.021	UP
cfosl1b	TRG	1	0.429	0.105 - 1.569	0.047 - 3.272	0.049	DOWN
cfosl2	TRG	1	0.936	0.437 - 2.237	0.178 - 4.691	0.829	

6.2.4 TLE35 vs 1AE(5+30)

Supplementary Figure S49. Expression ratios, a comparison between TL AA treated (35 minute incubated) (TLE(5+30)) vs panx1a KO AA treated (35 minute incubated)(1AE(5+30)). Expression levels and statistical analysis preformed with REST 2009 software (Qiagen). P(H1) is the P-value. Std. Error is the standard error. 95% C.I is the 95% confidence interval. Result shows whether the gene is significantly regulated.

Gene	Type	Reaction Efficiency	Expression	Std. Error	95% C.I.	P(H1)	Result
p2rx8	TRG	1	0.623	0.155 - 3.046	0.043 - 6.964	0.34	
p2ry11	TRG	1	0.698	0.244 - 1.918	0.122 - 3.010	0.329	
p2ry12	TRG	1	1.188	0.148 - 6.314	0.056 - 15.562	0.77	
p2rx5	TRG	1	0.754	0.420 - 1.503	0.172 - 2.428	0.239	
p2rx7	TRG	1	0.422	0.157 - 1.246	0.067 - 2.770	0.032	DOWN
p2rx4a	TRG	1	1.048	0.259 - 4.141	0.080 - 7.362	0.912	
IL-1b	TRG	1	0.7	0.253 - 1.752	0.148 - 5.736	0.32	
IL-6	TRG	1	0.608	0.199 - 1.919	0.065 - 3.972	0.24	

IL-4	TRG	1	0.91	0.323 - 2.975	0.099 - 4.993	0.825	
IL-10	TRG	1	1.269	0.179 - 5.879	0.046 - 66.257	0.746	
Trpa1a	TRG	1	0.694	0.222 - 1.703	0.166 - 3.031	0.236	
Trpa1b	TRG	1	0.725	0.286 - 1.745	0.149 - 2.789	0.317	
cfosAA	TRG	1	0.57	0.288 - 1.133	0.158 - 1.454	0.021	DOWN
cfosAB	TRG	1	0.404	0.238 - 0.712	0.093 - 0.953	0.001	DOWN
cfosB	TRG	1	0.78	0.248 - 1.868	0.124 - 3.074	0.463	
cfosl1a	TRG	1	0.802	0.374 - 1.748	0.199 - 2.362	0.401	
cfosl1b	TRG	1	0.95	0.242 - 3.662	0.055 - 6.635	0.92	
cfosl2	TRG	1	0.65	0.328 - 1.154	0.240 - 2.071	0.049	DOWN

6.2.5 TLE120 vs 1AE(5+115)

Supplementary Figure S50. Expression ratios, a comparison between TL AA treated (120 minute incubated) (TLE(5+115)) vs panx1a KO AA treated (120 minute incubated)(1AE(5+115)). Expression levels and statistical analysis preformed with REST 2009 software (Qiagen). P(H1) is the P-value. Std. Error is the standard error. 95% C.I is the 95% confidence interval. Result shows whether the gene is significantly regulated.

Gene	Type	Reaction Efficiency	Expression	Std. Error	95% C.I.	P(H1)	Result
p2rx4a	TRG	1	1.566	0.865 - 2.718	0.607 - 5.502	0.054	
TRPa1a	TRG	1	1.064	0.387 - 3.859	0.043 - 6.498	0.89	
TRPa1b	TRG	1	1.055	0.608 - 1.682	0.371 - 2.549	0.776	
TRPC4b	TRG	1	1.004	0.436 - 2.180	0.257 - 4.228	0.987	
p2ry11	TRG	1	0.791	0.303 - 1.692	0.149 - 3.972	0.488	
p2ry12	TRG	1	1.151	0.424 - 3.626	0.098 - 7.945	0.75	
p2rx5	TRG	1	1.127	0.537 - 2.376	0.299 - 3.891	0.632	
cfosAA	TRG	1	0.948	0.387 - 2.193	0.179 - 4.170	0.862	
cfosAB	TRG	1	0.756	0.214 - 2.515	0.117 - 6.681	0.485	

cfosB	TRG	1	1.038	0.247 - 6.120	0.064 - 10.556	0.935	
cfosl1a	TRG	1	1.373	0.191 - 6.517	0.096 - 22.785	0.571	
cfosl1b	TRG	1	0.912	0.396 - 2.004	0.247 - 4.823	0.744	
cfosl2	TRG	1	1.172	0.494 - 3.058	0.174 - 4.659	0.596	

6.3 ATP assay

Supplementary Figure S51. ATP assay stats. Comparison between Control TL (60 min incubated vs AA treated TL (5 min AA treatment followed by 55 minute incubation)

Treatment	P value	P value summary	Unpaired T-test t, df	ATP Concentration Control (nm/µg)	ATP Concentration AA (nm/µg)
Control TL vs AA Treated TL (5+55)	**0.2755**	**ns**	**t=1.262, df=4**	**4.368**	**4.849**

6.4 RNA Seq

Supplementary Figure S52. RNA sequencing data. Expression ratios of genes of interest in Panx1a KO compared to TL.

GeneName	log2FoldChange	pvalue	padj
fosaa	-0.17330848	0.642525	0.926808
fosab	-0.301644779	0.671673	0.938191
fosb	-3.957390948	0.2082	0.635527
fosb	-1.046561131	0.370599	0.791348
fosb	-0.398905466	0.630713	0.922789
fosb	0	1	1
fosl1a	0.342181814	0.689425	0.94408
fosl1a	0.614547656	0.691081	0.944367
fosl1b	1.172011855	0.112562	0.477064
fosl2	0.249327512	0.394885	0.808136
il10	-1.147203811	0.562532	NA
il10ra	-0.045817014	0.876862	0.985593
il10rb	0.242013764	0.220302	0.649447
il1b	-2.697233122	0.143651	0.538406
il1b	-2.697233122	0.143651	0.538406

il1b	0.119929072	0.763506	0.962108
il4	0.675113007	0.660515	NA
il4r.1	-3.049671017	0.00079	0.019239
il4r.1	0.319957769	0.198238	0.622821
il4r.1	-0.031879092	0.869641	0.984038
il4r.2	7.961457105	0.002418	0.043463
il4r.2	-0.496381738	0.069736	0.374189
il4r.2	1.67181596	0.231435	0.663755
il6	-1.145229974	0.66763	NA
il6r	-0.838468682	0.032798	0.245167
il6r	-0.259872188	0.538298	0.886856
p2rx1	0.723464145	0.598376	0.911159
p2rx1	0.036055128	0.745	0.958472
p2rx2	0.13515696	0.392828	0.806612
p2rx2	-0.156852822	0.796636	0.969268
p2rx3a	0.027448241	0.902279	0.989447
p2rx3b	-0.076258608	0.705799	0.948457
p2rx3b	0.239317417	0.896839	NA
p2rx4a	-0.256914783	0.145413	0.540802
p2rx4a	2.188338254	0.469027	0.853657
p2rx4b	-2.45050996	0.12689	NA
p2rx4b	-0.087608754	0.782939	0.966396
p2rx5	-0.26480521	0.353951	0.780665
p2rx7	-1.12651694	8.8E-08	1.03E-05
p2rx8	-1.582087937	0.014882	0.151792
p2ry1	2.615777682	0.614542	NA
p2ry1	-0.075266609	0.710981	0.950338
p2ry10	-0.59355328	0.569221	NA
p2ry11	-0.392984135	0.618202	0.918364
p2ry12	-0.823014462	0.301049	0.736085
p2ry13	0.771638898	0.583061	NA
p2ry13	0.957722113	0.803104	NA
P2RY14	0.43542926	0.685276	NA
trpa1a	0.651266652	0.119012	0.491117
trpa1b	-1.588343502	0.117318	0.487805
trpa1b	0.949081447	0.152352	0.551895
trpa1b	-0.287562711	0.817565	0.974025

6.5 Immunohistochemistry

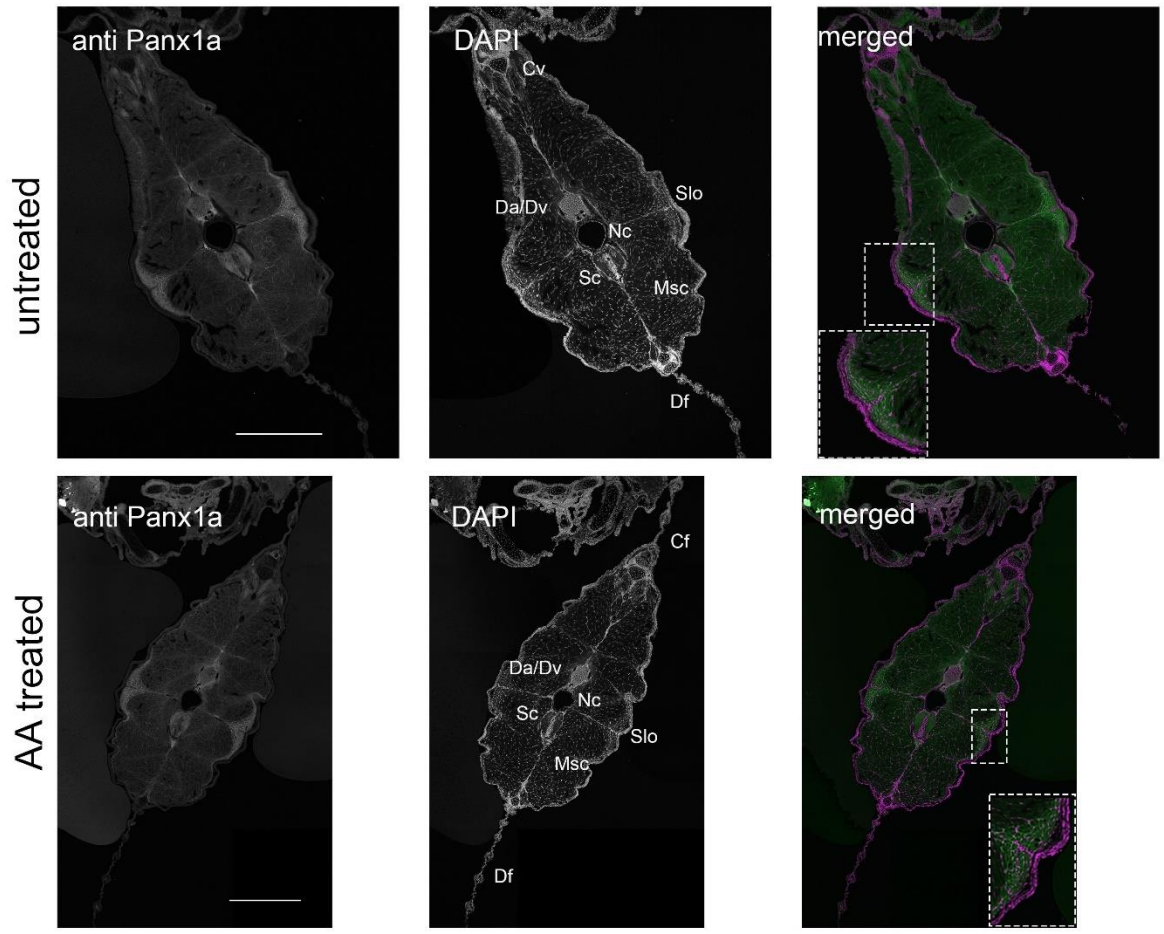

Supplementary Figure S53: Panx1a immunohistochemistry of zebrafish larvae. 6dpf TL larvae were cryo-sectioned at a mid-body position. After staining frontal sections with a custom-made anti-Panx1 antibody (Safarain et al. 2020) sections of untreated (upper row) and AA treated larvae (lower row) were imaged using the LSM700 confocal microscope and identical settings. The insets show enlarged sections of highly innervated areas below the skin. Abbreviations: Df, Cf dorsal and caudal fin. Da/Dv dorsal artery and vein, Nc notochord, Sc spinal cord, Msc muscle. Scale bar = 100µm.

6.6 2 Way ANOVA tables behavioral assays

6.6.1 Burst level activity TL Panx1a KO

Supplementary Figure S54: Time point 1s – 150s. Two-way ANOVA followed by. “P-value” shows the p-value of the interaction factors (column or row) for significance. Row

factor; Genotypes used TL and panx1a KO. Column Factor; Egg water or AA concentration 0.01%.

ANOVA table	SS	DF	MS	F (DFn, DFd)	P value
Interaction	0.000001851	1	0.000001851	F (1, 92) = 0.0004403	P=0.9833
Row Factor (Genotype)	0.001494	1	0.001494	F (1, 92) = 0.3554	P=0.5525
Column Factor (AA Treatment)	0.5618	1	0.5618	F (1, 92) = 133.7	P<0.0001
Residual	0.3866	92	0.004203		

Supplementary Figure S55: Time point 151s – 300s. Two-way ANOVA followed by. "P-value" shows the p-value of the interaction factors (column or row) for significance. Row factor; Genotypes used TL and panx1a KO. Column Factor; Egg water or AA concentration 0.01%.

ANOVA table	SS	DF	MS	F (DFn, DFd)	P value
Interaction	0.0009416	1	0.0009416	F (1, 92) = 0.1534	P=0.6962
Row Factor (Genotype)	0.0005941	1	0.0005941	F (1, 92) = 0.09679	P=0.7564
Column Factor (AA Treatment)	0.3063	1	0.3063	F (1, 92) = 49.91	P<0.0001
Residual	0.5647	92	0.006138		

Supplementary Figure S56: Time point 1s – 150s. Two-way ANOVA followed by. "P-value" shows the p-value of the interaction factors (column or row) for significance. Row factor; Genotypes used TL and panx1a KO. Column Factor; Egg water or AA concentration 0.005%.

ANOVA table					
Interaction	0.03504	1	0.03504	F (1, 92) = 12.41	P=0.0007
Row Factor (Genotype)	0.02669	1	0.02669	F (1, 92) = 9.450	P=0.0028
Column Factor (AA Treatment)	0.3335	1	0.3335	F (1, 92) = 118.1	P<0.0001
Residual	0.2598	92	0.002824		

Supplementary Figure S57: Time point 151s – 300s. Two-way ANOVA followed by. "P-value" shows the p-value of the interaction factors (column or row) for significance. Row

factor; Genotypes used TL and panx1a KO. Column Factor; Egg water or AA concentration 0.005%.

ANOVA table	SS	DF	MS	F (DFn, DFd)	P value
Interaction	0.001779	1	0.001779	F (1, 92) = 0.4876	P=0.4867
Row Factor (Genotype)	0.0003685	1	0.0003685	F (1, 92) = 0.1010	P=0.7513
Column Factor (AA Treatment)	0.4057	1	0.4057	F (1, 92) = 111.2	P<0.0001
Residual	0.3356	92	0.003648		

Supplementary Figure S58: Time point 1s – 150s. Two-way ANOVA followed by. “P-value” shows the p-value of the interaction factors (column or row) for significance. Row factor; Genotypes used TL and panx1a KO. Column Factor; Egg water or AA concentration 0.0025%.

ANOVA table	SS	DF	MS	F (DFn, DFd)	P value
Interaction	0.004267	1	0.004267	F (1, 92) = 1.388	P=0.2418
Row Factor (Genotype)	0.0006407	1	0.0006407	F (1, 92) = 0.2084	P=0.6491
Column Factor (AA Treatment)	0.2973	1	0.2973	F (1, 92) = 96.71	P<0.0001
Residual	0.2829	92	0.003075		

Supplementary Figure S59: Time point 151s – 300s. Two-way ANOVA followed by. “P-value” shows the p-value of the interaction factors (column or row) for significance. Row factor; Genotypes used TL and panx1a KO. Column Factor; Egg water or AA concentration 0.0025%.

ANOVA table	SS	DF	MS	F (DFn, DFd)	P value
Interaction	0.002794	1	0.002794	F (1, 92) = 0.8256	P=0.3659
Row Factor (Genotype)	0.005018	1	0.005018	F (1, 92) = 1.483	P=0.2265
Column Factor (AA Treatment)	0.2309	1	0.2309	F (1, 92) = 68.24	P<0.0001
Residual	0.3113	92	0.003384		

Supplementary Figure S60: Time point 1s – 150s. Two-way ANOVA followed by. “P-value” shows the p-value of the interaction factors (column or row) for significance. Row factor; Genotypes used TL and panx1a KO. Column Factor; Egg water or AA concentration 0.00125%.

ANOVA table	SS	DF	MS	F (DFn, DFd)	P value
Interaction	0.002542	1	0.002542	F (1, 92) = 1.085	P=0.3003
Row Factor (Genotype)	0.004433	1	0.004433	F (1, 92) = 1.892	P=0.1723
Column Factor (AA Treatment)	0.03355	1	0.03355	F (1, 92) = 14.32	P=0.0003
Residual	0.2155	92	0.002342		

Supplementary Figure S61: Time point 151s – 300s. Two-way ANOVA followed by. "P-value" shows the p-value of the interaction factors (column or row) for significance. Row factor; Genotypes used TL and panx1a KO. Column Factor; Egg water or AA concentration 0.00125%.

ANOVA table	SS	DF	MS	F (DFn, DFd)	P value
Interaction	0.01146	1	0.01146	F (1, 92) = 3.644	P=0.0594
Row Factor (Genotype)	0.009394	1	0.009394	F (1, 92) = 2.986	P=0.0873
Column Factor (AA Treatment)	0.04106	1	0.04106	F (1, 92) = 13.05	P=0.0005
Residual	0.2894	92	0.003146		

6.6.2 Freeze Duration TL Panx1a KO

Supplementary Figure S62: Time point 1s – 150s. Two-way ANOVA followed by. "P-value" shows the p-value of the interaction factors (column or row) for significance. Row factor; Genotypes used TL and panx1a KO. Column Factor; Egg water or AA concentration 0.01%.

ANOVA table	SS	DF	MS	F (DFn, DFd)	P value
Interaction	0.0004915	1	0.0004915	F (1, 92) = 0.05881	P=0.8089
Row Factor (Genotype)	0.003027	1	0.003027	F (1, 92) = 0.3622	P=0.5488
Column Factor (AA Treatment)	0.9152	1	0.9152	F (1, 92) = 109.5	P<0.0001
Residual	0.7689	92	0.008357		

Supplementary Figure S63: Time point 151s – 300s. Two-way ANOVA followed by. "P-value" shows the p-value of the interaction factors (column or row) for significance. Row factor; Genotypes used TL and panx1a KO. Column Factor; Egg water or AA concentration 0.01%.

ANOVA table	SS	DF	MS	F (DFn, DFd)	P value
Interaction	0.008984	1	0.008984	F (1, 92) = 0.7641	P=0.3843
Row Factor (Genotype)	0.000489	1	0.000489	F (1, 92) = 0.04160	P=0.8388
Column Factor (AA Treatment)	0.4474	1	0.4474	F (1, 92) = 38.06	P<0.0001
Residual	1.082	92	0.01176		

Supplementary Figure S64: Time point 1s – 150s. Two-way ANOVA followed by. “P-value” shows the p-value of the interaction factors (column or row) for significance. Row factor; Genotypes used TL and panx1a KO. Column Factor; Egg water or AA concentration 0.005%.

ANOVA table	SS	DF	MS	F (DFn, DFd)	P value
Interaction	0.06763	1	0.06763	F (1, 92) = 10.55	P=0.0016
Row Factor (Genotype)	0.04189	1	0.04189	F (1, 92) = 6.537	P=0.0122
Column Factor (AA Treatment)	0.5809	1	0.5809	F (1, 92) = 90.66	P<0.0001
Residual	0.5895	92	0.006408		

Supplementary Figure S65: Time point 151s – 300s. Two-way ANOVA followed by. “P-value” shows the p-value of the interaction factors (column or row) for significance. Row factor; Genotypes used TL and panx1a KO. Column Factor; Egg water or AA concentration 0.005%.

ANOVA table	SS	DF	MS	F (DFn, DFd)	P value
Interaction	0.01239	1	0.01239	F (1, 92) = 1.469	P=0.2286
Row Factor (Genotype)	0.0008486	1	0.0008486	F (1, 92) = 0.1006	P=0.7518
Column Factor (AA Treatment)	0.7037	1	0.7037	F (1, 92) = 83.42	P<0.0001
Residual	0.7761	92	0.008436		

Supplementary Figure S66: Time point 1s – 150s. Two-way ANOVA followed by. “P-value” shows the p-value of the interaction factors (column or row) for significance. Row factor; Genotypes used TL and panx1a KO. Column Factor; Egg water or AA concentration 0.0025%.

ANOVA table	SS	DF	MS	F (DFn, DFd)	P value
Interaction	0.01102	1	0.01102	F (1, 92) = 1.901	P=0.1713
Row Factor (Genotype)	0.000551	1	0.000551	F (1, 92) = 0.09505	P=0.7585
Column Factor (AA Treatment)	0.5566	1	0.5566	F (1, 92) = 96.01	P<0.0001
Residual	0.5334	92	0.005797		

Supplementary Figure S67: Time point 151s – 300s. Two-way ANOVA followed by. “P-value” shows the p-value of the interaction factors (column or row) for significance. Row factor; Genotypes used TL and panx1a KO. Column Factor; Egg water or AA concentration 0.0025%.

ANOVA table	SS	DF	MS	F (DFn, DFd)	P value
Interaction	0.004651	1	0.004651	F (1, 92) = 0.6934	P=0.4072
Row Factor (Genotype)	0.001101	1	0.001101	F (1, 92) = 0.1642	P=0.6863
Column Factor (AA Treatment)	0.4166	1	0.4166	F (1, 92) = 62.10	P<0.0001
Residual	0.6171	92	0.006708		

Supplementary Figure S68: Time point 1s – 150s. Two-way ANOVA followed by. “P-value” shows the p-value of the interaction factors (column or row) for significance. Row factor; Genotypes used TL and panx1a KO. Column Factor; Egg water or AA concentration 0.00125%.

ANOVA table	SS	DF	MS	F (DFn, DFd)	P value
Interaction	0.01502	1	0.01502	F (1, 92) = 2.398	P=0.1249
Row Factor (Genotype)	0.01358	1	0.01358	F (1, 92) = 2.170	P=0.1442
Column Factor (AA Treatment)	0.08644	1	0.08644	F (1, 92) = 13.81	P=0.0003
Residual	0.5761	92	0.006261		

Supplementary Figure S69: Time point 151s – 300s. Two-way ANOVA followed by. “P-value” shows the p-value of the interaction factors (column or row) for significance. Row factor; Genotypes used TL and panx1a KO. Column Factor; Egg water or AA concentration 0.00125%.

ANOVA table	SS	DF	MS	F (DFn, DFd)	P value
Interaction	0.03898	1	0.03898	F (1, 92) = 5.602	P=0.0200
Row Factor (Genotype)	0.01859	1	0.01859	F (1, 92) = 2.671	P=0.1056
Column Factor (AA Treatment)	0.07497	1	0.07497	F (1, 92) = 10.77	P=0.0015
Residual	0.6402	92	0.006959		

6.6.3 PROB burst level activity

Supplementary Figure S70: Time point 1s – 150s. Two-way ANOVA followed by. “P-value” shows the p-value of the interaction factors (column or row) for significance. Row factor; Prob treated TL and TL. Column Factor; Egg water or AA concentration 0.005%.

ANOVA table	SS	DF	MS	F (DFn, DFd)	P value
Interaction	0.0144	1	0.0144	F (1, 92) = 2.928	P=0.0904
Row Factor (No prob/Prob)	0.02734	1	0.02734	F (1, 92) = 5.558	P=0.0205
Column Factor (AA Treatment)	0.3419	1	0.3419	F (1, 92) = 69.50	P<0.0001
Residual	0.4526	92	0.004919		

Supplementary Figure S71: Time point 151s – 300s. Two-way ANOVA followed by. “P-value” shows the p-value of the interaction factors (column or row) for significance. Row factor; Prob treated TL and TL. Column Factor; Egg water or AA concentration 0.005%.

ANOVA table	SS	DF	MS	F (DFn, DFd)	P value
Interaction	0.01727	1	0.01727	F (1, 92) = 3.414	P=0.0679
Row Factor (No prob/Prob)	0.05182	1	0.05182	F (1, 92) = 10.25	P=0.0019
Column Factor (AA Treatment)	0.4306	1	0.4306	F (1, 92) = 85.13	P<0.0001
Residual	0.4653	92	0.005057		

6.6.4 PROB freeze duration activity

Supplementary Figure S72: Time point 1s – 150s. Two-way ANOVA followed by. “P-value” shows the p-value of the interaction factors (column or row) for significance. Row

factor; Prob treated TL and TL. Column Factor; Egg water or AA concentration 0.00125%.

ANOVA table	SS	DF	MS	F (DFn, DFd)	P value
Interaction	0.02484	1	0.02484	F (1, 140) = 4.443	P=0.0368
Row Factor (No prob/Prob)	0.04361	1	0.04361	F (1, 140) = 7.800	P=0.0060
Column Factor (AA Treatment)	0.4899	1	0.4899	F (1, 140) = 87.63	P<0.0001
Residual	0.7827	140	0.005591		

Supplementary Figure S73: Time point 1s – 150s. Two-way ANOVA followed by. “P-value” shows the p-value of the interaction factors (column or row) for significance. Row factor; Prob treated TL and TL. Column Factor; Egg water or AA concentration 0.00125%.

ANOVA table	SS	DF	MS	F (DFn, DFd)	P value
Interaction	0.09123	1	0.09123	F (1, 140) = 11.58	P=0.0009
Row Factor (No prob/Prob)	0.1305	1	0.1305	F (1, 140) = 16.57	P<0.0001
Column Factor (AA Treatment)	0.7015	1	0.7015	F (1, 140) = 89.04	P<0.0001
Residual	1.103	140	0.007879		

Supplementary Figure S74: Time point 1s – 150s. Two-way ANOVA followed by. “P-value” shows the p-value of the interaction factors (column or row) for significance. Row factor; Prob treated TL and TL. Column Factor; Egg water or AA concentration 0.00125%.

ANOVA table	SS	DF	MS	F (DFn, DFd)	P value
Interaction	0.02449	1	0.02449	F (1, 92) = 2.480	P=0.1187
Row Factor (No prob/Prob)	0.06934	1	0.06934	F (1, 92) = 7.022	P=0.0095
Column Factor (AA Treatment)	0.6023	1	0.6023	F (1, 92) = 61.00	P<0.0001
Residual	0.9084	92	0.009874		

Supplementary Figure S75: Time point 1s – 150s. Two-way ANOVA followed by. “P-value” shows the p-value of the interaction factors (column or row) for significance. Row factor; Prob treated TL and TL. Column Factor; Egg water or AA concentration 0.00125%.

ANOVA table	SS	DF	MS	F (DFn, DFd)	P value
Interaction	0.02556	1	0.02556	F (1, 92) = 2.660	P=0.1063
Row Factor (No prob/Prob)	0.1182	1	0.1182	F (1, 92) = 12.30	P=0.0007

Column Factor (AA Treatment)	0.7432	1	0.7432	F (1, 92) = 77.34	P<0.0001
Residual	0.8841	92	0.009609		

6.6.5 Ibuprofen burst level activity

Supplementary Figure S76: Time point 1s – 150s. Two-way ANOVA followed by. “P-value” shows the p-value of the interaction factors (column or row) for significance. Row factor; Ibuprofen (25 ug/L) treated TL and TL. Column Factor; Egg water or AA concentration 0.005%.

ANOVA table	SS	DF	MS	F (DFn, DFd)	P value
Interaction	0.01253	1	0.01253	F (1, 92) = 3.794	P=0.0545
Row Factor	0.04702	1	0.04702	F (1, 92) = 14.24	P=0.0003
Column Factor	0.4237	1	0.4237	F (1, 92) = 128.3	P<0.0001
Residual	0.3038	92	0.003302		

Supplementary Figure S77: Time point 151s – 300s. Two-way ANOVA followed by. “P-value” shows the p-value of the interaction factors (column or row) for significance. Row factor; Ibuprofen (25 ug/L) treated TL and TL. Column Factor; Egg water or AA concentration 0.005%.

ANOVA table	SS	DF	MS	F (DFn, DFd)	P value
Interaction	0.007013	1	0.007013	F (1, 92) = 1.744	P=0.1899
Row Factor	0.01128	1	0.01128	F (1, 92) = 2.804	P=0.0974
Column Factor	0.4667	1	0.4667	F (1, 92) = 116.1	P<0.0001
Residual	0.3699	92	0.004021		

Supplementary Figure S78: Time point 1s – 150s. Two-way ANOVA followed by. “P-value” shows the p-value of the interaction factors (column or row) for significance. Row factor; Ibuprofen (50 uM) treated TL and TL. Column Factor; Egg water or AA concentration 0.005%.

ANOVA table	SS	DF	MS	F (DFn, DFd)	P value
Interaction	0.03872	1	0.03872	F (1, 92) = 11.54	P=0.0010

Row Factor	0.0009796	1	0.0009796	F (1, 92) = 0.2921	P=0.5902
Column Factor	0.4008	1	0.4008	F (1, 92) = 119.5	P<0.0001
Residual	0.3086	92	0.003354		

Supplementary Figure S79: Time point 151s – 300s. Two-way ANOVA followed by. “P-value” shows the p-value of the interaction factors (column or row) for significance. Row factor; Ibuprofen (50 uM) treated TL and TL. Column Factor; Egg water or AA concentration 0.005%.

ANOVA table	SS	DF	MS	F (DFn, DFd)	P value
Interaction	0.006169	1	0.006169	F (1, 92) = 1.763	P=0.1875
Row Factor	0.02195	1	0.02195	F (1, 92) = 6.274	P=0.0140
Column Factor	0.3267	1	0.3267	F (1, 92) = 93.37	P<0.0001
Residual	0.3219	92	0.003499		

6.6.6 Ibuprofen freeze duration activity

Supplementary Figure S80: Time point 1s – 150s. Two-way ANOVA followed by. “P-value” shows the p-value of the interaction factors (column or row) for significance. Row factor; Ibuprofen (25 ug/L) treated TL and TL. Column Factor; Egg water or AA concentration 0.00125%.

ANOVA table	SS	DF	MS	F (DFn, DFd)	P value
Interaction	0.05717	1	0.05717	F (1, 92) = 7.224	P=0.0085
Row Factor	0.0002756	1	0.0002756	F (1, 92) = 0.03483	P=0.8524
Column Factor	0.6884	1	0.6884	F (1, 92) = 86.98	P<0.0001
Residual	0.7281	92	0.007914		

Supplementary Figure S81: Time point 151s – 300s. Two-way ANOVA followed by. “P-value” shows the p-value of the interaction factors (column or row) for significance. Row factor; Ibuprofen (25 ug/L) treated TL and TL. Column Factor; Egg water or AA concentration 0.00125%.

ANOVA table	SS	DF	MS	F (DFn, DFd)	P value

Interaction	0.02057	1	0.02057	F (1, 92) = 2.276	P=0.1348
Row Factor	0.0137	1	0.0137	F (1, 92) = 1.516	P=0.2213
Column Factor	1.25	1	1.25	F (1, 92) = 138.4	P<0.0001
Residual	0.8314	92	0.009037		

Supplementary Figure S82: Time point 1s – 150s. Two-way ANOVA followed by. “P-value” shows the p-value of the interaction factors (column or row) for significance. Row factor; Ibuprofen (25 ug/L) treated TL and TL. Column Factor; Egg water or AA concentration 0.005%.

ANOVA table	SS	DF	MS	F (DFn, DFd)	P value
Interaction	0.00948	1	0.00948	F (1, 92) = 1.367	P=0.2454
Row Factor	0.1001	1	0.1001	F (1, 92) = 14.42	P=0.0003
Column Factor	0.6976	1	0.6976	F (1, 92) = 100.6	P<0.0001
Residual	0.6382	92	0.006937		

Supplementary Figure S83: Time point 151s – 300s. Two-way ANOVA followed by. “P-value” shows the p-value of the interaction factors (column or row) for significance. Row factor; Ibuprofen (25 ug/L) treated TL and TL. Column Factor; Egg water or AA concentration 0.005%.

ANOVA table	SS	DF	MS	F (DFn, DFd)	P value
Interaction	0.005619	1	0.005619	F (1, 92) = 0.7228	P=0.3974
Row Factor	0.02149	1	0.02149	F (1, 92) = 2.765	P=0.0998
Column Factor	0.8251	1	0.8251	F (1, 92) = 106.1	P<0.0001
Residual	0.7152	92	0.007774		

Supplementary Figure S84: Time point 1s – 150s. Two-way ANOVA followed by. “P-value” shows the p-value of the interaction factors (column or row) for significance. Row factor; Ibuprofen (50 uM) treated TL and TL. Column Factor; Egg water or AA concentration 0.00125%.

ANOVA table	SS	DF	MS	F (DFn, DFd)	P value
Interaction	0.009494	1	0.009494	F (1, 92) = 1.899	P=0.1715
Row Factor	0.03261	1	0.03261	F (1, 92) = 6.524	P=0.0123

Column Factor	0.0006202	1	0.00062	F (1, 92) = 0.1241	P=0.7255
Residual	0.4599	92	0.004999		

Supplementary Figure S85: Time point 151s – 300s. Two-way ANOVA followed by. “P-value” shows the p-value of the interaction factors (column or row) for significance. Row factor; Ibuprofen (50 uM) treated TL and TL. Column Factor; Egg water or AA concentration 0.00125%.

ANOVA table	SS	DF	MS	F (DFn, DFd)	P value
Interaction	0.003311	1	0.003311	F (1, 92) = 0.7501	P=0.3887
Row Factor	0.03731	1	0.03731	F (1, 92) = 8.453	P=0.0046
Column Factor	0.06626	1	0.06626	F (1, 92) = 15.01	P=0.0002
Residual	0.4061	92	0.004414		

Supplementary Figure S86: Time point 1s – 150s. Two-way ANOVA followed by. “P-value” shows the p-value of the interaction factors (column or row) for significance. Row factor; Ibuprofen (50 uM) treated TL and TL. Column Factor; Egg water or AA concentration 0.005%.

ANOVA table	SS	DF	MS	F (DFn, DFd)	P value
Interaction	0.1027	1	0.1027	F (1, 92) = 13.82	P=0.0003
Row Factor	0.004676	1	0.004676	F (1, 92) = 0.6294	P=0.4296
Column Factor	0.7321	1	0.7321	F (1, 92) = 98.53	P<0.0001
Residual	0.6836	92	0.00743		

Supplementary Figure S87: Time point 151s – 300s. Two-way ANOVA followed by. “P-value” shows the p-value of the interaction factors (column or row) for significance. Row factor; Ibuprofen (50 uM) treated TL and TL. Column Factor; Egg water or AA concentration 0.005%.

ANOVA table	SS	DF	MS	F (DFn, DFd)	P value
Interaction	0.05428	1	0.05428	F (1, 92) = 6.789	P=0.0107
Row Factor	0.03338	1	0.03338	F (1, 92) = 4.174	P=0.0439
Column Factor	0.6728	1	0.6728	F (1, 92) = 84.13	P<0.0001
Residual	0.7356	92	0.007996		